VIII-th INTERNATIONAL CONFERENCE

on

ION IMPLANTATION AND OTHER APPLICATIONS OF IONS AND ELECTRONS

June 14-17, 2010
Kazimierz Dolny, Poland

Edited by **Jerzy Żuk**
and **Janusz Filiks**

The Market Square in Kazimierz Dolny
drawn by Józef Tarłowski

Published by Lublin University of Technology Press
20-109 Lublin, 13 Bernardyńska Str.
e-mail: wydawnictwo@pollub.pl

ISBN 978-83-7497-092-1

Printed by Printing House Ex-libris
20-484 Lublin, 3 Inżynierska Str.

CHAIRPERSONS

Dariusz Mączka – honorary chairman
Jerzy Żuk – chairman, Maria Curie-Skłodowska University
Paweł Żukowski – co-chairman, Lublin University of Technology
Jerzy Zdanowski – co-chairman, Wrocław University of Technology

INTERNATIONAL SCIENTIFIC COMMITTEE

V.M. Anishchik (Belarus)
A.V. Belushkin (Russia)
R.L. Boxman (Israel)
K.P. Homewood (United Kingdom)
R. Hurley (Northern Ireland)
J. Jagielski (Poland)
F.F. Komarov (Belarus)
Z.W. Kowalski (Poland)
A. Kozanecki (Poland)
D. Machajdík (Slovakia)
F. Nickel (Germany)
J. Piekoszewski (Poland)
A.D. Pogrebnjak (Ukraine)
L. Pranevičius (Lithuania)
B. Rajchel (Poland)
M. Rubel (Sweden)
J. Sielanko (Poland)
W. Skorupa (Germany)
B. Słowiński (Poland)
L. Thomé (France)
A. Turos (Poland)
Z. Werner (Poland)
K. Wieteska (Poland)

LOCAL ORGANIZING COMMITTEE

Maria Curie-Skłodowska University
J. Filiks (Secretary)
M. Kulik
A. Markowski
M. Turek
K. Pyszniak
A. Droździel

Lublin University of Technology
Cz. Karwat
M. Kozak
J. Partyka
P. Węgierek

Monday 14 June	Tuesday 15 June	Wednesday 16 June	Thursday 17 June
	7:30 – 8:30 Breakfast		
	8:30 K. Potzger – Tu-1	**Young Scientist Session**	8:30 F.F. Komarov – Th-1
	9:00 A. Maziewski – Tu-2	Oral presentations	9:00 W. Skorupa – Th-2
10:00 **Registration**	9:30 A. Misiuk – Tu-3	8:30 K. Pągowska – We-1	9:30 B. Nycz – Th-3
	10:00 Z. Werner – Tu-4	8:50 A. Stępkowska – We-2	9:50 R. Hurley – Th-4
	10:30 J. Fedotova – Tu-5	9:10 O. Yastrubchak– We-3	10:20 C. Cherkouk – Th-5
	10:50 *Coffee break*	9:30 S. Abd El Aal – We-4	10:40 *Coffee break*
	11:15 L. Thomé – Tu-6	9:50 J. Lehmann – We-5	11:00 B. Słowiński – Th-6
	11:45 J. Jagielski – Tu-7	10:10 M. Sochacki– We-6	11:30 T. Wilczyńska – Th-7
	12:15 POSTER SESSION I	10:30 S. Prucnal – We-7	11:50 M. Turek – Th-8
		8:30-10:50 Posters	12:10 P. Szałański – Th-9
		I.A. Chugrov – We-1P	
13:00 *Lunch*	14:00 *Lunch*	A. Mikhaylov – We-2P	

14:00 **Opening of the Conference**	15:00 J. Sullivan – Tu-8	R. Ratajczak – We-3P	12:30 **Closing of the Conference**
14:15 L. Pranevičius – Mo-1	15:30 G.M. Wu – Tu-9	V. Tsvyrko – We-4P	13:00 *Lunch*
14:45 J. Piekoszewski – Mo-2	15:50 A. Turos – Tu-10	10:50 *Coffee break*	14:00 *Departure*
15:15 A.D. Pogrebnjak – Mo-3	16:10 W. Wierzchowski – Tu-11	11:00 POSTER SESSION II	
15:45 D.L. Alontseva – Mo-4	16:40 G. Gawlik – Tu-12	13:00 *Lunch*	
16:05 *Coffee break*	17:00 F. Nickel – Tu-13	14:00 *Excursion*	
16:30 M. Ali – Mo-5	17:30 Z. Wroński – Tu-14		
16:50 A. Michel – Mo-6			
17:20 P. Konarski – Mo-7			
17:40 I. Jóźwik – Mo-8			
18:00 Scientific Committee Meeting			
	18:00 *Dinner*		
19:15 *Wellcome dinner*	19:30 *Organ concerto Fara Chuch*	20:00 *Barbecue*	

CONTENTS

ORAL PRESENTATIONS 17

Mo-1 *Liudvikas Pranevicius, Darius Milcius, Liudas Pranevicius, Claude Templier*, Hydrogen separation under molecular ion implantation in nanocrystalline Mg films 18

Mo-2 *Jerzy Piekoszewski, Ludwik Dąbrowski, Bożena Sartowska, Cezary Pochrybniak, Marek Barlak, Paweł Stoch, Wojciech Starosta, Lech Waliś, Zbigniew Werner, Katarzyna Bocheńska, Barbara Nycz*, The effect of chromium on formation of nitrogen expanded austenite phase in Fe-Cr alloy induced by high intensity nitrogen pulses 19

Mo-3 *A.D. Pogrebnjak, Yu.N. Tyurin, Marek Opielek*, Application of plasma jets for fabrication of coatings from metals, hard alloys, ceramics, and their combination 20

Mo-4 *D.L. Alontseva, S.A. Ivanov, S.Ya. Misevra, A.D. Pogrebnjak, N.V. Prokhorenkova, A.A. Timofeev*, The structural phase changes in Ni –Cr- and Co-Cr based coatings deposited by plasma detonation and the results of coatings' modification by duplex treatment 21

Mo-5 *Mona Ali, A. Shaaban, G. Mahgoub, A. Sihame, A. Turos, A. Korman, A. Stonert,* The use of PIXE in evaluation of Coptic Wall Paintings conservation (Case Study) 22

Mo-6 *A. Michel, A. Fillon, G. Abadias, C. Jaouen*, Interaction between energy of deposited species and intrinsic stress build-up in thin solid films grown by magnetron sputtering 23

Mo-7 *P. Konarski, K. Kaczorek, J. Senkara,* Vacuum annealing effects in nickel alloys applied in aviation industry – Depth profile analysis by secondary ion mass spectrometry (SIMS) and glow discharge mass spectrometry (GDMS) 25

Mo-8 *I. Jozwik, J. Jagielski, T. Runka, L. Dobrzanski, A. Zamojski*, Thermal annealing of carbon layers formed via ion-beam induced hydrocarbons decomposition 26

Tu-1 *K. Potzger*, Ion-beam synthesis of magnetic semiconductors 27

Tu-3 *Andrzej Misiuk, Jadwiga Bak-Misiuk, Adam Barcz, Lee Chow, Barbara Surma*, Properties of Si:V annealed under enhanced hydrostatic pressure 28

Tu-4 *Zbigniew Werner, Jerzy Piekoszewski, Marek Barlak, Cezary Pochrybniak, Katarzyna Bocheńska*, The effects of He irradiation in manganese implanted silicon 29

Tu-5 *Julia Fedotova, Dmitry Ivanou, Yulia Ivanova, Alexander Fedotov, Alexander Mazanik, Ivan Svito, Eugen Streltsov, Anis Saad, Serguey Tyutyunnikov, Tomasz N. Koltunowicz, Serguey Demyanov, Vera Fedotova*, Magnetoresistance in n-Si/SiO_2/Ni nanostructures manufactured by swift heavy ion-induced modification technology 30

Tu-6 *Lionel Thomé, Jacek Jagielski, Aurélien Debelle, Frédérico Garrido, Gaël Sattonnay*, On the damage build-up in ion-irradiated ceramics..... 31
Tu-7 *J. Jagielski, A. Piatkowska, P. Aubert, S. Labdi, O. Maciejak, L. Thomé, I. Jozwik, A. Debelle, A. Wajler, M. Boniecki*, Effect of grain size on mechanical properties of irradiated mono- and polycrystalline $MgAl_2O_4$..... 32
Tu-8 *J.L. Sullivan, S.O.Saied*, Deposition and Properties of ultra fast deposited diamond-like hydrogenated carbon films..... 33
Tu-9 G.*M. Wu, Y.F. Chen, H.C. Lu*, Aluminum-doped zinc oxide thin films prepared by sol-gel and RF magnetron sputtering 34
Tu-10 *A. Turos, R. Ratajczak, K. Pągowska, L. Nowicki, A. Stonert*, Stopping power and energy straggling of channeled He-ions in GaN 35
Tu-11 *Wojciech Wierzchowski, Krzysztof Wieteska, Dariusz Mączka, Marcin Turek, Krzysztof Pyszniak*, X-ray diffraction studies of strain distibution in 6H SiC repeatedly implanted with Al ions..... 36
Tu-12 *Grzegorz Gawlik, Jerzy Sarnecki, Iwona Jóźwik, Jacek Jagielski, Marta Pawłowska*, Ion and electron beam induced luminescence of rare earth doped YAG crystals..... 37
Tu-13 *F. Nickel*, News about the precise numerical value of the em fine structure constant..... 38
Tu-14 *Z. Wroński, J. Filiks*, Diagnostics of ion-cathode interaction of glow discharges..... 39
We-1 *K. Pągowska, R. Ratajczak, A. Stonert, A. Turos, L. Nowicki, A. Muecklich,* RBS\channeling and TEM study of damage buildup in ion bombarded III-N compounds..... 41
We-2 *Aneta Stępkowska, Grażyna Przybytniak, Dariusz M. Bieliński*, Application of electron beam radiation to modify crosslink structure in rubber vulcanizates and its tribological consequences..... 42
We-3 *O. Yastrubchak, H. Krzyżanowska, M. Kulik, K. Pyszniak, A. Droździel, J. Żuk, J.Z. Domagała, R. Szymczak, T. Andrearczyk, J. Sadowski, T. Wosiński*, Application of the ion implantation for the synthesis and modification of the (Ga,Mn)As ferromagnetic semiconductors..... 43
We-4 *Shaaban Abd El Aal*, Identification of painting layers of Sennefer Tomb by ion beam analysis..... 45
We-5 *J. Lehmann, L. Rebohle, A. Kanjilal, M. Voelskow, M. Helm, W. Skorupa*, Wear-out phenomena in Si-based light emitting devices with ion beam implanted europium..... 46
We-6 *Mariusz Sochacki, Norbert Kwietniewski, Jan Szmidt, Paweł Kowalczyk*, Reactive ion etching (RIE) of 4H-SiC in fluorinated plasma for device fabrication..... 47
We-7 *S. Prucnal, M. Turek, A. Droździel, K. Pyszniak, A. Wójtowicz, A. Kanjilal, A. Shalimov, W. Skorupa, J. Żuk*, Optical and microstructural properties of In(As,N) quantum structure made by ion implantation and flash lamp processing..... 48

We-1P *Ivan A. Chugrov, Alexey V. Ershov, Andrew A. Ershov, Alexey N. Mikhaylov, David I. Tetelbaum*, Effect of ion doping on optical properties of multilayered *nc*-Si/high-*k*-oxide structures 49
We-2P *Alexey Mikhaylov, Alexey Belov, Alexey Kostyuk, Alexey Ershov, Oleg Gorshkov, David Tetelbaum*, Ion-beam synthesis and modification of light-emitting silicon and silicon-carbon nanoclusters in oxide layers 50
We-3P *R. Ratajczak, A. Turos, A. Stonert, L. Nowicki*, Defect transformations in ion bombarded InGaAsP 51
We-4P Viktor Tsvyrko, Yury Pokotilo, Alexander Kamyshan, Formation of H-donors and radiation defects in proton implanted SiGe 52
Th-1 *F. Komarov, L. Vlasukova, O. Milchanin, J. Żuk, A. Mudryi, K. Pyszniak, M. Kulik*, Nanocrystal- and dislocation-related luminescence in (As+In) implanted Si 53
Th-2 *W. Skorupa, C.Wündisch, M. Posselt, V. Heera, T. Herrmannsdörfer, D. Buca, S. Mantl, S. Haeberlein, R. Fendler, Thoralf Gebel*, Advances in Si & Ge millisecond processing: From silicon-on-insulator to superconducting Ge 54
Th-3 *Barbara Nycz, Marek Barlak, Jerzy Piekoszewski, Bożena Sartowska, Cezary Pochrybniak, Katarzyna Bocheńska*, Diagnostics of high intensity pulsed plasma beams by ex-post analysis of morphology of the irradiated silicon surface 55
Th-4 *R. Hurley, P. Rainey, Y.W. Low, P. Baine, D.W. McNeill, S.J.N. Mitchell, H.S. Gamble and B.M. Armstrong*, Hydrogen and helium implantation in germanium for semiconductor layer transfer applications 56
Th-5 *C. Cherkouk, L. Rebohle, W. Skorupa, M. Helm*, Estrogen detection in waterish solutions by silicon based light emitters 57
Th-6 *B. Słowiński, P. Duda, P. Hładki*, Space structure and fluctuation of electromagnetic cascades produced by 100-3500 MeV gamma quanta in heavy amorphous media 58
Th-7 *Teresa Wilczyńska, Marek Barlak, Roland Wiśniewski, Piotr Konarski, Bożena Sartowska, Wojciech Starosta, Barbara Nycz*, The changes of manganin thermoresistance properties induced by Nb, Ti, C low energy and then Kr high energy ion implantation 60
Th-8 *M. Turek, A. Droździel, K. Pyszniak, S. Prucnal, D. Mączka*, Plasma ion source with an internal evaporator 61
Th-9 *P.J. Szalanski, R.Brzozowski, M.Proba, C.Oprea, I. A.Oprea*, Analysis of the iron state in ferric and ferrous iron containing pharmaceutical products available in Poland by Mössbauer spectroscopy 63

POSTER PRESENTATIONS, Tuesday, June 15, 2010 64
P-Tu-1 *Shaaban Abd El Aal*, Identification of the Vine Tomb multi-layers composition by means of ion beam analysis 65

P-Tu-2 *M.M. Abd El Hady, A.Turos, H.S. Kotb, A. Korman, A. Stonert, F. Munnik*, Characteristics of ancient Egyptian glazed ceramic objects as revealed by ion beam analysis 66
P-Tu-3 *D.L. Alontseva*, Modification of mechanical properties of the Ni-Cr based alloy by continuous electron irradiation 67
P-Tu-4 *Igor Azarko, Oleg Ignatenko, Igor Karpovich, Vladimir Odzhaev, Mihail Puzyrev, Oleg Yankovski*, Laser beam interaction with boron nitride based composites 68
P-Tu-5 *I.I. Azarko, A. Bakulin, E.I. Kozlova, V.P. Kurchenko, L.V. Ajayeva*, Melanin complexes as a radiation bioprotector 69
P-Tu-6- *Marek Barlak, Jerzy Piekoszewski, Zbigniew Werner, Bożena Sartowska, Lech Waliś, Wojciech Starosta, Andreas Kolitsch, Rainer Gröetzchel, Cezary Pochrybniak, Katarzyna Bocheńska, Barbara Nycz*, Wettability of carbon ceramics induced by their surface alloying with Ti, Zr and Cu elements using high intensity pulsed plasma beams 70
P-Tu-7 *Katarzyna Bocheńska, Marek Barlak, Jerzy Piekoszewski, Bożena Sartowska, Cezary Pochrybniak, Barbara Nycz*, Mass loss of the solid irradiated with intense plasma pulses: sputtering or ablation? 71
P-Tu-8 *Jarosław Domaradzki, Danuta Kaczmarek, Eugeniusz L. Prociow, Zbigniew Radzimski*, Study of structure densification in TiO_2 coatings prepared by magnetron sputtering under low pressure of oxygen plasma discharge 72
P-Tu-9 *Hamid Ghomi, Mansour Khoramabadi*, Positive and negative ion temperature effects on the sheath structure in the electronegative plasmas 73
P-Tu-10 *H. Ghomi, M. Kulik, A. Heidarnia, S. Ghasemi*, Fabrication and characterization of diamond-like carbon by DC magnetron sputtering 74
P-Tu-11 J. Baranowska, S. Fryska, Influence of deposition parameters on properties of S-phase coatings 75
P-Tu-12 *Aleksandras Iljinas, Saulius Burinskas, Julius Dudonis, Darius Milčius*, Synthesis of bismuth oxide solid electrolyte thin films deposited by reactive magnetron sputtering 76
P-Tu-13 *Zydrunas Kavaliauskas, Liutauras Marcinauskas, Liudvikas Pranevicius, Pranas Valatkevicius*, Enhanced capacitance of porous carbon electrodes through deposition of small amounts of NiO_2 77
P-Tu-14 *K. Kiszczak, D. Mączka, B. Słowiński, J. Zubrzycki*, The utilization of molecular ions for implantation purposes 78
P-Tu-15 *Tomasz N. Koltunowicz, Pawel Zhukowski, Vera V. Fedotova, Anis M. Saad, Alexander K. Fedotov*, The features of real part of admittance in the nanocomposites $(Fe_{45}Co_{45}Zr_{10})_x(Al_2O_3)_{(100-x)}$ manufactured by ion-beam sputtering technique with Ar ions 79

P-Tu-16 *T.N. Koltunowicz, P. Zhukowski, V.V. Fedotova, A.M. Saad, A.K. Fedotov*, Hopping conductance in nanocomposites $(Fe_{45}Co_{45}Zr_{10})_x(Al_2O_3)_{100-x}$ manufactured by ion-beam sputtering of complicated target in $Ar+O_2$ ambient 80
P-Tu-17 *F.F. Komarov, A.S. Kamyshan*, Peculiarities of swift proton transmission through tapered glass capillaries 81
P-Tu-18 *Zbigniew W. Kowalski*, Comprehensive analysis of ion beam induced stainless steel surface morphology 82
P-Tu-19 *Michał Krysztof, Witold Słówko*, Numerical modelling of the charged particles flow at the variable gas pressure 84
P-Tu-20 *Giedrius Laukaitis, Darius Virbukas, Julius Dudonis, Oresta Katkauske, Darius Milcius*, The influence of technological parameters on the zirconium and cerium based thin films properties 85
P-Tu-21 *N. Levintant-Zayonts, S. Kucharski*, Mechanical properties of nitrogen ion implanted near-surface layers on NiTi Shape Memory Alloy 86
P-Tu-22 *S. Kucharski, N. Levintant-Zayonts*, Influence of high dose nitrogen ion implantation into pseudoelastic behavior of NiTi Shape Memory Alloy 87
P-Tu-23 *Z. Swiatek, M. Michalec, N. Levintant-Zayonts, A. Budziak, O. Bonchyk, G. Savitskij*, Structural evolution of near-surface layers in NiTi alloy caused by an ion implantation 88
P-Tu-24 *P. Mazalski, A. Maziewski, B. Liedke, M.O. Liedke, J. Fassbender*, Studies of Ga+ jons irradiated magnetic Pt/Co/Pt nanostructures 89
P-Tu-25 *A. Meftah, W. Assmann, N. Khalfaoui, F. Studer, M. Toulemonde, C. Trautmann, and K.-O. Voss*, Electronic sputtering of $Gd_3Ga_5O_{12}$ and $Y_3Fe_5O_{12}$ garnets: yield, stoichiometry and comparison to track formation 90
P-Tu-26 *R. Brzozowski, K. Dolecki, B. Pawłowski, M. Moneta*, Phase transformation of Fe-based thin films after ion irradiation 91
P-Tu-27 *A. Puszkarz, M. Moneta*, Role of Ta replacing Nb in Finemet™ 92
P-Tu-28 *A.E. Muñoz-Castro, R. López-Callejas, R. Valencia Alvarado, R. Peña-Eguiluz, A. Mercado-Cabrera, S.R. Barocio, B.G. Rodríguez-Méndez, A. de la Piedad-Beneitez*, Aluminium morphological modification by nitrogen-argon mixture PIII 93
P-Tu-29 *A.R. Niknam, S. Abdi, A.R. Rastkar*, Investigation of direct current discharge plasma in a coaxial structure 94
P-Tu-30 *Alexander D. Pogrebnjak, Mannab Tashmetov, Maxim Il'yashenko, Nemat A.Makhmudov, Vyacheslav M. Beresnev, Oleksey Borysenko, Igor Kulik, Mikhail Kaverin, Ivan Yakuschenko, Janusz Partyka, Bogdan Postolnyi*, Physical-chemical, mechanical, thermal, and radiation resistance of hard and super-hard nano-structured coatings 95

P-Tu-31 *A.D. Pogrebnjak, V.M. Beresnev, M.V. Kaverin, Cz. Karvat, N.A. Makhmudov, M.V. Il'yashenko, O.V. Sobol, A.P. Pshyk, V.A. Baidak, A.A. Dem'yanenko*, Structure and mechanical properties of superhard nanocomposite coatings on Hf-Ti-Si-N base 96
P-Tu-32 *A.D. Pogrebnjak, V.M. Bersnev, M.V. Il'yashenko, M.K. Kylyshkanov, A.P. Shypilenko, M.V. Kaverin, N.K. Erdybaeva, P.V. Zukovski, F.F. Komarov, Yu.Zh. Tuleushev*, Multilayers nanocomposite coatings Ti-N-Al/Ti-N/Al_2O_3/substrate, their structure and properties 97
P-Tu-33 *A.D. Pogrebnjak, O.V. Sobol, V.M. Beresnev, M. Kozak, N.A. Makhmudov, M.V. Il'yashenko, A.P. Shypylenko, M.V. Kaverin, M.Yu. Tashmetov, V. Rogoz, A.V. Pshyk*, Phase composition, thermal stability, and properties of hard ZrN and superhard on base Zr-Ti-Si-N nanocomposite coatings 98
P-Tu-34 *Serhiy Protsenko, Helena Fedchenko, Marta Marszalek, Pawel Zukowski*, Computation of diffusion processes in nanoscale thin films system based on Fe and Cr 99
P-Tu-35 *B. Rajchel, J. Kwiatkowska*, Application of Raman microspectroscopy to the studies of carbon-silver coatings formed by DB IBAD on polyurethane substrate 100
P-Tu-36 *A.V. Russakova, D.T. Berdaliev, O. P. Maksimkin, K.V. Tsay*, Martensite γ→α transformation in deformable stainless steels irradiated with ions and pulse electron flows 101
P-Tu-37 *A. Sallam, M. Fouad, B. Ismail, S. Abd El Aal*, Diagnosis and investigation strategies in the Coptic mural paintings in Upper Egypt 103
P-Tu-38 *A. Sallam, M. Fouad, B. Ismail*, Comparative study of the Stratagraphic Composition of mural painting in Qubbet el Hawa Monastery and Anba Hidra Monastery in the estern Bank in Aswan 104
P-Tu-39 *Bożena Sartowska, Jerzy Piekoszewski, Lech Waliś, Marek Barlak, Wojciech Starosta, Cezary Pochrybniak, Katarzyna Bocheńska*, Structure and composition of scales formed on AISI 316 L steel alloyed with Ce/La using high intensity plasma pulses after oxidation in 1000°C 106
P-Tu-40 *A.D. Pogrebnjak, V.M. Beresnev, M.V. Il'yashenko, A.P. Shypylenko, M.V. Kaverin, P.V. Zukovski, Yu.A. Kunitskyi, O.V. Kolisnichenko, N.A. Makhmudov*, Structure and properties nanocomposite and coating based on Ti-Si-N/WCCo-Cr 107
P-Tu-41 *Witold Słówko, Michał Krysztof*, Environmental equipment for a classic SEM enabling investigations of dielectric and wet surfaces 108
P-Tu-42 *C. Oprea, G. Mateescu, Zh. A. Kozlov, I. A. Oprea, V. A. Semenov, I. Padureanu, M. Ion, L. Craciun, P.J. Szalanski, M. Curuia, I. Stefanescu*, Vacuum system of the thermostat TS-3000K 109

P-Tu-43 *C.Oprea, A.I. Velichkov, D. V.Filossofov, I.A. Oprea, P.J. Szalanski, A.Mihul*, The method of perturbed angular correlations used to study the molecular dynamics in Satureia hortensis vegetal oil 110
P-Tu-44 *Witold Szmaja, Michał Cichomski, Katarzyna Kośla, Józef Balcerski*, TEM and AFM investigation of obliquely evaporated thin cobalt films 111
P-Tu-45 *Marek Tuleta*, Effect of argon plasma on the glass surface 112
P-Tu-46 *Marcin Turek*, Ionization efficiency of a source with a spherical ionizer 113
P-Tu-47 *V.V. Uglov, V.I. Shymanski, N.N. Cherenda, V.M. Astashynski, P. Konarski, A.V. Shashok*, Phase and chemical composition of titanium surface layer simultaneously alloyed with chromium and molybdenum atoms 115
P-Tu-48 *Pawel Zhukowski, Tomasz N. Koltunowicz, Pawel Wegierek, Julia A. Fedotova, Alexander K. Fedotov, Andrey V. Larkin*, The formation of noncoil-like inductance in nanocomposites $(Fe_{45}Co_{45}Zr_{10})_x(Al_2O_3)_{100-x}$ manufactured by ion-beam sputtering of complicated targets in $Ar+O_2$ atmosphere 116

POSTER PRESENTATIONS, Wednesday, June 16, 2010 117
P-We-1 *I.I. Azarko, A. Bakulin, E.I. Kozlova, V.P. Kurchenko, L.V. Ajayeva*, Melanin complexes as a radiation bioprotector 118
P-We-2 *J. Bak-Misiuk, P. Romanowski, E. Dynowska, J.Z. Domagala, A. Barcz, W. Caliebe, A. Hallen*, Investigation of defect structure of Mn-implanted GaSb 119
P-We-3 *M. Szymanska-Chargot, A. Gruszecka, A. Smolira, K. Bederski*, Mass – spectrometric investigations of silver clusters 121
P-We-4 *A.M. Chaplanov, C. Karwat, V.V. Kolos, M.I. Markevich, V.F. Stelmakh*, Effect of arsenium dose iimplanted in silicon substrate on titanium silicide growth during pulse photon processing 122
P-We-5 W*.L. Wang, H.W. Chien and G.M. Wu*, Improved phase change recording systems using silicon nitride dielectric layers prepared by mixed gas plasma 123
P-We-6 *Michał Cichomski, Katarzyna Kośla, Witold Szmaja, Witold Kozłowski, Jacek Rogowski*, Investigation of the structure of fluoroalkylsilanes on alumina surface by XPS and ToF-SIMS 124
P-We-7 *A. Fedotov, O. Korolik, A. Mazanik, N. Stas'kov, T.N. Kołtunowicz, P. Żukowski*, Influence of annealing on the electrical and structural properties of Cz Si wafers preliminary subjected to the hydrogen ion-beam treatment 125
P-We-8 *N.V. Frantskevich, A.K. Fedotov, A.V. Mazanik, A.V. Frantskevich, T.N. Kołtunowicz, P. Żukowski*, Formation of cone-shaped and crystallographically oriented defects on the Cz-Si wafer surface by the helium implantation and DC nitrogen plasma treatment 126

P-We-9 *P. Żukowski, D. Freik, Ya. Saliy, N. Stefaniv, L. Mezhylovska*, Distribution of radiation defects on thickness of IV-VI thin films at α-irradiation 127
P-We-10 *R. Kaliasas, M. Mikolajunas, L. Jakucionis, J. Baltrusaitis, D. Virzonis, J. Puiso, D. Adliene*, Scaling down the lateral dimensions of silicon nanopillars fabricated by RIE, using Au/Cr self-assembled clusters as an etch mask..... 128
P-We-11 *I.A. Karpovich, V.B. Odzhaev, O.N. Yankovsky, E.I.Kozlova*, Microwave diagnostics technology of ion-radiated silicon layers 129
P-We-12 *F. Komarov, O. Milchanin, J. Solovjov, A. Turtsevich, P. Zukowski, Cz. Karwat, K. Kiszczak, Cz. Kozak*, RBS measurements of the low temperature formation of Platinum silicide for Schottky high-power diodes 130
P-We-13 *F. Komarov, L. Vlasukova, O. Milchanin, W. Wesch, A. Mudryi, B. Dunetz*, Structure and optical properties of silicon layers with GaSb nanocrystals created by ion-beam synthesis..... 131
P-We-14 *F.F. Komarov, O.V. Milchanin, I. Konopljanik, K. Kiszczak, P. Zukowski, Cz. Karwat, Cz. Kozak*, Nickel-platinum silicide formation on silicon by IBAD..... 132
P-We-15 *M. Kulik, A. Droździel, Li Lin, S. Prucnal, K. Pyszniak, M. Rawski, M. Turek, J. Filiks, Ł.Gluba, J. Żuk*, Influence of hot implantation on residual radiation damage in silicon carbide 133
P-We-16 *M. Kulik, W. Rzodkiewicz, A. Droździel, K. Pyszniak, J.Żuk*, Application of the fractional-dimensional space approach to analysis of optical spectra in Al^+ hot-implanted GaAs..... 134
P-We-17 *Andrei Lagutin, Helena Gorodecka*, Ion beam analysis of agricultural plants..... 135
P-We-18 *Skirmantė Mockevičienė, Diana Adlienė, Igoris Prosyčevas, Asta Guobienė*, Structural changes in porous Si induced by high energy electron bombardment..... 136
P-We-19 *N. Vabishchevich, D. Brinkevich, V. Volobuev, M. Lukashevich, V. Prosolovich, Yu. Sidorenko, V. Odzhaev, J. Partyka*, Structure and electron-transport properties of photoresist implanted by Sb^+ ions..... 137
P-we-20 *D.I. Brinkevich, V.S. Prosolovich, Yu.N. Yankovski, S.A. Vabishchevich*, Strength of the silicon implanted by high-energy ions of inert gases..... 138
P-We-21 *S. Prucnal, W. Skorupa, B. Abendroth, K. Krockert, H.J. Möller*, Solar cell emitters fabricated by plasma immersion ion implantation and flash lamp millisecond annealing 139
P-We-22 *A. Grigonis, Z. Rutkuniene, V. Vinciunaite*, Different wavelength laser irradiation of amorphous carbon 140
P-We-23 *Jolita Sakaliūnienė, Jurgita Čyvienė, Brigita Abakevičienė*, Investigation of structural and optical properties of GDC thin films deposited by reactive magnetron sputtering..... 141

P-We-24 *Wojciech Słysz, Marek Guziewicz, Michał Borysiewicz, Jarosław Domagała, Iwona Pasternak, Krzysztof Hejduk, Jan Bar, Maciej Węgrzecki, Piotr Grabiec, Remigiusz Grodecki, Iwona Węgrzecka, Roman Sobolewski*, Thin superconducting NbN layers deposited on different substrates: Si, SiO_2, Si_3N_4, Al_2O_3 designed for superconducting single photon detectors 142
P-We-25 *Anna Smolira, Robert Bicki, Agnieszka Gruszecka, Monika Szymańska-Chargot*, Influence of target materials on silver benzoate ion formation in LD ion source of time of flight mass spectrometer..... 143
P-We-26 *Joanna Wessely-Szponder, Barbara Majer-Dziedzic, Anna Smolira, Ryszard Bobowiec*, Detection of cathelicidins from porcine neutrophils by MALDI time of flight mass spectrometry 144
P-We-27 *Kazimierz Reszka, Mieczysław Szczypiński, Małgorzata Pomorska*, Influence of substrate local heating on morphology of Al and Al_2O_3 nanofilms..... 145
P-We-28 *E. Szot, L. Wojcik, K. Głuch*, Mass spectrometric study of the kinetic energy release of isopropanon isomer ions..... 146
P-We-29 *E. Szot, L. Wojcik, K. Głuch*, Double focusing mass spectrometer in molecular structure investigatnios 147
P-We-30 *M.I. Tarasik, A.K. Fedotov, A.M. Yanchenko, A.N. Pyatlitski, T.V. Piatlitskaya, S.V. Shvedov, P. Węgierek, P. Zhukowski*, Recombination properties of the ion-implanted silicon..... 148
P-We-31 *N.A. Poklonski , N.I. Gorbachuk , M.I. Tarasik, S.V. Shpakovski , V.A. Philipenya, V.A. Skuratov, A. Wieck, T. Kołtunovicz*, Effect of fluences of irradiation with 107 MeV krypton ions on recovery charge of silicon p^+n-diodes..... 149
P-We-32 *Igor Tashlykov, Anton Turavets, Pawel Zukowski*, Influence of Xe^+ irradiation on topography and wettability of graphite surface 150
P-We-33 *Iya I. Tashlykova-Bushkevich, Czeslaw Kozak, Vasiliy G. Shepelevich*, Effect of annealing on dope depth profiles in rapidly solidified Al-Ge alloys..... 151
P-We-34 *T. Tsvetkova, S. Takahashi, P. Sellin, I. Gomez-Morilla, O. Angelov, D. Dimova-Malinovska, J. Żuk*, Optical pattern fabrication in amorphous silicon carbide with high-energy focused ion beams 152
P-We-35 *V.V. Uglov, N.T. Kvasov, Yu.A. Petukhou, R.S. Kudaktsin, V.M. Astashynski, A.M. Kuzmitski, V.A. Ukhov, A.V. Shashok, P. Konarski*, Modification of "zirconium-on-silicon" system by dense compression plasma..... 153
P-We-36 *Paweł Węgierek and Piotr Billewicz*, Hopping mechanism of electric conductivity in the n-type silicon implanted with Ne^+ neon ions 154
P-We-37 *Yury Pokotilo, Alla Petukh, Aleksey Giro, Paweł Węgierek*, Formation of submicron n^+-layers in silicon implanted with H^+-ions..... 155
P-We-38 *Ewa Taranko, Małgorzata Wiertel, Ryszard Taranko*, Time-dependent electron transport through the quantum dot based devices..... 156

P-We-39 *Leszek Wójcik and Artur Markowski*, Mass spectrometric study of ion-molecule reactions in H_2S and CH_4 mixtures 157
P-We-40 *Leszek Wójcik and Artur Markowski*, Ion-molecule reactions in carbon tetrafluoride-helium mixtures 158
P-We-41 *B. H. Tsai, C. F. Wu, S. F. Kung, G. M. Wu*, Improved light extraction efficiency by two-dimensional triangular photonic crystal arrays using focused ion beams 159
P-We-42 *Paweł Żukowski, Paweł Węgierek, Piotr Billewicz, Tomasz Kołtunowicz*, Mechanisms of electric conductivity in gallium arsenide exposed on poly-energy implantation of H^+ ions..... 160
P-We-43 *V. Wojcik, Ya. Saliy, P. Zukovskiy, D. Freik*, Calculation of concentration and mobility of free charge carriers and own defects in monocrystal epitaxial films PbTe at α-irradiation 161
P-We-44 *V.B. Odzhaev, V.S. Prosolovich, Yu.N. Yankovski, V.A. Belous, P. Zhukowski*, Features annealing of silicon implanted with argon ions 162
Authors Index 163

ORAL PRESENTATIONS

Mo-1 (Invited)

Hydrogen separation under molecular ion implantation in nanocrystalline Mg films

Liudvikas Pranevicius[1)], *Darius Milcius*[2)], *Liudas Pranevicius*[1)], *Claude Templier*[3)]

[1)] *Vytautas Magnus University, 8 Vileikos St., LT-44404 Kaunas, Lithuania*
[2)] *Lithuanian Energy Institute, 3 Breslaujos St., LT-44403 Kaunas, Lithuania*
[3)] *Université de Poitiers, SP2MI, Bd Marie et Pierre Curie, 30179 Futuroscope, France*

High purity H_2 gas streams are increasingly important for a variety of applications including feed gases for fuel cells and hydrogen storage. The potential of hydrogen gas as primary energy source has generated considerable interest in hydrogen separation technologies. We have been investigating a method to separate hydrogen from molecules containing hydrogen employing molecular ion implantion.

2 μm thick magnesium films have been magnetron sputter deposited on stainless steel (AISI 316L) substrates and hydrogenated at 450 K by plasma immersion ion implantation (PIII) technique using $CH_4(H_2O)$+Ar gases at 10 Pa pressure. Variety of molecular ions containing hydrogen are extracted from plasma and accelerated by 1-10 keV bias voltage for implanting hydrogen into near surface region. Molecular ions upon entering the substrate break up into constituent atoms and separation of hydrogen occurs. The depth profiles of C, O and H atoms across the Mg film have been analyzed using Nuclear Reaction Analysis (NRA) and secondary ion mass spectrometry (SIMS) techniques. The identification of phases has been performed using X-ray diffraction (XRD) technique and the surface topography of as-deposited and hydrogenated films analyzed by scanning electron microscopy.

It is shown that after plasma treatment of Mg film in $CH_4(H_2O)$+Ar plasmas, C and O atoms accommodate in the near surface region while H atoms are transported at elevated temperature along grain boundaries into the bulk of nanocrystalline Mg film. In this way, hydrogen separation and formation of Mg hydrides have been performed avoiding hydrogen gas purification process.

Mo-2 (Invited)

The effect of chromium on formation of nitrogen expanded austenite phase in Fe-Cr alloy induced by high intensity nitrogen pulses

Jerzy Piekoszewski[1,2)], Ludwik Dąbrowski[3)], Bożena Sartowska[2)], Cezary Pochrybniak[1,3)], Marek Barlak[1,2)], Paweł Stoch[3)], Wojciech Starosta[2)], Lech Waliś[2)], Zbigniew Werner[1)], Katarzyna Bocheńska[1)], Barbara Nycz[1)]

[1]*The Andrzej Sołtan Institute for Nuclear Studies, Otwock/Świerk, Poland*
[2]*Institute of Nuclear Chemistry and Technology, Warszawa, Poland*
[3]*Institute of Atomic Energy, Otwock/Świerk, Poland*

Several authors have shown that the presence of expanded austenite phase (called "S" or γ_N phase) in stainless steel, increases its surface hardnessand and wearing resistance. Some of the authors claim explicitly that regardless of the method of nitriding, the γ_N phase can be formed only when Fe, Cr (>15 wt. %) and Ni (>5 wt. %) are available. However, in our previous experiments it was shown that any kind of the steel including pure Fe can be austenized and γ_N can be formed if the substrate is treated with high intensity pulsed nitrogen plasma beams (HIPPB). The intention of the present experiments is to get inside into more details about the role of Cr in formation of γ_N in chromium alloys. An amount components was limited to only Fe and Cr with different Cr content: 2.55, 4.97, 9.94, 20.86, 41.97 at. %. The samples were subjected to HIPPB treatment to incorporate 17.51±2 at % of N in the near surface layer. The samples were characterized by CEMS, XRD and EDX. Also the "*ab initio*" calculatations s were performed. Main conclusions are:

1) Incorporation of nitrogen results in the transition from magnetic to paramengetic state for all Cr contents and the fraction of CEMS spectra representing γ_N phase decreases with an increase of Cr concentration.
2) "ab initio" calculations seems to support Williamson's model [1, 2] of trapping nitrogen at chromium.

References

[1] Williamson D L, Ozturk O, Wei R, Wilbur PJ. Surf.Coat Technol. 1994;65:15
[2] Blawert C, Mordike B L, Collins G A, Short K T, Jiraskova Y, Schneeweis O, PerinaV. Surf. Coat. Technol. 2000; 128-129: 219

Mo-3 (Invited)

Application of plasma jets for fabrication of coatings from metals, hard alloys, ceramics, and their combination

A.D. Pogrebnjak[1)], *Yu.N. Tyurin*[2)], *Marek Opielek*[3)]

[1)] *Sumy State University, Sumy Institute for Surface Modification, 40007 Sumy, Ukraine*
[2)] *E.O.Paton Welding Institute, NAS of Ukraine, Kiev, Ukraine*
[3)] *Lublin University of Technology, Lublin, Poland*

The report is concerned with the current status of research on the use of plasma jets for the modification of surface properties of metalware, as well as of investigations of doping and mass transfer of elements. The effect of thermal plasma parameters on the efficiency of surface processing of metal materials is discussed. The structure and properties of protective coatings produced by exposure to pulsed plasmas are analyzed. A new direction for the production of combined coatings is considered. Their structure and properties were studied by the example of Fe, Cu, steels, and alloys, including titanium alloys; the modification process was shown to be controllable by the action of pulsed plasma jets. The physical factors that affect the modification process and the coating deposition, and their effect on the structure and properties of metallic, ceramic ± metal, and ceramic coatings were analyzed.

We have considered one avenue in technology. the use of thermal plasmas for producing new materials and nanodimensional powders, depositing combined and protective coatings, and modifying the surfaces of materials by exposing them to pulsed plasma jets. We have shown that the findings of an investigation into this technological sphere may be used to advantage in many branches of industry. At present, the employment of pulsed high-speed jets offers promise as a tool for obtaining new composite, highly doped materials on the surfaces of articles made of constructional materials.

The thermal plasma processing of metal surfaces is under development and will soon enjoy wide use for the compaction of powdered materials, coatings, plasma-chemical vapor phase coating deposition, and the synthesis of fine powders with nanometer-sized grains. The industrial development of these technologies is largely dependent on the progress andapplication of the methods for efficient inspection of the technology, and the resultant coatings and materials.

Mo-4

The structural phase changes in Ni –Cr- and Co-Cr based coatings deposited by plasma detonation and the results of coatings' modification by duplex treatment

D.L. Alontseva[1)], *S.A. Ivanov*[2)], *S.Ya. Misevra*[1)], *A.D. Pogrebnjak*[3)], *N.V. Prokhorenkova*[1)], *A.A. Timofeev*[4)]

[1)] *East-Kazakhstan State Technical University, 69 Protozanov St., 070004, Ust-Kamenogorsk, Kazakhstan, e-mail: dalontseva@mail.ru*
[2)] *Interactive Corporation representative office in Moscow, 14 Gubkina Street, Office 23, Moscow 117312, Russian Federation, e-mail: iac@microanalysis.ru*
[3)] *Sumy Institute for Surface Modification, PO BOX 163, 40030, Sumy, Ukraine, e-mail: alexp@i.ua*
[4)] *«MEPhI», National University for Nuclear Research, 31 Kashirsky Freeway, 115409, Moscow, Russian Federation, e-mail: alexmail21@mail.ru*

Keywords: plasma detonation, electron irradiation, Transmission Electronic Microscopy (TEM), XRD-method, nanocrystalline structure, nanograins, crystal-lattice orientation, cellular precipitation

This paper presents the analysis of new results of experimental investigating of the structure-phase state and mechanical properties of Ni-Cr and Co-Cr-based composite powder coatings. The coatings were deposited on stainless substrates by plasma detonation in air. The coated samples were exposed to e-beam in vacuum or re-exposed to pulsed plasma jet without powder coating.

The main experiment methods were selected as follows: TEM, and SEM with EDS, topography by AFM, ESCA, XRD, micro-hardness measurement, and wear and corrosion tests.

It was empirically established that before irradiation the PG-19N-01 coating consists of Ni-based nanocrystalline γ-phase and CrNi3 microcrystalline phase. The morphology of new phase particles found in the coating suggests that it is cellular precipitation. The particles are structurally inhomogeneous to the Ni base, and glow in the dark field.

TEM and XRD tests defined the size of nanograins and microcrystallites, angles of their off-orientation, types and parameters of their lattices, morphology of their precipitation, and their volume concentration in the material. We suggested the thermodynamic model of CrNi3 precipitate formation.

It was found that depositing PG-10N-01, PG-19N-01, and AN-35 powder coatings by plasma detonation with the duplex treatment of the surface results in forming multi-phase dense coatings with intermetallic hardening compounds, oxides and carbides. We have detected improvement of mechanical properties of the coatings after their modification by e-beam or by re-exposed to pulsed plasma jet. Their microhardness and corrosion resistance in sea water is increased compared to the properties of not irradiated coatings. Therefore the Ni-Cr and Co-Cr coatings with the duplex treatment can be used for protection of valves and other components working in aggressive environments.

Mo-5

The use of PIXE in evaluation of Coptic Wall Paintings conservation (Case Study)

Mona Ali[1)], A. Shaaban[2)], G. Mahgoub[2)], A. Sihame[3)], A. Turos[4,5)], A. Korman[4)], A. Stonert[4)]

[1)] *Cairo University, Faculty of Archaeology, Conservation Dept., Egypt, monalyeg@yahoo.com*
[2)] *Fayoum University, Faculty of Archaeology, Conservation Dept., Egypt, smm00@fayoum.edu.eg*
[3)] *National Research Center, Dokki, Cairo, Egypt*
[4)] *Soltan Institute of Nuclear Studies, 05-400 Swierk/Otwock, Poland*
[5)] *Institute of Electronic Materials Technology, Wólczyńska 133, 01-919 Warszawa, Poland*

Egypt has a lot of ancient Monasteries and churches, which were decorated with different kinds of wall paintings. Structure of these wall pintings consists of support, plaster and painting layers [1]. Paintings deterioration is primarily due to physiochemical, natural and human factors. The most detrimental factors are bat patches, old varnish and organic waste of birds. All these lead to the gradual disappearance of paintings. New technology of conservation is focused on application of new materials for cleaning of wall paintings. Here we report on the use of enzymes, for cleaning surface of coptic wall paintings.

Analytical techniques such as PIXE, XRD, FTIR and LOM were used to evaluate the enzymatic cleaning processes of coptic wall paintings and to identify the chemical composition of red, yellow and white pigments. PIXE and XRD results indicated that there is no change in the chemical composition of the materials and pigments. FTIR and LOM results confirmed the stability of organic medium before and after enzymatic cleaning of different kind of patches.

Fig. 1. PIXE Spectra of Coptic Wall Paintings, Object No7953, Coptic Museum, Cairo, Egypt.

References

[1] Paul T. Nicholson, Ian Shaw, Ancient Egyptian materials and technology Cambridge University Press, 2000.

Mo-6 (Invited)

Interaction between energy of deposited species and intrinsic stress build-up in thin solid films grown by magnetron sputtering

A. Michel, A. Fillon, G. Abadias, and C. Jaouen

Institut P', CNRS - Université de Poitiers - ENSMA, UPR 3346, Département Physique et Mécanique des Matériaux, SP2MI - Téléport 2, Boulevard Marie et Pierre Curie, BP 30179 86962 Futuroscope-Chasseneuil Cedex, FRANCE

The use of sputtering deposition techniques, due to the versatility of the deposition parameters, is becoming more common in the ever-growing field of nanostructure thin films. Due to their small dimensions, nanostructure thin films can demonstrate new and sometimes unexpected physical properties, while possible applications for novel electrical, optical or mechanical devices are already proposed. However, a fine control on the film microstructure is mandatory, therefore, the ability to fine tune the energy of the deposited species is a major advantage of magnetron sputtering.

A key issue in thin films is the stress generation and development during growth; a lot of attention has been devoted to this subject, which is of importance not only to the properties of the films, but also to their stability as devices. Several mechanisms of stress evolution can be found in the literature (as the compressive-tensile-compressive model in the case of high mobility materials deposited by thermal evaporation, or the point defect creation model at high deposition energy). The proposed models, although sometimes contradictory, mainly depend on the mobility of the thin film constituents for the mechanisms of the energy transfer from the incoming particles or plasma ions to the film. Nevertheless, stress evolution during sputtering growth has not been exhaustively investigated and this contribution is focussed on stress in low mobility films; in more detail, Mo, a refractory metal, has be chosen as a model system, and MoxSi1-x solid solutions proved to be an interesting counterpart to pure Mo for a more general approach to polycrystalline sputter-deposited thin films.

In situ stress measurements during deposition are obtained using a multi-beam laser set-up providing a real time determination of the substrate curvature. These observations are coupled with ex-situ structural and microstructural investigations using XRD, and atomic force and transmission electron microscopies.

The influence of sputtering pressure, substrate bias voltage, and growth rate were examined; whereas the analysis was straightforward concerning the pressure, the influence of growth rate was apparent only under specific energy conditions. Additionally, the thin film microstructure was investigated, and the use of Mo_xSi_{1-x} alloys grown on different buffer layers provided an elegant way of tuning the lateral grain size of thin films, since a variation in the range between 20 nm and ~1 μm [1] has been observed. For pure Mo films, a typical stress evolution from tensile to compressive was observed in the final growth stages with decreasing pressure and increasing bias voltage. However, etching of the Si substrate or growth of an amorphous Si buffer layer induces significant stress changes in the early growth stages. For $Mo_{1-x}Si_x$ alloy films grown on Si, stress evolution with film thickness strongly depends on the Si content. Different stages were identified for crystalline solid solutions ($x<0.19$), while for amorphous alloys the stress reached rapidly a steady-state

compressive value. For $Mo_{1-x}Si_x$ alloy films grown on a Mo buffer layer in turn, the stress is essentially compressive.

The comparative study of stress evolution for pure Mo films and solid solutions brings into light the role of defect creation energy, as the displacement energy is lowered in disordered alloys. The whole of the observations illustrate that stress generation is located at the grain boundaries, and that grain boundary diffusion participates in the mechanisms for stress evolution. This result is in contrast to deposition methods involving higher energy deposited species (as Direct Ion Beam Sputtering), where a key role is attributed to point defects creation inside the grains. Finally, this work shows that with an in depth understanding of the stress generation mechanisms, it can be possible to tailor the average stress level in thin films.

References

[1] A. Fillon, G. Abadias, A. Michel, C. Jaouen, P. Villechaise, Phys. Rev. Lett. 104, 096101 (2010).

Mo-7

Vacuum annealing effects in nickel alloys applied in aviation industry – Depth profile analysis by secondary ion mass spectrometry (SIMS) and glow discharge mass spectrometry (GDMS)

P. Konarski[1)], *K. Kaczorek*[1)], *J. Senkara*[2)]

[1)] *Tele and Radio Research Institute, Ratuszowa 11, 03-450 Warszawa*
[2)] *Warsaw University of Technology, Narbutta 85, 02-524 Warszawa, Poland*

Heat treatment in vacuum environment of steels and nickel alloys is frequently used in the material production and its processing. Vacuum annealing is also employed for out-gassing elements in ultra-high vacuum systems or for surface activation in different production purposes. A number of phenomena (diffusion, segregation, selective vaporization of elements) are going on in the course of heating the material in vacuum in the near surface region leading to changes in its chemical composition and structure. In the present work heating procedure in vacuum was applied for selected nickel alloys and steels used in aviation technology.

Two depth profile analytical techniques were applied: secondary ion mass spectrometry (SIMS) and glow discharge mass spectrometry (GDMS). Compositional changes were observed in nanometer depth ranges for analysed alloys. SIMS depth profiles were obtained using 5 keV Ar^+ ion beam scanning performed over 1 mm x 0.6 mm area. In GDMS depth profile analysis was performed over 1.5 mm diameter spot eroded due to 1500 V, DC glow discharge in 1 Tr argon.

Performed analyses show depletions as well as enrichments of alloy components with respect to the bulk concentration. The results are compared for the two analytical techniques applied in this study.

This work is supported by the Polish Ministry of Science and Higher Education in years 2007-10 as research development project No R15 055 03.

Mo-8

Thermal annealing of carbon layers formed via ion-beam induced hydrocarbons decomposition

I. Jozwik[1)], *J. Jagielski*[1)], *T. Runka*[2)], *L. Dobrzanski*[1)], *A. Zagojski*[1)]

[1)] *Institute of Electronic Materials Technology, Warszawa, Poland*
[2)] *Faculty of Technical Physics, Poznan University of Technology, Poznan, Poland*

The exceptional electrical and mechanical properties of graphene motivated the need of searching for the new methods of its fabrication. This work presents the analysis of structural and electrical properties of carbon layers formed by ion-beam decomposition of hydrocarbons followed by thermal annealing. The Si substrates covered with SiO_2 layers (100 nm thick) and deposited Au contacts were bombarded at room temperature with 50 keV Ar or He ions up to fluences 1e16, 3e16 and 1e17 cm^{-2}. The irradiations were performed in the presence of hydrocarbon vapours. Thermal annealing of the carbon layers deposited on the SiO_2/Si substrates was performed in 200-600°C range in 100°C steps.

The RBS/C (Rutherford Backscattering/Channeling) method was applied to evaluate the thickness of deposited carbon layers, which is in tens of nanometers range. Surface morphology was analysed by scanning electron microscopy technique (SEM) and allowed us to determine specific morphological features of deposited layers. Structure of layers was investigated by means of μ-Raman spectroscopy. This last method revealed that the annealing resulted in the structural changes in carbon films leading to the increase of the sp^2 to sp^3 ratio and formation of small domains of micro-crystalline graphite.

The measurements of electrical parameters showed the increase of the conductivity after each step of annealing, what confirmed the thermal restructurisation and gradual graphitization of carbon layers. Special emphasise in the discussion will be given to the identification of graphene and differences between this material and other forms of carbon-based layers.

Tu-1 (Invited)

Ion-beam synthesis of magnetic semiconductors

K. Potzger

Forschungszentrum Dresden-Rossendorf, Bautzner Landstraße 400, 01328 Dresden

In recent years, ion implantation has been considered as a powerful tool for the doping of semiconductors with magnetic elements far from thermal equilibrium. For instance, research on diluted magnetic semiconductors (DMS) became very popular due to their large potential in future spintronics devices like spin valves or current-induced magnetic switches. The research faces, however, serious difficulties due to the appearance of tiny magnetic secondary phases, spinodal decomposition or magnetically active defects in the semiconductor induced by the implantation/oversaturation. It was found that those effects lead to ferromagnetic as well as magneto-transport properties which, by mistake, could be interpreted as intrinsic DMS. In this paper, I will focus on the discussion of pitfalls during magnetic and structural analysis, especially on element-specific analysis methods for the identification of the source of the ferromagnetic signal. Moreover, possibilities to overcome those difficulties will be presented.

Tu-3 (Invited)

Properties of Si:V annealed under enhanced hydrostatic pressure

Andrzej Misiuk[1)], *Jadwiga Bak-Misiuk*[2)], *Adam Barcz*[1,2)], *Lee Chow*[3)] *and Barbara Surma*[4)]

[1)] *Institute of Electron Technology, Al. Lotnikow 46, 02-668 Warszawa, Poland*
[2)] *Institute of Physics, PAS, Al. Lotnikow 32/46, 02-668 Warszawa, Poland*
[3)] *University of Central Florida, Orlando, FL 32816, USA*
[4)] *Institute of Electronic Materials Technology, 01-919 Warszawa, Poland*

Implantation of silicon with some transition metals, vanadium among them, and processing of resulting Si:TM at high temperature (HT)-hydrostatic pressure (HP) can lead to magnetic ordering within the buried TM-enriched area. In particular, magnetic ordering has been reported for Si:V and similar structures [1,2].

This work presents new data concerning structure and related properties of Si:V (D_{V+}=1x10^{12}-5x10^{15} cm^{-2}, E_{V+}=200 keV, projected range of V^+, R_p=170 nm), as implanted and processed for up to 5 h at HT ≤ 1400 K under HP ≤ 1.2 GPa. Secondary Mass Spectrometry, TEM, X-ray, synchrotron and photoluminescence methods were used for characterisation of the samples.

Strongly damaged and even amorphous (aSi) area is produced near R_p in effect of implantation. At HT-HP the aSi layer is subjected to Solid Phase Epitaxial Re-growth (SPER). Depending on HP, the formation of the VSi_2 phase and distinct SPER were observed at HT≥900 K. Usually the maximum V concentration was detected below R_p, at a depth of about 280 nm.

HP applied at processing results in the improved crystallographic perfection of Si:V. This is caused, among others, by the effect of HP on diffusivity of V^+ and of implantation-induced point defects.

Our results can be useful for development of the new family of magnetic semiconductors.

References

[1] Misiuk A, Barcz A, Chow L, Surma B, Bak-Misiuk J, Prujszczyk M, Solid State Phen. 2008;131-133:375.
[2] Misiuk A, Barcz A, Chow L, et al., Phys. Tekhn. Vys. Davlenii 2008;18:105.

Tu-4 (Invited)

The effects of He irradiation in manganese implanted silicon

Zbigniew Werner, Jerzy Piekoszewski, Marek Barlak, Cezary Pochrybniak, Katarzyna Bocheńska

Andrzej Soltan Institute for Nuclear Studies, Świerk, 05-400 Otwock, Poland
Institute of Nuclear Chemistry and Technology, Dorodna 16, 03-195 Warszawa, Poland

Silicon samples implanted with 160 keV Mn^+ ions to a dose of 1×10^{16} cm^{-2} were irradiated with 350 keV He^+ ions [1] to doses up to 1.5×10^{18} cm^{-2} at temperatures around 400^0C. The samples were next analysed using channeled RBS technique. The analysis of the RBS spectra reveals that He irradiation leads to a substantial depth reduction of the implantation-induced amorphous layer. The results are analysed in terms of consequences of the revealed process for preparation of spintronic materials.

References

[1] C.H. Chen, H.Niu, H.H.Hsieh, C.Y. Cheng, D.C. Yan C.C.Chi, J.J.Kai, S.C.Wu, Journal of Magnetism and Magnetic Materials 2009;321:1130.

Tu-5

Magnetoresistance in n-Si/SiO_2/Ni nanostructures manufactured by swift heavy ion-induced modification technology

Julia Fedotova[1)], Dmitry Ivanou[2)], Yulia Ivanova[2)], Alexander Fedotov[2)], Alexander Mazanik[2)], Ivan Svito[2)], Eugen Streltsov[2)], Anis Saad[3)], Serguey Tyutyunnikov[4)], Tomasz N. Koltunowicz[5)], Serguey Demyanov[6)], Vera Fedotova[6)]

[1)] *National Center of Particles and High Energy Physics of BSU, Minsk, Belarus*
[2)] *Belarusian State University, Minsk, Belarus*
[3)] *Al-Balqa Applied University, Salt, Jordan*
[4)] *Joint Institute for Nuclear Research, Dubna, Russia*
[5)] *Lublin University of Technology, Lublin, Poland*
[6)] *Scientific-Practical Material Research Centre NAS of Belarus, Minsk, Belarus*

In this work the comparative study of transport and magnetotransport of carriers in garanular Ni films and n-Si/SiO_2/Ni nanostructures with granular Ni nanorods in pores (or NanoRods-In-Pores – NRIPs) has been studied at 2 - 300 K and magnetic fields up to 8 T.

To produce n-Si/SiO_2/Ni nanostructures with Ni NRIPs we used underpotential electro-deposition of Ni nanoparticles into mesapores in SiO_2 layer created on n-Si(100) substrate. To produce latent tracks, SiO_2 layer was irradiated by scanned beams of swift heavy 350 MeV $^{197}Au^{26+}$ ions with fluences of $5 \cdot 10^8$ cm^{-2}. Pores with diameters of 100 - 250 nm and heights about 400 - 500 nm were then formed by chemical etching of the irradiated SiO_2 layer. Mesapores filled with Ni allowed to form a system of NRIPs randomly distributed inside the SiO_2 layer.

Comparison of magnetoresistive (MR) effect in Ni films and n-Si/SiO_2/Ni nanostructures has shown that the last in electric sense are similar to two Si/Ni Schottky diodes switched on oppositely to each other and connected by interfacial n-Si/SiO_2 layer enriched by electrons due to the band bending. So such system display 3 contributions in MR effect: negative anisotropic MR in Ni nanorods (predominating in weak magnetic fields and at temperatures higher 100 K); positive Lorenz-like MR in Ni nanorods and n-Si/SiO_2 interfacial layer (predominating at temperatures lower than 20 K and in high magnetic fields); gigantic positive contribution to MR effect (~1000% at 8 T) at 15 - 40 K due to impurity avalanche mechanism in the n-Si/SiO_2 interfacial layer.

Tu-6 (Invited)

On the damage build-up in ion-irradiated ceramics

Lionel Thomé[1)], *Jacek Jagielski*[2,3)], *Aurélien Debelle*[1)], *Frédérico Garrido*[1)], *Gaël Sattonnay*[4)]

[1)] *Centre de Spectrométrie Nucléaire et de Spectrométrie de Masse, CNRS-IN2P3, Université Paris-Sud, 91405 Orsay, France*
[2)] *Institute of Electronic Materials Technology, Wolczynska 133, 01-919 Warszawa, Poland*
[3)] *The Andrzej Soltan Institute for Nuclear Studies, 05-400 Swierk/Otwock, Poland*
[4)] *LEMHE-ICCMO-Université Paris-Sud, 91405 Orsay, France*

The evaluation of radiation damage in materials placed in a radiative environment is a challenging problem for electronic, space and nuclear industries. Ion beams delivered by various types of accelerators are very efficient tools to simulate the interactions involved during the slowing-down of energetic particles. This work aims at presenting new insight on the damage build-up of crystalline ceramics submitted to either nuclear ballistic collisions or electronic excitation after irradiation with ions of respectively low or high energies. Two specific topics are concerned: (i) the different damage build-ups determined for the two slowing-down regimes of incoming ions (nuclear and electronic); (ii) the nature of the defects created in for the different materials investigated.

RBS/C data show that the damage build-up follows a one-step process for high-energy ion irradiation (>1 MeV/amu) and a multi-step process for low-energy ion irradiation (<10 keV/amu). Results are accounted for in the framework of a model referred to as MSDA (Multi-Step Damage Accumulation). TEM data show that the nature of the defects formed at saturation (i.e. at high fluences) essentially depends on the physico-chemical properties of irradiated crystals, the influence of the slowing-down regime being weak for a given material. A surprising effect is also reported for SiC: the recovery by electronic excitation of the damage created by ballistic collisions.

Tu-7 (Invited)

Effect of grain size on mechanical properties of irradiated mono- and polycrystalline $MgAl_2O_4$

J. Jagielski[1,2], A. Piatkowska[1], P. Aubert[3], S. Labdi[4], O. Maciejak[4], L. Thomé[5], I. Jozwik[1], A. Debelle[5], A. Wajler[1] and M. Boniecki[1]

[1] *Institute of Electronic Materials Technology, Warszawa, Poland*
[2] *The Andrzej Soltan Institute for Nuclear Studies, Swierk/Otwock, Poland*
[3] *Institut d'Electronique Fondamentale, Université Paris-Sud, Orsay, France*
[4] *Université d'Evry-Val d'Essonne, Evry, France*
[5] *Centre de Spectrométrie Nucléaire et de Spectrométrie de Masse CNRS-IN2P3, Université Paris-Sud, Orsay, France*

The influence of the size of crystalline regions on mechanical properties of irradiated oxides has been studied using a magnesium aluminate spinel. The samples of different grain size, varying from sintered $MgAl_2O_4$ ceramics with grains of few micrometers in size up to single crystals, were used in the experiments. The samples were irradiated at room temperature with 320 keV Ar ions up to fluences reaching 5×10^{16} cm^{-2}. Nanomechanical properties (nanohardness and Young's modulus) were measured by using a nanoindentation technique and the resistance to crack formation by measurement of the total crack lengths made by Vickers indenter. The results revealed several effects: correlation of nanohardness evolution with the level of accumulated damage, radiation-induced hardness increase in grain-boundary region and significant improvement of material resistance to crack formation. This last effect is especially surprising as the typical depth of cracks formed by Vickers indenter in unirradiated material exceeds several tens of micrometers, i.e. is more than hundred times larger than the thickness of the modified layer.

Tu-8 (Invited)

Deposition and properties of ultra fast deposited diamond-like hydrogenated carbon films

J.L. Sullivan and S.O. Saied

Surface Science Group, SEAS, Aston University, Aston Triangle, B4 7ET, United Kingdom

The paper describes a novel method for the deposition of hydrogenated diamond like carbon films and the characterisation of the films so produced on a variety of substrates, including silicon (100), glass and plastics. The deposition is by a PECVD process employing acetylene as the precursor gas, with a cascade-arc plasma source and Ar as carrier gas. A major advantage of the method described is that the films are formed at deposition rates orders of magnitude higher than those produced by other methods for films of similar quality. Further advantages are that the films are deposited at very low ion energies and low substrate temperatures. Good homogeneous, adherent films have been grown in the range 20 nm to 1.5 μm, above which delamination from the substrate begins to occur.

The films have been characterized in terms of sp^3 content, surface roughness, hardness, adhesion, and optical properties. Deposition rates up to 20 nm/sec have been achieved at substrate temperatures below 100°C with ion energies less that 1 eV. The typical sp^3 content of 60-75% in the films was determined by a combination of XPS and XAES techniques The hardness and adhesion of the films was measured using a MicroMaterials Nano-Test Indenter/Scratch tester. Hardness was found to vary from 5 to 12 GPa depending on the admixed acetylene flow. Plasma power was found to have an important role in growth rate and area of deposition, whereas the substrate temperature drastically influences the adhesion to the substrate. Optical and thickness measurements on thinner films were made using elipsometry.

The role of plasma surface pre-treatment on film deposition and adhesion is also reported.

Keywords: diamond-like carbon, cascaded arc plasma source, ultra fast PECVD, hardness, adhesion.

Tu-9

Aluminum-doped zinc oxide thin films prepared by sol-gel and RF magnetron sputtering

G.M. Wu, Y.F. Chen and H.C. Lu

Institute of Electro-Optical Engineering, Chang Gung University, Taoyuan 333, Taiwan R.O.C.

Zinc oxide (ZnO) thin films have become technologically important materials due to their wide range of electrical and optical properties. The characteristics can be further adjusted by adequate doping processes, along with their high chemical and mechanical stabilities. This has made doped ZnO thin films with promising applications in solar cells, transparent conductors, gas sensors, transducers, luminescent materials, heat mirrors, and semiconductor heterojunctions. In this paper, aluminium-doped zinc oxide (AZO) thin films have been prepared on glass substrates using a sol-gel route and the radio-frequency (RF) magnetron sputtering process. The stoichiometry could be easily adjusted by controlling the nano-sized precursor concentration and the thickness by dip-coating cycles. On the other hand, the mixed N_2O/Ar plasma gas provided adequate N doping for the RF sputtering process. The results showed the low electrical resisitivity of 21.5 Ω-cm with the carrier concentration of -3.21×10^{18} cm^{-3} for the n-type AZO film. They were 34.2 Ω-cm and $+9.68\times10^{16}$ cm^{-3} for the p-type AZO film. The optical transmittance has been as high as 85-90% in the 400-900 nm wavelength range. The AZO (Al-2 at.%) films exhibited the hexagonal wurzite structure with (002) preferred crystal orientation. The electrical characteristics were depicted by the gradual increase in N and NO that occupying the oxygen vacancies.

Corresponding author: e-mail: wu@mail.cgu.edu.tw

Tu-10

Stopping power and energy straggling of channeled He-ions in GaN

A. Turos[1,2], *R. Ratajczak*[2], *K. Pągowska*[2], *L. Nowicki*[2], *A. Stonert*[2]

[1] *Institute of Electronic Materials Technology, 01-919 Warsaw, Wolczynska 133, Poland*
[2] *Soltan Institute of Nuclear Studies, 05-400 Świerk/Otwock, Poland*

GaN epitaxial layers are usually grown on sapphire substrates. To avoid disastrous effect of the large lattice mismatch a polycrystalline GaN nucleation layer of about 40nm thickness is grown at 500^{o}C followed by the deposition of thick GaN template at much higher temperature. Remnants of the nucleation layer provide a very useful depth marker for the measurement of channeled ions stopping power.

Random and aligned spectra of He ions incident at energies ranging from 1.7 to 4.0 MeV have been measured and evaluated using the Monte Carlo simulation code McChasy. Impact parameter dependent stopping power has been calculated for channeling direction and its parameters have been adjusted according to experimental data. Defects produced by ion implantation largely influence the stopping power. Influence on stopping power of two types of defects: randomly displaced atoms and dislocations were studied.

For channeled ions the variety of possible trajectories leads to different energy loss at a given depth, thus producing much larger energy straggling than that for the random path. Beam energy distributions at different depths were calculated using the McChasy code. They are significantly broader than those predicted by the Bohr formula for random direction.

Tu-11 (Invited)

X-ray diffraction studies of strain distibution in 6H SiC repeatedly implanted with Al ions

Wojciech Wierzchowski[1)], Krzysztof Wieteska[2)], Dariusz Mączka[2)], Marcin Turek[3)], Krzysztof Pyszniak[3)]

[1)] *Institute of Electronis Materials Technology, ul. Wólczyńska 133, 01-919 Warsaw, Poland*
[2)] *Institute of Atomic Energy POLATOM, 05-400 Otwock-Świerk, Poland*
[3)] *Maria Curie-Skłodowska University, Pl. M. Curie-Skłodowskiej 1, 20-031 Lublin, Poland*

The important difficulty in manufacturing of electrically active layers in SiC based semiconductor technology is the implantation of necessary high fluences of doping ions without amorphization. That may be realized only by repeatable implantation combined with the annealing of defects introduced by partial implantation.

In the present case the results of triple subsequent RT implantation with 250 keV Al^+ ions to the fluences of $3\times10^{15}cm^{-2}$ separated by the annealing for 3 hours at 500ºC were examined. The samples cut out from the good quality 6H SiC wafer manufactured by CREE Inc. were studied after each of subsequent operation. The samples were characterized by taking local rocking curves, white beam section and pin-hole topography using synchrotron radiation.

The investigations confirmed that the triple implantation combined with annealing allowed achieving the fluence of $9\times10^{15}cm^{-2}$ without the amorphization of the SiC crystal. After each subsequent implantation a significant increase of lattice parameter was observed which was only reduced but not comlpletely removed after the following annealing process.

The synchrotron investigations were supported by the HASYLAB project II-20060165 EC.

Tu-12

Ion and electron beam induced luminescence of rare earth doped YAG crystals

Grzegorz Gawlik, Jerzy Sarnecki, Iwona Jóźwik, Jacek Jagielski, Marta Pawłowska

Institute of Electronic Materials Technology, Wólczyńska 133, 01-919 Warszawa, Poland

Luminescence of the material may provide useful information about composition and structure of the solid. Visible light emission can be produced under ion beam bombardment of solids as a result of ion collisions with target atoms. Epitaxial YAG layers doped with rare earth ions are widely used for optoelectronic devices. Ion beam induced luminescence (IBIL) may be used as analytical method in wave-guide fabrication in these laser materials by ion implantation. The motivation of this work was investigation of the ion beam induced luminescence of YAG epitaxial layers doped with rare earth (RE) Nd, Tm, Ho, Pr, Tm and Yb in comparison with cathodoluminescence (CL) as alternative characterization technique. IBIL has been excited by 100keV H_2^+ ion beam with ion current density of 0.1μA - 5μA/cm^2. The IBIL signal was detected by fiber-optic mini spectrometer with CCD detector in the wavelength range of 300-1000 nm and spectral resolution of about 1nm. CL spectra of the same samples have been measured using scanning electron microscope (SEM) in the wavelength range of 360-800 nm. Obtained IBIL spectra are reach of details with well separated emission lines. The measured IBIL and CL spectra consist of the same emission lines within registered wavelength range. However, relative ratios of spectral lines excited by IBIL and CL were different. It suggests that IBIL is more effective for excitation of some states than CL. Moreover the IBIL may be carried out in the same target chamber as ion implantation process. Concluding, the IBIL may be useful method for detection of RE elements in the oxide materials and for characterization of the RE doped YAG as a method integrated with ion implantation.

Tu-13 (Invited)

News about the precise numerical value of the em fine structure constant

F. Nickel

GSI Darmstadt, Germany

We had proposed [1] a simple equation for the em fine structure constant α at lowest energies, and could show that our formula has a solid physical background. We only referred to considerations about the so-called running coupling constant discussed in special GUT theories, and on small modifications due to QED-calculations of the so-called ´vacuum polarization´ (VP) in the low-energy regime. This formula reads:

$$\alpha^{-1} = 16\pi \cdot e \cdot Q \, .$$

with

$$\begin{aligned} Q &= 1 + \left(5/4 + \varsigma(4)/\pi^4\right) \cdot \alpha/\pi \\ &= 1 + 1.26111111111 \cdot \alpha/\pi \\ &= 1.002929333 \, . \end{aligned}$$

In this talk it will be shown, that Q can be accurately determined by higher-order QED-calculations of the VP, and by the mass m_e of the electron.

From the above formula the numerical value of α^{-1} is calculated to 137.0359992264....., and has to be compared with the current experimental value α^{-1}_{exp} = 137.03599921(15), deduced from the newest three most-accurate experimental values taken from measurements of the g-factor of the free electron, and the Rydberg-constants of Rb and Cs atoms.

The consequences of our investigations on the numerical values of other fundamental physical constants will be discussed.

References

[1] F. Nickel, talk (see book of abstracts) at the VII-th International Conference ION 2008, Kazimierz Dolny, Poland, June 16, 2008.

Tu-14 (Invited)

Diagnostics of ion-cathode interaction of glow discharges

Z. Wroński, J. Filiks

Institute of Physics, M. Curie-Skłodowska University, 20-031 Lublin, Poland,
e-mail: zdzislaw.wronski@poczta.umcs.lublin.pl

The plasma – cathode interface (P-CI) of glow discharges (GD) is very often used as a source of species deposited on a substrate or studied with the use of optical emission diagnostics owing to its great efficiency of these species production (excited solid atoms) and its simple „technical" structure.

However, the measured physical characteristics of GDP-C interfaces are complex, e.g.:

- the radial distribution of cathode etching efficiency affecting the depth profile $\Delta h = f(r)$ of the cathode surface exposed to plasma, see Fig. 1,
- the space structure of line emission, see Fig. 2, *etc*.

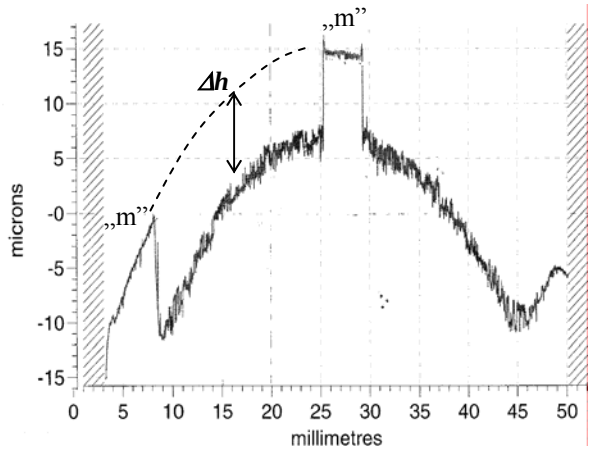

Fig. 1. Depth profile $\Delta h = f(r)$ of the crater etched with the plasma. "m" – traces of masks used for measurement of etched craters depth. O_2/Ni discharge: j_d = 0.5 mA/cm^2, p ~ 0.06 torr, L_{cf} ~ 2 cm, U_{cf} = 1750 V, Δt ~ 24 h[1].

The dependence of the craters depth Δh on the radial position r, where the maximum etching at the cathode edge is observed, is different from the dependence $I_\lambda = f(x, r_n)$ where a maxi-mum line emission of sputtered Ni atom appears at the discharge axis.

[1] j_d – discharge current density, p – gas pressure, L_{cf} – space length of cathode voltage fall U_{cf}, x - distance from cathode, $r_n = r/r_c$ – normalised radius of flat circular cathode, Δt – time of exposition of cathode to plasma, $Q_{p\text{-}p}$ – cross sections of species-species interactions.

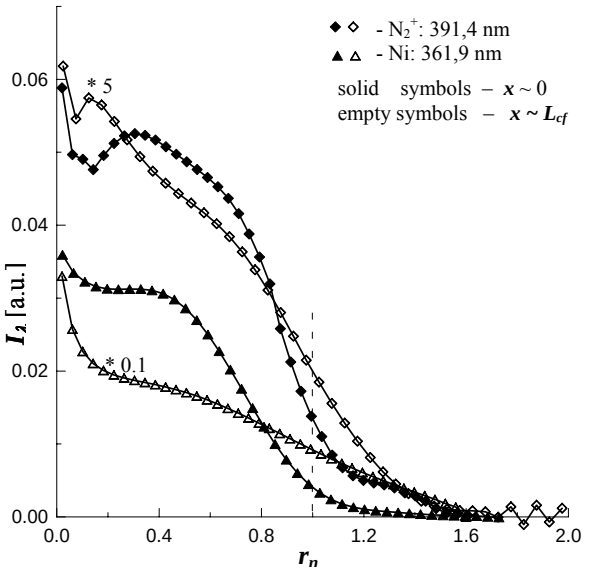

Fig. 2. Space distributions $I_\lambda = f(x, r_n)$ of the emission intensity I_λ of lines N_2: 391.4 nm and Ni: 361.9 nm. N_2/Ni discharge: $j_d = 0.5$ mA/cm^2, $p \sim 0.11$ torr, $L_{cf} \sim 2$ cm, $U_{cf} \sim U_{ac} = 2750$ V. Radius of flat circular cathode $r_c = 2.4$ cm[1].

The numerical modelling, assuming the parameters $(p, j_d, U_{ac}, L_{cf}, Q_{p\text{-}p}$[1]$)$ as fundamental and important data, allows initially to assess the angle-energy spectra $F(\varepsilon,\alpha)$ of particles bombarding the cathode surfaces as well as electrons exciting in the plasma and finally to asses the space distribution $n_s(x, r)$ of the sputtered species as well as to the explain above discussed problems. This modelling explains also high intensities of the lines emitted by the sputtered sputtered atoms as well as by the fast atoms O and N and their dependence on the discharge parameters (j_d, p).

We-1

RBS\channeling and TEM study of damage buildup in ion bombarded III-N compounds

K. Pągowska[1)], R. Ratajczak[1)], A. Stonert[1)], A. Turos[1,2)], L. Nowicki[1)] and A. Muecklich[3)]

[1)] *Soltan Institute for Nuclear Studies, 05-400 Świerk/Otwock, Poland*
[2)] *Institute of Electronic Materials Technology, 01-919 Warszawa, Wólczyńska 133, Poland*
[3)] *Forschungszentrum Dresden-Rossendorf, POB 510119, D-01314 Dresden, Germany*

Structural defect buildup in 320 keV Ar-ion bombarded $Al_xGa_{1-x}N$ ($0 \le x \le 1$) epitaxial layers has been reported. Ion fluences ranged from $5x10^{12}$ to $1x10^{17}$ at/cm^2. 1μm thick epitaxial layers were grown on sapphire substrates using the MOVPE technique. RBS\channeling with 1.7 MeV ^{4}He beam was applied for analysis. As a complementary method Transmission Electron Microscopy (TEM) has been used. The later has revealed the presence of extended defects like dislocations and loops. New version of the Monte Carlo simulation code McChasy has been developed that makes it possible to analyze such defects on the basis of the bent channel model. Accumulation curves for two distinct types of defects, i.e. randomly displaced atoms and extended defects have been determined. They were evaluated in the frame of the multistep MSDA model, allowing numerical parameterization of defect transformations occurring upon ion bombardment. Displaced atoms buildup is a three step process for GaN and $Al_{0.1}Ga_{0.9}N$ whereas for $Al_{0.44}Ga_{0.56}N$ and AlN it is a two step process. Extended defect buildup is always a two step process.

We-2

Application of electron beam radiation to modify crosslink structure in rubber vulcanizates and its tribological consequences

Aneta Stępkowska[1)], *Grażyna Przybytniak*[2)], *Dariusz M. Bieliński*[1,3)]

[1)] *Institute for Engineering of Polymer Materials & Dyes, Division of Elastomers & Rubber Technology, Harcerska 30, 05-820 Piastów, Poland*
[2)] *Institute of Nuclear Chemistry & Technogy, Dorodna 16, 03-195 Warszawa, Poland*
[3)] *Institute of Polymer & Dye Technology, Technical University of Łózź Stefanowskiego 12/16, 90-924 Łódź, Poland*

The aim of this work was the modification of crosslink density and structure of rubber vulcanizates in order to control surface energy, mechanical strength under static as well as dynamic conditions and in the consequence tribological properties of the materials. Sulphur vulcanizates of isoprene (IR) and styrene-butadiene rubber (SBR), filled with carbon black, were subjected to electron beam radiation in the range from 50 to 250 kGy. Changes to crosslink density and structure were determined applying the method of selective swelling of rubber in "hard" and "soft" solvents. The modification influences the ability of material to energy dissipation and its surface wettability. The changes are discussed from the friction and abrasion of rubber point of view.

Keywords: rubber, EB radiation, modification, friction and wear

We-3

Application of the ion implantation for the synthesis and modification of the (Ga,Mn)As ferromagnetic semiconductors

O. Yastrubchak[1)*], *H. Krzyżanowska*[1)], *M. Kulik*[1)], *K. Pyszniak*[1)], *A. Drożdziel*[1)], *J. Żuk*[1)], *J.Z. Domagała, R. Szymczak, T. Andrearczyk*[2)], *J. Sadowski*[2,3)] *and T. Wosiński*[2)]

[1)] *UMCS, Institute of Physics, Pl. Marii Curie-Skłodowskiej 1, 20-031 Lublin, Poland*
[2)] *Institute of Physics, Polish Academy of Sciences, 02-668 Warszawa, Poland*
[3)] *MAX-Lab, Lund University, 22100 Lund, Sweden*

Ferromagnetic semiconductors (FMS), such as the thoroughly investigated (Ga,Mn)As, are especially promising as the materials for spintronics since they interrelate both semiconducting and magnetic properties. Extensive research activity aimed at clarifying structural features of thin (Ga,Mn)As films grown at low temperature (LT, 230°C) on GaAs substrates caused significant progress in the improving their magnetotransport properties and the increasing of the Curie temperature(T_C). Nevertheless, the nature of the conducting carriers mediating the ferromagnetic state in the (Ga,Mn)As material is not clear so far as well as was not observed the ferromagnetism at the room temperature. The resolution of this issue is needed for the in-depth understanding of carrier-mediated ferromagnetism in this prototypical III-V feromagnet and also for assessment of its potential for spintronic device concepts.

In this work we have employed the complementary characterization techniques such as photoreflectance spectroscopy, micro-Raman spectroscopy, high resolution X-ray diffractometry (XRD) and superconducting quantum interference device (SQUID) magnetometery to study the fundamental properties of (Ga,Mn)As thin films with diverse Mn doping level (x = 0%, 1% and 6%) such as T_C, hole density (p) and hole effective masses. The PR measurement yields the direct observation of the electronic transitions for the Γ point (E_0) in (Ga,Mn)As.

A number of complementary characterisation techniques have been used with the aim to study an effect of ion implantation on (Ga,Mn)As thin film properties. It was revealed that the implantation with a low fluence of either O or Ne or He ions suppressed the conductivity and ferromagnetism in the films. Both the high resolution X-ray diffraction technique and the Raman spectroscopy showed significant changes in the structural and optical properties of the films caused by ion implantation. A mechanism responsible for ion-implantation-induced suppression of the conductivity and ferromagnetism in (Ga,Mn)As layers, which could be applied as a method for tailoring nanostructures in the layers, is discussed. Contrary to this the incorporation of transition metal such as Mn into the GaAs host exhibits ferromagnetism at room temperature and opens the possibility of applications in spin-dependent semiconductor-magnetic hybrid devices. The micro-Raman scattering have been used to study the evolution of the host lattice recrystallization in Mn+-implanted GaAs depending on the annealing temperature. The topography of the samples surface was probed by the

* *E-mail: yastrub@hektor.umcs.lublin.pl*

atomic force microscopy (AFM). Magnetic Force Microscopy (MFM) and SQUID was used for revealing of the magnetism in the implanted samples.

Dr Oksana Yastrubchak acknowledges financial support by the Polish Ministry of Science and Higher Education (MSHE) under Grant POL-POSTDOC III, N PBZ/MNiSW/07/2006/33.

Identification of painting layers of Sennefer Tomb by ion beam analysis

Shaaban Abd El Aal

Conservation Dept, Faculty of Archaeology, Fayoum University, Egypt, smm00@fayoum.edu.eg

Egypt has many pharaonic tombs for kings, queens and noblemen. Sennefer tomb is one of the most important noblemen tombs, which is located in the southern hillside of Sheikh Abd El – Qurna- west side of Loxor .It is dated back to 1439-1413BC (18th Dynasty) and is usually referred as the Tomb of Vines; due to the large part of the ceiling of the burial chamber. The vine tomb was carved inside a mountain, its walls are covered with plaster and have been painted using the tempera technique (pigments mixed with organic binding medium).

The analysis was performed by using PIXE, μPIXE and optical microscope [1] for red, yellow, grey and blue pigments and for ground layers of the tomb in order to identify the composition of plaster layers and pigments. These data about the nature of these materials are indispensable for conservation and cleaning [2].

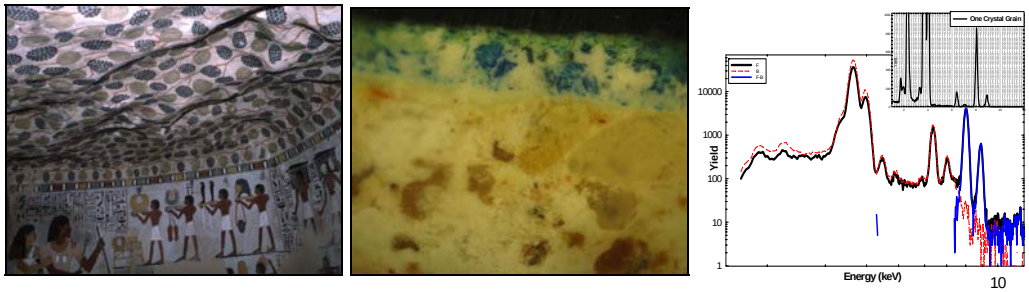

Fig. 1. PIXE,μPIXE and LOM Spectra of The tomb of Vines.

References

[1] Shaaban A, Turos A, Korman A, Stonert A, Munnik F, Ion beam analysis of ancient Egyptian wall paintings; Vacuum 2009; 83: s4-s8.

[2] Nicholson P, Shaw I, Ancient Egyptian Materials and Technology 2000; Cambridge University Press.

Wear-out phenomena in Si-based light emitting devices with ion beam implanted europium

J. Lehmann[*] *, L. Rebohle, A. Kanjilal, M. Voelskow, M. Helm, W. Skorupa*

Institute of Ion-Beam Physics and Materials Research (FWI), Research Center Dresden-Rossendorf (FZD), Dresden, Germany

Recently, efficient electroluminescence (EL) from UV to IR could be obtained by implanting lanthanides into the oxide layer of metal-oxide semiconductor (MOS) structures [1]. With these electrically driven Si-based light emitting devices (MOSLEDs) an integrated biosensor can be built for the detection of organic molecules like estrogene [2]. For this purpose, the intensity and stability of the EL are critical properties of the light emitters. Usually, lanthanide implanted MOSLEDs show a quenching of the EL-signal with time. However, Eu-implanted MOSLEDs can show a rise of the EL-signal during the operation time of the device [3]. For this reason, Eu-implanted MOSLEDs offer the possibility to build devices with an extremely stable EL-emission if the occurring processes can be better understood. Therefore, an intensive investigation was performed on Eu-implanted MOSLEDs exposed to different annealing temperatures and times. Transmission electron microscopy (TEM) and Rutherford backscattering spectroscopy (RBS) were used to trace the growth of Eu / Eu oxide clusters and the diffusion of Eu to the interfaces of the gate oxide layer, respectively. Resonant nuclear reaction analysis (rNRA) was used to measure the hydrogen depth profile, while current-voltage characteristics, the EL decay times and the evolution of the voltage as well as the EL were studied under constant current injection to reveal details of the wear-out mechanism. Correlating the microstructural, the electrical and the EL properties, a qualitative model for the anomalous wear-out phenomenon is proposed.

References

[1] L. Rebohle and W. Skorupa, Materials Science Forum 590, 117 (2008).
[2] C. Cherkouk, et al. Journal of Colloid and Interface Science 337, 375 (2009)
[3] S. Tyagulskiy, et al. Microelectronic Engineering, 86, 1954 (2009)

[*] Corresponding author, Address: Institute of Ion-Beam Physics and Materials Research (FWI), Research Center Dresden-Rossendorf, Bautzner Landstraße 400, 01328 Dresden, Germany.
Tel.: +49 351 2602912.
E-Mail address: j.lehmann@fzd.de

Reactive ion etching (RIE) of 4H-SiC in fluorinated plasma for device fabrication

Mariusz Sochacki[1)], *Norbert Kwietniewski*[1)], *Jan Szmidt*[1)], *Paweł Kowalczyk*[2)]

[1)] *Warsaw University of Technology, Koszykowa 75, 00-662 Warszawa, Poland*
[2)] *University of Łódź, Pomorska 149/153, 90-236 Łódź*

Reactive ion etching (RIE) of 4H-SiC in fluorinated plasma (CF_4 and SF_6 with oxygen addition) has been investigated. The influence of process parameters on etching rate and roughness was examined. The most satisfying results taking into account both factors were achieved for SF_6/O_2 plasma. The rms surface roughness measured by AFM technique for 2 μm x 2 μm area is smaller than 2 nm and 20 nm for etching rate of 40-70 nm/min and 150 nm/min, respectively. The oxygen addition and SF_6/O_2 flow ratio have defined the surface roughness. The etching rate depends strongly on working pressure for SF_6/O_2 mixture.

The resistance of SiO_2/Cr layers and S1818 fotoresist films against etching agents was analyzed. The stoichiometry and surface chemical bonds have been investigated after etching process by Auger Electron Spectroscopy (AES) and X-ray Photoelectron Spectroscopy (XPS). The AES and XPS spectra analysis confirmed the surface graphitization, C=O bonds and flour compounds on the surface leading to modification of silicon carbide electronic properties.

Acknowledgement

The work was funded under Polish Ministry of Science and Higher Education silicon carbide programme as grant no. PBZ-MEiN-6/2/2006.

We-7

Optical and microstructural properties of In(As,N) quantum structure made by ion implantation and flash lamp processing

S. Prucnal[1,2], M. Turek[1], A. Droździel[1], K. Pyszniak[1], A. Wójtowicz[1], A. Kanjilal[2], A. Shalimov[2], W. Skorupa[2] and J. Żuk[1]

[1] *Maria Curie-Skłodowska University, Pl. M. Curie-Sklodowskiej 1, 20-035 Lublin, Poland*
[2] *Institute of Ion Beam Physics and Materials Research, Forschungszentrum Dresden-Rossendorf, P.O. Box 510119, 01314 Dresden, Germany*

The In(As, N) quantum structures were formed in silicon, SiO_2 and Si_3N_4 films by sequential ion implantation and subsequent thermal annealing. Samples were characterized by μ-Raman spectroscopy, Rutherford backscattering spectrometry (RBS), low temperature photoluminescence (PL), high resolution transmission electron microscopy (HRTEM) and X-ray diffraction (XRD). Two kinds of crystalline InAs nanostructures were successfully synthesized: quantum dots (QDs) and nanopyramides (NPs). The Raman spectrum shows two peaks at 215 and 235 cm^{-1} corresponding to the transverse optical (TO) and longitudinal optical (LO) InAs phonon modes, respectively. The narrow PL band at around 1.3 μm from the InAs QDs with an average diameter 7.5 ± 0.5 nm was observed.

The InAs NPs were found only in samples annealed for 20 ms at temperature range from 1000 up to 1200 ^oC. The crystallinity and pyramidal shape of InAs quantum structures were confirmed by high resolution transmission electron microscopy (HRTEM) (see Fig. 1) and X-ray diffraction (XRD). The average size of the NPs is 50 nm base and 50 nm high and they are oriented parallel to the Si (001) planes. The InAs nanopyramids grow in silicon due to liquid phase epitaxy. The InN crystals are formed on the top of silicon nitride layer due to outdiffusion of indium and in Si_3N_4 film. The PL measurements shows narrow band at around 1.35 μm originated from hexagonal InN nanocrystals due to quantum confinement size effect. μ-Raman scattering study shows two peaks at 495 and 588 cm^{-1}, which correspond to (TO) of E_2^h and (LO) of A_1 phonon modes, respectively.

We-1P

Effect of ion doping on optical properties of multilayered *nc*-Si/high-*k*-oxide structures

Ivan A. Chugrov, Alexey V. Ershov, Andrew A. Ershov, Alexey N. Mikhaylov and David I. Tetelbaum

N.I. Lobachevski State University of Nizhny Novgorod, 23/3 Gagarin prospect, 603950 Nizhny Novgorod, Russia

Current investigations of silicon nanocrystal (NC) are focused on the preparation of ensembles of Si quantum dots in SiO_2 host. An original method was established based on the preparation of *a*-SiO/SiO_2 superlattices which enables independent control of size, size distribution, position and density of the NCs. On the other hand, the decrease in device dimensions leads to the need for alternative, high dielectric constant (*k*) oxides to replace SiO_2 as the gate dielectric in CMOS devices.

In our report the results of investigations of photoluminescence (PL), Raman scattering and FTIR-spectra of the *a*-Si(*a*-SiO_x)/high-*k*-oxide (ZrO_2 or Al_2O_3) multilayered (up to 70 layers) nanoperiodic (period of 5-20 nm) structures (MNSs) prepared by vacuum evaporation are discussed. The high-temperature annealing (HTA) at 1000-1100 °C results in formation of Si NCs with sizes 3-5 nm. Raman scattering of the annealed MNSs gives evidence that sizes of Si NCs, which are responsible for visible PL band, depend on thickness of the silicon-contained layer. In comparison with PL of NC in the Si/SiO_2 MNSs prepared at same conditions, PL intensity was 10-50 times smaller. The influence of kind of oxide layer material on MNS PL intensity and spectrum is discussed from the view point of chemical interactions which lead to the formation of intermediate silicate layers at heteroboundaries of the nanostructure.

Implantation of boron and phosphorus ions and followed HTA results in quenching or enhancement of different PL bands. Post-hydrogenation gives rise to enhancement of PL band (~500 nm) caused by radiative defects and/or small Si NCs, and of 750-850 nm band associated with (3-5 nm)-NCs of Si, as well.

Support through the Federal Targeted Programme “Scientific and pedagogical cadres of innovative Russia”, grant of the RF President (MK-185.2009.2) and RFBR project (10-02-00995) is gratefully acknowledged.

Ion-beam synthesis and modification of light-emitting silicon and silicon-carbon nanoclusters in oxide layers

Alexey Mikhaylov, Alexey Belov, Alexey Kostyuk, Alexey Ershov, Oleg Gorshkov, David Tetelbaum

Physico-Technical Research Institute of N.I. Lobachevski State University of Nizhny Novgorod, 23/3 Gagarin prospect, 603950 Nizhny Novgorod, Russia

New applications of silicon as optoelectronic material initiate numerous investigations of Si-based nanostructures. Quantum confinement of carriers in Si nanocrystals embedded into a wide-band matrix provides size-dependent luminescence at room temperature in a broad spectral range of 500-1000 nm, as well as robust charge storage. Such nanostructures are promising candidates for new-generation light emitters, non-volatile memory, solar cells, etc. Successful application of these new materials requires detailed information on optimal conditions of fabrication, peculiarities of structure and composition of both the matrix and the nanocrystals and their interfaces. In the present report, original results of comprehensive investigation of optical properties, structure and phase composition are generalized for a set of combinations of the oxide matrices (SiO_2, Al_2O_3 and ZrO_2) and the ion-synthesized nanoclusters (nc-Si, nc-Si_xC_y).

In order to form Si nanocrystals, the oxide layers were implanted with Si^+ ions to the peak concentrations of 5-30 at.% and annealed at 700-1100 °C. Carbon-rich nanoclusters were grown by annealing of Si^+ and C^+ co-implanted SiO_2 films or C^+-implanted deposited SiO_x films. Ion doping with shallow impurities and annealing in controllable oxygen-containing atmosphere were used to modify the synthesized nanoclusters ensembles that emit light in a wide visible/near-IR spectral range. The main factors that determine possibility of nanoclusters synthesis and control of their luminescence were found. The most important of them include chemical interaction between the implanted atoms and the host matrix atoms, mechanical stresses at the interfaces and their relaxation. Some electro-optical properties were demonstrated in the ITO/oxide:nc-Si/Si diode structures.

Support through the Federal Targeted Programme “Scientific and pedagogical cadres of innovative Russia”, grant of the RF President (MK-185.2009.2) and RFBR project (10-02-00995) is gratefully acknowledged.

We-3P

Defect transformations in ion bombarded InGaAsP

R. Ratajczak[1)], A. Turos[1,2)], A. Stonert[1)], L. Nowicki[1)]

[1)] Sołtan Institute of Nuclear Studies, 05-400 Świerk/Otwock, Poland
[2)] Institute of Electronic Materials Technology, 01-919 Warszawa, Wólczyńska 133, Poland

Damage buildup and defect transformations at temperatures ranging from 18K (LT) to 300K (RT) in ion bombarded $In_xGa_{1\_x}As_yP_{1\_y}$ ($0<x,y<1$) epitaxial layers on InP were studied by in situ RBS/channeling measurements using 1.4 MeV ^{4}He ions. Ion bombardment was performed using 150 keV N ions and 580 keV As ions to fluences ranging from 5×10^{12} to 6×10^{14} at/cm^2. Damage distributions were determined using the McChasy Monte Carlo simulation code assuming that they consist of randomly displaced lattice atoms. Steep damage buildup up to amorphisation with increasing ion fluence was observed. Defect production rate increases with the ion mass and decreases with the implantation temperature. Parameters of damage buildup were evaluated in the frame of the Multi-Step Damage Accumulation model. Following ion bombardment at LT defect transformations upon warming up to RT have also been studied. Defect migration beginning at 100K was revealed leading to a broad defect recovery stage.

Formation of H-donors and radiation defects in proton implanted SiGe

Viktor Tsvyrko, Yury Pokotilo, Alexander Kamyshan

Belorussian State University, Nezavisimosty av. 4, Minsk, Belarus

Schottky diodes on the base of pure silicon and $Si_{1-x}Ge_x$ (x=1,4-5,5 %) were implanted by 300 keV protons a dose of 1×10^{15} cm^{-2} to form hydrogen donors (H-donors). It is established, that the conditions of thermal treatment for formation of H-donors in SiGe coincide with a conditions of thermal treatment in Si. From Fig. 1 it is visible, that concentration of H-donors changes with change of germanium content in SiGe alloy not monotonously. The concentration of H-donors in SiGe is lower in 5-10 times, than in the pure silicon irradiated with the same dose of protons. Taking into account dependence of concentration of H-donors from Ge content in an alloy and that the concentration of H-donors in an alloy is much less, than in pure Si, it is possible to assume, that there is a sink for hydrogen atoms. Presence of a sink can substantially decrease concentration of H-donors and cause effect of not monotonous dependence of concentration of H-donors from Ge content in an alloy. Possibly, atoms Ge incused by proton irradiation or radiation defects (RD) is the sink for hydrogen atoms.

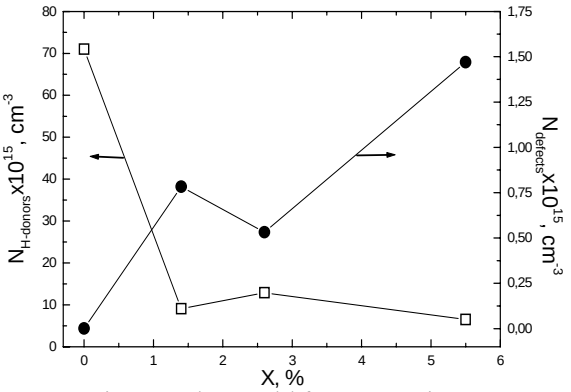

Figure 1: H-donors and defects concentration in Si (x=0%) and SiGe alloys.

With change of Ge fraction in SiGe concentration of H-donors and RD increases, passes over maximum and falls. Thus, in SiGe and Si correlation of properties of H-donors and RD is observed which shows some influence of RD concentration and Ge content in an alloy on H-donors concentration.

It is suppose, that H-donors is extended polyatomic interstitial-related clusters [1, 2], essential factor for which formation are RD. It is obvious, in SiGe in comparison with Si it is possible to explain high content of RD by absence of passivation of RD by hydrogen because of an additional sink of hydrogen atoms on atoms Ge. In this connection it is possible to suppose, that an impurity of germanium in SiGe alloys substantively decreases efficiency of H-donors formation, but RD is a catalyst for formation of H-donors.

References

[1] Abdullin, Kh.A. Mater. Sci. in Semicond. Proc. 2004; 7: 447.
[2] Abdullin, Kh.A. Physica B 2003; 340-342: 692.

Th-1 (Invited)

Nanocrystal- and dislocation-related luminescence in (As+In) implanted Si

F. Komarov[1)], L. Vlasukova[1)], O. Milchanin[1)], J. Żuk[2)], A. Mudryi[3)], K. Pyszniak[2)], M. Kulik[2)]

[1)] *Belarusian State University, Nezavisimosti ave. 4, 220030 Minsk, Belarus*
[2)] *Maria Curie-Skłodowska University, pl. M.Curie-Skłodowskiej 1, 20-031 Lublin, Poland*
[3)] *Scientific and Practical Materials Research Center, National Academy of Sciences of Belarus, P. Brovki str. 17, 220072 Minsk, Belarus*

A silicon based optoelectronics progress is restrained because of the absence of effective light source – light emitting diode or laser. The main problem is the indirect band gap nature of silicon, resulting in inefficient light emission. A number of approaches to overcome this problem were reported including the synthesis of A^3B^5 quantum dots [1], or the intentional formation of structural defects [2] in Si matrix. In this work, we present the results of structural and optical characterizations of Si layers with InAs nanocrystals ion-beam synthesized in Si. (100) Si wafers were implanted at 25 and 500 °C subsequently with As (245 keV, 4.1×10^{16} cm^{-2}) and In ions (350 keV, 3.7×10^{16} cm^{-2}). Part of the samples was additionally exposed to H_2^+ ions (100 keV, 1.2×10^{16} cm^{-2} in terms of atomic hydrogen). This procedure was performed to obtain an internal getter. Afterwards, the samples were annealed at 600, 900 and 1050 °C in an inert ambient using RTA. The depth distributions of embedded impurities and the structure-phase transformations within the implanted layers were evaluated by means of RBS/C and TEM/TED technique. The optical properties of samples have been characterized using low-temperature photoluminescence (PL). It has been shown that an annealing of samples at 950 °C results in Pl spectra with dominant dislocation-related lines [2]. An increase of annealing temperature up to 1050 °C results in the appearance of a broad band in an energy range of 0.75–1.1 eV. This feature is ascribed to the InAs nanocrystals formation [1]. An additional low intensive dislocation-related peak at 0.8 eV appears in PL spectra of the samples with getter annealed at 1050 °C. Ion-implantation induced formation and evolution of nanocrystals and crystal defects in silicon as a function of annealing parameters have been discussed.

References

[1] Komarov F, Vlasukova L, Wesch W *et al*, Nucl. Instr. and Meth. 2008; B.266: 3557.
[2] Sobolev N, Emel'yanov A, Shek E *et al*, J. Luminescence 2002;B91-92:167.

Th-2 (Invited)

Advances in Si & Ge millisecond processing: From silicon-on-insulator to superconducting Ge

W. Skorupa[1)], C. Wündisch[1)], M. Posselt[1)], V. Heera[1)], T. Herrmannsdörfer[1)], D. Buca[2)], S. Mantl[2)], S. Haeberlein[3)], R. Fendler[3)], Thoralf Gebel[4)]

[1)] *Institute of Ion Beam Physics & Materials Research, Forschungszentrum Dresden-Rossendorf, POB 510119, Dresden, Germany*
[2)] *Institute of Bio-and Nanosystems, Forschungszentrum Jülich, Jülich, Germany*
[3)] *FHR GmbH, Ottendorf-Okrilla, Germany*
[4)] *DTF Technology GmbH i.G., Dresden, Germany*

Recently we could demonstrate that advanced SOI material can be treated in advantageous manner regarding USJ formation [1]. Especially, strained Si and SiGe/Si heterostructures on insulator are promising channel materials for future nanoelectronics devices. Their successful integration into new device architectures depends on the ability of forming ultra shallow and ultra steep junctions. We present results for dopant activation in SOI, sSOI, HOI and sHOI [2]. FLA allows complete suppression of diffusion while obtaining sheet resistances lower than 500 Ω/□ in both, SOI and sSOI. Strained and unstrained SiGe heterostructures indicated significant diffusional broadening of Sb implant profiles and low electrical activation. In contrast, B shows higher activation but significant dopant loss in the near surface region. Moreover, we demonstrate that, after diamond and silicon, the third elemental group-IV semiconductor, germanium, exhibits superconductivity at ambient pressure [3]. For the first time, techniques of the state-of-the-art semiconductor processing as ion implantation and FLA were used to fabricate such material, i.e. a highly Ga-doped Ge (Ge:Ga) layer in near-intrinsic Ge. It is shown that superconductivity can be generated and tailored in the Ge host at temperatures as high as 0.5 K. Results of critical-field measurements demonstrate the quasi-two-dimensional character of superconductivity in the 60 nm thick Ge:Ga layer.

References

[1] F. Lanzerath, D. Buca, H. Trinkaus, M. Goryll, S. Mantl, J. Knoch, U. Breuer, W. Skorupa, B. Ghyselen, J. Appl. Phys. 104 (2008), 044908

[2] R. A. Minamisava, W. Heiermann, D. Buca, H. Trinkaus, J. Hartmann, W. Skorupa, U. Breuer, B. Ghyselen, S. Mantl, Proc. 215th ECS Meeting, Vol. 19, Issue 1, May 24-29, 2009

[3] T. Herrmannsdörfer, V. Heera, O. Ignatchik, M. Uhlarz, A. Mücklich, M. Posselt, H. Reuther, B. Schmidt, K.-H. Heinig, W, . Skorupa, M. Voelskow, C. Wündisch, R. Skrotzki, M. Helm, J. Wosnitza, Phys. Rev. Lett., 102 (2009) 217003, Supercond. Sc. & Techn., 23 (2010) 034007

Th-3

Diagnostics of high intensity pulsed plasma beams by ex-post analysis of morphology of the irradiated silicon surface

Barbara Nycz[1)], Marek Barlak[1,2)], Jerzy Piekoszewski[1,2)], Bożena Sartowska[2)], Cezary Pochrybniak[1,3)], Katarzyna Bocheńska[1)]

[1)] The Andrzej Sołtan for Nuclear Studies, 05-400 Otwock-Świerk, Poland
[2)] Institute of Nuclear Chemistry and Technology, Dorodna 16, 03-195 Warszawa, Poland
[3)] Institute of Atomic Energy POLATOM, 05-400 Otwock-Świerk, Poland

Pulse of energy deposited on the surface of solid is immediately (10^{-12} s) transformed into heat. At sufficiently short (20 ns-1.0 μs) and intense (10^6-10^8 W/cm^2) pulse, the near surface layer (of 0.1-2.0 μm) of the solid can reach a temperature of melting point or above. After rapid (10^6-10^8 k/s) quenching and solidification the top layer is modified as compare to its initial state The pulse can be delivered by: laser, electron, ion or plasma beams. The diagnostic of the plasma beams is especially difficult since plasma in the diagnosed region behaves as a very good electrically conductive fluid. Analysis of the "as pulsed" surface may be helpful since rapid melting and solidification of the surface layer results in creation of variety of morphological features: cracks, ripples, rims, craters and so on. In the present work the set of mono and polycrystalline silicon samples were irradiated by argon plasma pulses of energy densities between 2 to 5 J/cm^2. The irradiated samples were analyzed with respect to the surface roughness and the dependence of the deepest craters as function of an energy pulse density was determined. These results were compared with the values of the melting depth calculated for energy density used in experiment for various pulse durations using the ETLIT package program.

The main results are:

1) Pulse duration increases with an increase of energy density.
2) For the energy range 2 to 5 J/cm^2 the maximum pulse durations expressed as FWHM are in the range 0.1-0.7 μs.

Th-4 (Invited)

Hydrogen and helium implantation in germanium for semiconductor layer transfer applications

R. Hurley, P. Rainey, Y.W. Low, P. Baine, D.W. McNeill, S.J.N. Mitchell, H.S. Gamble and B.M. Armstrong

Northern Ireland Semiconductor Research Centre, The Queen's University of Belfast, Ashby Building, Stranmillis Road, Belfast UK BT9 5AH.

The development of germanium on insulator technology (GOI) for high performance CMOS and other specialised applications is discussed. The technique of ion-cut using ion implantation is described and the results of measurements made on devices. The results suggest that implantation species and conditions of implantation have an effect on electrical device performance and can lead to the creation of acceptor states extending significantly below the the implant depth (measured after annealing out of damage). These have been investigated using resistance spreading measurements and Raman spectroscopy whilst surface profiling measurements have been used to identify the effect of helium co-implanted with hydrogen on the activation energies for surface blistering.

Th-5

Estrogen detection in waterish solutions by silicon based light emitters

C. Cherkouk, L. Rebohle, W. Skorupa, M. Helm

FZD-Forschungszentrum Rossendorf-Dresden, Bautzner Landstrasse 400, D-01314 Dresden, Germany, e-mail: c.cherkouk@fzd.de

The immediate and accurate monitoring of chemical and biological substances is essential in environmental analysis for minimizing the health risk for citizens and their exposure to pollutants. Recently, considerable attention has been focused on endocrine-disrupting compounds (EDCs), such as estrogens, which constitute a wide group of environmental pollutants, especially in drinking water.

A new concept for measuring the concentration of such organic compounds by using Si-based, integrated light sources for fluorescence analysis is presented. In that concept the analyte, estrogen in this example, is labelled with a fluorescence marker and is immobilized at the passivated surface of the light emitter by receptor molecules.

The ion beam technology is one of the most essential steps of the light emitter fabrication. The integrated light emitters are based on a metal-oxide-semiconductor (MOS) structure. This oxide layer is implanted with Ge or rare earth ions (Gd and Tb) followed by annealing and SiON deposition. Depending on the implanted element there is a broad palette of MOS devices emitting light from the UV up to the red spectral region. The combination between Si-based integrated light emitter and this kind of biosensing opens a way to extremely small device dimensions and is of great interest for point-of-care measurements.

The current system was investigated Fourier-Transform infrared spectroscopy (FTIR), x-ray-photoelectron spectroscopy, photoluminescence (PL) and electroluminescence (EL) measurements.

Space structure and fluctuation of electromagnetic cascades produced by 100-3500 MeV gamma quanta in heavy amorphous media

B. Słowiński[1)], *P. Duda*[2)], *P. Hładki*[2)]

[1)] *Institute of Atomic Energy POLATOM, Otwock-Świerk, Poland*
[2)] *Faculty of Physics, Warsaw University of Technology, Warsaawa, Poland*

In actual practice the longitudinal distributions of energy deposition or profiles, *(-dE/dt),* of the electromagnetic cascades (ECs or showers) initiated in dense amorphous materials are usually approximated by a gamma function (for example, [1]). Nevertheless, such a simple model is not too good, especially at an increasing depth t and at the very beginning of the cascade [1]. Therefore, a thorough analysis of EC created in most popular media (liquid xenon, PWO, $CdWO_4$, GaAs, NaI, Pb, lead glass and BGO) by gamma quanta (GQ) of energy E_γ =100÷3500 MeV has been performed with the help of extended version of EGS4 package [2]. The goal of the work was to describe both average longitudinal (LP) and transverse (TP) profiles of ECs, as well as the corresponding fluctuation in a unified way, i.e. using the approximating function:

$$\left(-dE/dt\right) = \alpha_t \left(t - \varepsilon_t\right)^{\beta_t} \exp\left(-\gamma_t t^{\delta_t}\right) \tag{1}$$

for LP and longitudinal fluctuation. Here α_t, β_t, δ_t, γ_t, ε_t are the fit parameters depending on cut-off energy $E_{c.o.}$ of cascade particles and material properties. They are determined as a result of statistic approximation to calculated data. Next, the relationship between the values of parameters β_t, δ_t, γ_t and ε_t, and the initial GQ energy and media properties was investigated [3, 4]. To characterize different media the so-called material coefficient W was defined as $W=(A/Z)\rho$, where A is the mean mass number of components of the material, Z is the mean atomic number of its elements, ρ – material density. Similarly, the transverse cascade's profiles and relevant fluctuation have been described with the help of approximating function:

$$\left(-dE/dt\right) = \alpha_r \exp\left(-\gamma_r t^{\delta_r}\right), \tag{2}$$

where α_r, γ_r and δ_r are, as above, functions of the cut-off energy ($E_{c.o}$) and material properties. These functions were determined by means of statistic fitting to modeled data.

The modeling has been performed for $E_{c.o}$=1.2 MeV as commonly used in experimental practice. The results of modeling were examined using ROOT programming environment.

Two ways of analytical description of shower fluctuation were used [1]. One of them is to count the value of standard deviation of the mean energy deposited to a given distance t from the point, where a shower was initiated (also called a shower depth). The other is the distribution of the shower depth, up to which an amount of energy exceeding the so-called threshold energy (TE) was deposited. Three values of TE were considered: 50%, 70% and 90% of the total shower energy E_γ. The same approach is applied when analyzing TPs, but instead of shower depth, a distance from the shower axis (also called a shower radius) was used.

The performed analysis has led to conclusion that function (1) turned out to be a very good fit to all modeled longitudinal distributions, both average and relevant fluctuation. Nevertheless, a problem appeared that even at large enough statistics of modeled events there is no clear and simple relationships between fit parameters and the initial energy E_γ or material coefficient W at different threshold energy deposition. The same conclusion holds for TPs and formula (2). In the case of LPs a simple power relationship between fit parameters p (i.e. β_t and γ_t) and initial energy E_γ

$$p = aE_\gamma^b + c \tag{3}$$

and a logarithmic dependence for TPs parameters

$$p = a \ln E_\gamma + b \tag{4}$$

has been taken.

All the obtained approximating formulas reveal a quite acceptable description of electromagnetic cascade process initiated by gamma quanta of transient energy interval 100÷3500 MeV in the most often used dense materials. They can be applied both for hard gamma detection and radiation shielding construction.

References

[1] B. Słowiński. Phys. Part. Nucl. 25 (2) March-April 1994.
[2] D.W.O. Rogers, I. Kawrakow, J.P. Seuntjens, B.R.B. Walters, E. Mainegra-Hing. NRCC Report PIRS-702(revB), 2005.
[3] P. Dziekan. MSc Thesis. WUT, Warsaw, 2009.
[4] B. Słowiński, P. Duda and P. Hładki. Ann. Rep. of IAE, 2008, p. 41.

Th-7

The changes of manganin thermoresistance properties induced by Nb, Ti, C low energy and then Kr high energy ion implantation

Teresa Wilczyńska[1)], *Marek Barlak*[2)], *Roland Wiśniewski*[1)], *Piotr Konarski*[3)], *Bożena Sartowska*[4)], *Wojciech Starosta*[4)] *and Barbara Nycz*[2)]

[1)] *Institute of Atomic Energy POLATOM, Świerk, 05-400 Otwock-Świerk, Poland*
[2)] *The Andrzej Sołtan Institute for Nuclear Studies, Świerk, 05-400 Otwock-Świerk, Poland*
[3)] *Tele & Radio Research Institute, 11 Ratuszowa Str., 03-450 Warszawa, Poland*
[4)] *Institute of Nuclear Chemistry and Technology, 16 Dorodna Str., 03-195 Warszawa, Poland*

Manganin is very important Cu based alloy for resistance standard, applied e.g. in the electrotechnics, electronics, high-pressure measurements. However, its R(T) characteristic plateau is about 10 Celsius degree only [1].

The investigations carried out in Institute of Atomic Energy POLATOM show, that above mentioned plateau became 2-3 times more wide by using niobium, titanium, carbon elements and heavy noble gas ion implantation.

Nb, Ti and C elements were implanted firstly, using about 2,5e17 ion cm^{-2} fluence and 30 keV ions energy. Secondly, Kr implantation (about 2,5e13 ion cm^{-2} fluence and to 250 MeV energy) was applied in order to make the above mentions ions lying more deep. In the third step, the sample annealing was applied at 130ºC for 100 h.

Basic investigations of specimens were pressure-temperature tests. Other properties of samples were fixed using following methods: Scanning Electron Microskopy SEM, Electron Probe Microanalysis EPMA, Secondary Ion Mass Spectrometry SIMS and Grazing-angle X-Ray Diffraction GXRD.

References

[1] Wiśniewski R, Czachor A, Wilczyńska T, Semina V, High Pressure Research 2007;27:193

Plasma ion source with an internal evaporator

M. Turek[1)], A. Drożdziel[1)], K. Pyszniak[1)], S. Prucnal[1)], D. Mączka[2)]

[1)] Institute of Physics, Maria Curie-Sklodowska University in Lublin, pl. M. Curie-Sklodowskiej 1, 20-031 Lublin, Poland
[2)] Institute of Atomic Energy POLATOM, Otwock-Świerk, Poland

Development of new electronic and optoelectronic devices, especially those involving semiconductor or metalic quantum dots [1] or e.g highly Al^+ doped SiC layers requires high dose (10^{16}-10^{17} ions/cm^{-2}) implantations with ions of solids, both metalic and non-metalic. In order to cope with those demands, especially those concernig implantations of rare earths ions, the authors developed an innovative plasma ion source with an internal evaporator heated by arc discharge. This construction, described in details in [2], is suitable especially for high melting point feeding material – the source provides e.g 40 μA of Er^+ and 60 μA of Al^+.

The novel ion source design (see the figure on the left) presented in the paper is another solution involving an internal evaporator (crucible) placed inside the hollow cathode. The source is characterised by high efficiency, compact design, very low energy consumption and simple maintenance. The arc discharge burns between the front mount (2) of the cathode and a tip of a funnel-shaped anode (3), which is also a front cap of the source. The molybdenum crucible with a load of feeding substance is surrounded by a spiral cathode (4) made of tungsten.

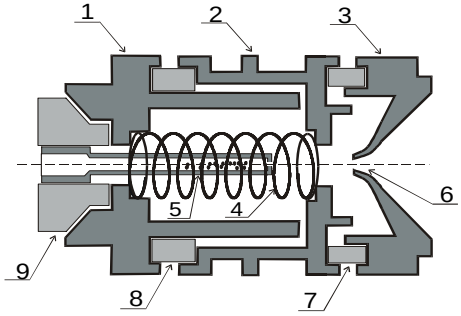

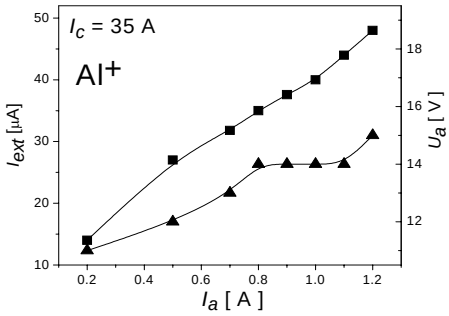

The arc discharge area is very close to the extraction hole (6). This enables production of intense ion beams, even if very low anode current (1 A) is applied. The paper presents construction of the source and its characteristics for selected elements: rare gases (He, Ne Xe) and .solids (Al, Mn and the like). The dependencies of extracted currents I_{ext} on: the discharge current I_a, cathode current I_c and the strength of magnetic field the discharge chamber is immersed in, are under investigation. One can see (the figure on the right) that extracted current of Al^+ ions (squares) reaches almost 50 μA for I_a=1.2 A. It should be noted that similar efficiency was achieved using the source with cylindrical anode [2,3], but using much higher discharge currents ($I_a \approx 4$ A). The discharge current was restricted up to 1.2 A during our present research (Knurr-Heinzinger PNC 1500-1200 power supply). One may conclude that the source is able

to produce ion currents larger by factor of 2 or 3 if more powerful anode power supply is applied.

Acknowledgement

The work was funded under Polish Ministry of Science and Higher Education silicon carbide programme as grant no. PBZ-MEiN-6/2/2006.

References

[1] F. Komarov, L. Vlasukova *et al.* Nucl. Instr. And Meth. B 266 (2008) 3557
[2] M Turek, S. Prucnal *et al.* Rev. Sci. Instr. 80 (2009) 043304
[3] M. Turek, K. Pyszniak, A. Droździel, S. Prucnal, J. Żuk, to be published in Przegląd Elektrotechniczny (2010)

Th-9

Analysis of the iron state in ferric and ferrous iron containing pharmaceutical products available in Poland by Mössbauer spectroscopy

P.J. Szalanski[1)], R. Brzozowski[1)], M. Proba[1)], C. Oprea[2)], I. A. Oprea[2)]

[1)] *Faculty of Physics and Applied Informatics, Łódź University, Łódź, Poland*
[2)] *Joint Institute for Nuclear Research, 141980 Dubna, Russia,*

Mössbauer spectroscopy is a very useful technique for chemical analysis of iron-containing compounds in various subjects [1-4]. An analysis of the iron state in commercial pharmaceuticals containing ferric and ferrous iron compounds, which are used for treatment of iron deficiency, was made by Mössbauer spectroscopy [5]. Characterization of the iron state in vitamins and dietary supplements containing ferrous compounds was made. The presence of ferrous and ferric impurities and iron compounds that were in good agreement with compounds announced by the manufacturer was detected by Mössbauer spectroscopy.

References

[1] Goldanskii V., Herber R. (Eds), Chemical Applications of Mössbauer Spectroscopy, Academic Press, New York and London, 1968.
[2] Gutlich P., Link R., Trautwein A., Mössbauer Spectroscopy and Transition Metal Chemistry, Springer–Verlag, Berlin– Heidelberg–New York, 1978.
[3] Vertes A., Korecz L., Burger K., Mössbauer Spectroscopy, Akadémiai Kiadó, Budapest, 1979.
[4] Herber R. (Ed.), Chemical Mössbauer Spectroscopy, Plenum, New York, 1984.
[5] Oshtrakh M., Milder O., Semionkin V., Analytica Chimica Acta 2004; 506: 156.

POSTER PRESENTATIONS

Tuesday, June 15, 2010

Identification of the Vine Tomb multi-layers composition by means of ion beam analysis

Shaaban Abd El Aal

Conservation Dept, Faculty of Archaeology, Fayoum University, Egypt, smm00@fayoum.edu.eg

Egypt has many kinds of ancient pharaoh tombs for kings, queens and Noblemen. One of the most important tombs from noblemen tombs is Sennefer Tomb. Located in a prominent position on the southern hillside of Sheikh Abd El- Qurna, close to several other tombs from the time of Amenhotep II (of the 18th Dynasty, about 1439-1413B.C.), It is usually referred to as the Tomb of Vines; because a large part of the ceiling of the burial (or coffin) chamber and all of that of its antechamber are decorated to give the impression of standing under an overhanging vine arbor, hung with large bunches of grapes.The vine tomb was carved inside Mountain, ancient Egyptian artist covered tomb walls with many layers to avoid disadvantages of the rock, then wall surface was ready for drawing with pigments which were mixed with organic medium.

Scientific analysis was carried out by PIXE, μPIXE not only to identify the composition of materials which were used on the surface of the tomb but also to identify the composition of the pigments. This also to get data about the nature of these materials and pigments to help in conservation process such as cleaning. Some samples from the vine tomb were analyzed by PIXE and μPIXE which are considered the most sensitive analytical methods. It is a non-destructive technique. The study was performed by using PIXE, μPIXE and light Optical Microscope (LOM) for red, yellow, grey and blue pigments and for ground layers of the tomb.

References

[1] Shaaban A, Turos A, Korman A, Stonert A, Munnik F, Ion beam analysis of ancient Egyptian wall paintings; vacuum 2009; 83: s4-s8.

[2] Nicholson P, Shaw I, Anceint Egyptian Materials and Technology 2000; Cambridge University Press.

P-Tu-2

Characteristics of ancient Egyptian glazed ceramic objects as revealed by ion beam analysis

M.M. Abd El Hady[1)*], *A. Turos*[2,3)], *H.S. Kotb*[2,4)], *A. Korman*[2)], *A. Stonert*[2)], *F. Munnik*[5)]

[1)] *Conservation Department, Faculty of Archaeology, Cairo University, Egypt*
[2)] *Sołtan Institute for Nuclear Studies, Hoża 69, 00-681 Warszawa, Poland*
[3)] *Institute for Electronic Materials Technology, Wólczynska 133, 01-919 Warszawa, Poland*
[4)] *Conservation Department, Faculty of Archaeology, Fayoum University, Egypt*
[5)] *Forschungszentrum Dresden, IIM, P.O. Box 510119, D-01314 Dresden, Germany*

Analytical studies of ancient glaze layers meet different challenge during investigation, preparing samples and identify chemical composition especially trace elements which were not appearing with different methods. Ion beam analysis solves many of these problems. With IBA, it is possible to avoid sampling; the technique is largely non-destructive [1], allowing for multiple data points to be taken across an object and finally, the resulting X-ray spectra are easily interpreted and understood by many conservators and archaeologists.

Al-Fustat, the oldest Islamic city and center of ceramic production in Egypt have different kinds and treasures of glazed ceramic. The role of trace elements and pigments was not studied before with IBA, elements and its effect in glaze colors and other aspects such as deterioration.

Eight glazed ceramic samples from Al-Fustat were analyzed with PIXE and μPIXE, samples were classified depending on color of glaze (white, blue, green, yellow, black, brown and terquaze).

Results showed that ancient potters used lead as flux agent and mix lead with alkaline to have different ranges of colors, potters control firing conditions to have ranges of colors.

References

[1] Demortier,G.: Ion Beam Techniques for the Non-destructive Analysis of Archaeological Materials in M. Uda et al. (eds.), X-rays for Archaeology, 67-100.

* Correspondence author: elhady_esna@yahoo.com & hsr00@fayoum.edu.eg

P-Tu-3

Modification of mechanical properties of the Ni-Cr based alloy by continuous electron irradiation

D.L. Alontseva

East-Kazakhstan State Technical University, 69 Protozanov St., 070004, Ust-Kamenogorsk, Kazakhstan, e-mail: dalontseva@mail.ru

Keywords*:* electron irradiation, structural and phase transformations, TEM, SEM, fractography

Using TEM, SEM with EDS and XRD methods we studied the structure-phase state of the industrial precision dispersion-hardening alloy on the Ni-Cr base after various modes of mechanic-thermal processing and e-beam irradiation.

The choice of the modes of electron irradiation is made on the basis of mathematical modeling of the temperature profile distribution during irradiation.

Mechanical test included the measurement of monoaxial static tension of the point of break σ_b, relative fluid limit σ_{02}, coefficient of elongation to fracture δ, and microhardness measurement.

The data of structure investigation were compared to the data received from investigation of kinetics of strength and plasticity properties which depend on the initial structure state and the time of electron irradiation.

We established the morphology of structure and phase transformations in the alloy at continuous electron irradiation.

The simultaneous increase of mechanical strength and plasticity characteristics of the alloy after an e-beam irradiation is revealed. The reasons of this phenomenon are analyzed.

The scientifically-proved schemes of mechanic-thermal processing of this alloy are developed, and the selection of modes of electron irradiation for optimization of its mechanical properties is proved.

P-Tu-4

Laser beam interaction with boron nitride based composites

Igor Azarko[1)], *Oleg Ignatenko*[2)], *Igor Karpovich*[1)], *Vladimir Odzhaev*[1)], *Mihail Puzyrev*[1)], *Oleg Yankovski*[1)]

[1)] *Belorusian State University, Nezavisimosti Ave. 4, Minsk, 220050 Belarus*
[2)] *State Scientific Organization " Integrated Institute of Solid State and Semiconductors Physics of the National Academy of Sciences of Belarus", P. Brovki str. 19, Minsk, 220072, Belarus, azarko@bsu.by*

Cubic boron nitride is widely used as the base material. For example, metal-containing composites reinforced with nano-powders of boron nitride, are used to protect against various types of radiation. High-strength ceramics from powders of metal bounded cubic BN is used as a cutting tool. Some superhard superconducting materials based on cubic boron nitride with MgB_2 were synthesized lately. The effects of laser radiation on superhard materials are widely studied now.

In our work we investigated the intermetallic compounds of Al and Ti on the basis of cubic boron nitride in the form of tablets and the original fine dispersed crystals of cubic boron nitride of various sizes. For irradiation of the samples there was the laser YAG: Nd3 + of Lotis-TII company used with a repetition rate of laser pulses of 5 Hz. Laser radiation wavelength λ = 1064 nm and pulse duration τ = 20 ns was focused by a lens onto the target. The power density of laser radiation was equal to 2.8 • 108 W/cm^2, and the number of laser pulses was varied from 1000 to 4000. The studies of the samples were carried out by the electron spin resonance method using the spectrometer "Varian" in the temperature range of 77-493 K. The possibilities of this method are considered in the studies of impurity-defect composition and electronic processes in the samples of composite materials based on cubic boron nitride.

To reveal the mechanism of transport carriers in the intermetallic compounds there were the temperature dependences of the resistivity studied for the samples synthesized at various ratios of metal and cubic boron nitride.

P-Tu-5

Melanin complexes as a radiation bioprotector

I.I. Azarko[1)], A. Bakulin[2)], E.I. Kozlova[1)], V.P. Kurchenko[1)], L.V. Ajayeva[3)]

[1)] Belorussian state university, Minsk, Republic of Belarus, azarko@bsu.by
[2)] "Bioingeneria" Center Russian Academy of Sciences, Moscow, Russia
[3)] 4 Hospital, Minsk, Republic of Belarus

A significant problem with most UV-visible radiation (photo-) protectors is phototoxic and photo allergic action they show in a varying extent. That is why it is important to search for some natural biopolymers, which efficiently absorb and dissipate the UV light energy. A special place in this aspect belongs to melanin pigments and their chitin complexes. Chitosan is non-toxic, has a high sorption capacity, and the potentialities of chitosan's chemical transformations can be applied to form a variety of new materials with different structure and properties.

The goal of the present study is to determine the best ratio of melanin and chitosan to prepare the most promising radiation safe melanin-chitosan complexes. Tinders and grapes were used as the source of melanin pigments to prepare the samples for the studies. The influence of UV-irradiation over the paramagnetic properties of melanin pigments and their chitosan compounds was studied by standard EPR method. All the samples show an intensive paramagnetic absorption line with g-factor of 2.0035. For the samples of pure chitosan, a similar signal is not detected. The studies of photo screening activity of the samples show that the investigated pigments absorbs radiation in all UV ranges.

The original melanins, like their chitosan complexes, show photo protective properties and participate the photochemical processes due to the presence in their molecules of such structures as free radicals, systems of poly-conjugated double bonds, highly reactive functional groups, capable of restorable oxidation. The photo induced paramagnetic centers appearing in the samples may be due to generation of anion- and cation-radical centers in the process of electrons transfer within the polymer granules. Moreover, the UV-irradiation is hard physical agent able to cause the polymer molecules lacing which may cause the reduction of the pigments capabilities of restorable oxidation.

The present studies show the effectiveness of the ESR-method to study both the initial melanin samples and their compounds with chitosan.

P-Tu-6

Wettability of carbon ceramics induced by their surface alloying with Ti, Zr and Cu elements using high intensity pulsed plasma beams

Marek Barlak[1,2], Jerzy Piekoszewski[1,2], Zbigniew Werner[2,3], Bożena Sartowska[1], Lech Waliś[1], Wojciech Starosta[1], Andreas Kolitsch[4], Rainer Gröetzchel[4], Cezary Pochrybniak[2,5], Katarzyna Bocheńska[2], Barbara Nycz[2]

[1] *Institute of Nuclear Chemistry and Technology, 16 Dorodna, 03-145 Warszawa, Poland*
[2] *The Andrzej Sołtan Institute for Nuclear Studies, 05-400 Otwock-Świerk, Poland*
[3] *Institute of Physical Chemistry, PAS, 44/52 Kasprzaka, 01-224 Warszawa, Poland*
[4] *Forschunzentrum Dresden-Rossendorf, Institute of Ion Beam Physics and Materials Research, PO Box 51 01 19, D-01314 Dresden, Germany*
[5] *Institute of Atomic Energy, 05-400 Otwock/Świerk, Poland*

Ceramics materials, such as: oxides, nitrides, borides, carbides and carbon are widely applied in modern constructions and devices. Their advantages are: low density, high mechanical strength and corrosion resistance at high temperature and favourable relationship high performance/weight rate. However, an application of these materials in joints or in composites with metals is very difficult, because usually the ceramics are non-wettable by liquid metals.

In the present work, we used high intensity plasma pulses technique for the preparation of carbon and silicon carbide surface before the wetting process by liquid copper. The Ti, Zr and Cu plasma was applied to induce the wettability.

The experiments were preceded by thermodynamical considerations. The prepared samples were investigated by sessile-drop tests, SEM observations, EPMA, GXRD analysis and RBS measurements.

The results of Ti and Zr plasma modifications were beneficial and similar to each other. The measured contact angles were below 90°. The results of Cu plasma were unfavorable with contact angles near 180°.

Mass loss of the solid irradiated with intense plasma pulses: sputtering or ablation?

Katarzyna Bocheńska[1)], Marek Barlak[1)], Jerzy Piekoszewski[1)], Bożena Sartowska[2)], Cezary Pochrybniak[1)], Barbara Nycz[1)]

[1)] The Andrzej Sołtan for Nuclear Studies, 05-400 Otwock-Świerk, Poland
[2)] Institute of Nuclear Chemistry and Technology, Dorodna 16, 03-195 Warszawa, Poland

Deposition of short (ns- μs) intense (10^6-10^8 W/cm^2) pulse of energy large on the surface of solid can rise its temperature to the melting point or above.

If the pulse is generated in the rod plasma injector type of device (accelerator) the two modes of operation are available. One, referred to as the pulsed implantation doping (PID) and the second referred to as deposition by pulsed erosion (DPE). In both cases the transport of both: portion of energy and mass occurs. In the PID, the beam contain almost exclusively ion of the working gas (any kind of gas volatile at normal conditions), whereas in DPE apart of ions as above also ion/atoms of the metallic electrodes takes place. In both cases melting of the near-surface layer occurs. The gravimetrical analysis of the properties of treated samples reveal that in some cases the mass of the substrate increases, when in others is reduced. Two mechanisms can be responsible for these effects: mass deposition + sputtering and mass deposition + ablation. The aim of the present work was to reveal which of these machanism is decisive. Three kinds of the substrate of substantially (x20) different heat conductivity i.e: cooper, yttrium and alundum were coated with titanium layer of about 1μm thick and then irradiated with 10 and 20 plasma pulses of energy density of 3.0 and 4.0 J/cm^2 in DPE mode with Ar as the working gas. The samples were analysed with EDX and gravimetric methods. The results of these examinations indicates that decisive mechanism responsible for the mass loss is rather evaporation then sputtering of atoms from the near-surface layer of the irradiated substrate.

P-Tu-8

Study of structure densification in TiO_2 coatings prepared by magnetron sputtering under low pressure of oxygen plasma discharge

Jarosław Domaradzki[1)], *Danuta Kaczmarek*[1)], *Eugeniusz L. Prociow*[1)], *Zbigniew Radzimski*[2)]

[1)] *Faculty of Microsystem Electronics and Photonics, Wroclaw University of Technology, Janiszewskiego 11/17, 50-372 Wroclaw, Poland*
[2)] *RaEn Tech, Inc., 4800 Eisan Avenue, Reno, NV 89506, USA*

It is well known that the structure evolution of thin films prepared by reactive magnetron sputtering is strictly dependent on the particle energy at the film nucleation site. The energy could be changed typically by: (1) additional heating of the substrates, (2) decrease in plasma pressure, (3) increase in the temperature of the sputtered target surface (hot target) and (4) increase the sputtering power. Present work presents results of studies on structural and optical properties of the TiO_2 thin films prepared by two methods: Low Pressure Hot Target Magnetron Sputtering (LP HTRS) and High Energy Reactive Magnetron Sputtering (HE RMS). Both these methods allow adjusting the process energy using all four options mentioned above. In both processes oxide thin films are deposited from metallic targets using oxygen gas only instead of usually used mixture of Ar-O_2. Additionally, in HE RMS, an increased amplitude of unipolar pulses powering the magnetron has been applied. It is shown that all prepared coatings were stoichiometric and by changing only the discharge voltage it is possible to influence the resulting structural phase and optical properties of prepared thin films. TiO_2 thin films prepared using LP HTRS had anatase structure with refraction index n=2.1 (λ=500 nm) whereas HE RMS allows to obtain high temperature stable rutile structure with n=2.52 (λ=500 nm), i.e. equal to the n value reported for the monolithic rutile. It is also shown that enhanced kinetic energy in HE RMS caused higher degree of densification of the coatings and a change in the type of stress from compressive to tensile.

Positive and negative ion temperature effects on the sheath structure in the electronegative plasmas

Hamid Ghomi[1)], *Mansour Khoramabadi*[2)]

[1)] *Laser and Plasma Research Institute, Shahid Beheshti University, Evin 1983963113 , Tehran, Iran*
[2)] *Plasma Physics Research Center, Science & Research Campus of I. Azad University, Tehran, Iran*

Using a fluid model of plasma we have investigated the ion temperature effects on the sheath parameters such as densities of charged particles, electric potential, ion flux into the wall and space charge, in an electronegative plasma-wall interface. Electronegative plasmas are constituted of electronegative gases such as oxygen, chlorine, SF_6 and fluorocarbons, and are used extensively in plasma processing reactors. Therefore, the knowledge of the sheath formation condition and sheath structure is important. In addition, in plasma diagnostics, knowing the sheath parameters is necessary for understanding the observed data.

We have numerically solved the plasma sheath equations to study the ion temperature effects on the sheath structure. For example, as one can see from following Figs. the positive ion temperature decreases the sheath width, while the negative ion temperature increases it.

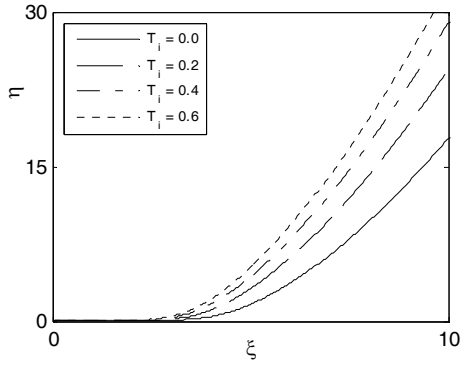

Fig. 1. Normalized electric potential $\eta = - e\phi/KT_e$-$e\phi/KT_e$ as as a function of the normalized distance from the from the sheath edge $\xi = x/\lambda_D$ for different values of positive values of ion temperature T_i.

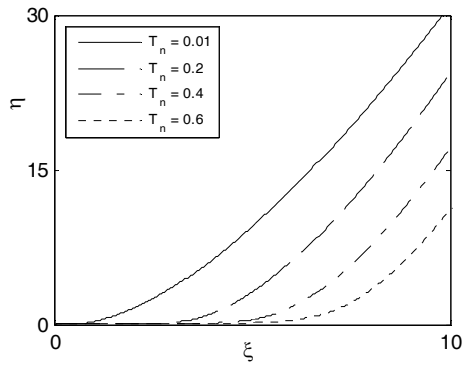

Fig. 2. Normalized electric potential η = a function of the normalized distance sheath edge $\xi = x/\lambda_D$ for different negative ion temperature T_n.

References

[1] Braithwaite N St J and Allen J E 1988 J. Phys. D: Appl. Phys. **21** 1733.
[2] Amemiya H 1990 J. Phys. D: Appl. Phys. **23** 999.

P-Tu-10

Fabrication and characterization of diamond-like carbon by DC magnetron sputtering

H. Ghomi[1)], *M. Kulik*[2)], *A. Heidarnia*[1)], *S. Ghasemi*[1)]

[1)] *Laser and Plasma research Institute, Shahid Beheshti University, Evin 1983963113 Tehran, Iran*
[2)] *Institute of Physics, Maria Curie-Skłodowska University, Pl. M. Curie-Skłodowskiej 1, 20-031 Lublin, Poland*

In this paper, diamond-like carbon (DLC) thin films were deposited on silicon and glass substrates by home a DC magnetron sputtering system. The films structure were characterized by Raman spectroscopy Figure 1 and the morphology of the surface was examined using AFM and SEM (Fig.2). AFM showed that the roughness of DLC surface is 2.02nm and 3.45nm for glass and silicon substrates respectively. Also by Scanning Electron Microscopy it was observed that DLC clusters formed on silicon substrates. The thickness of the DLC films was estimated to be about 100 nm by a Dektak 8000 surface profiler.

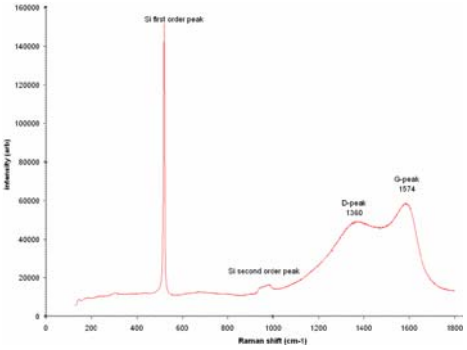

Fig. 1.

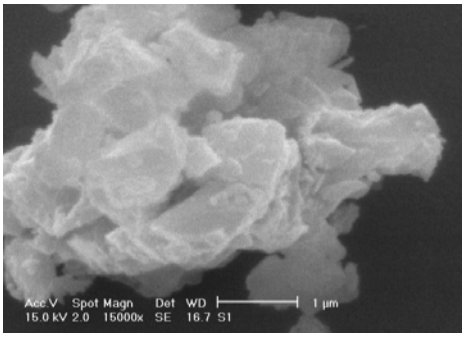

Fig. 2.

P-Tu-11

Influence of deposition parameters on properties of S-phase coatings

J. Baranowska, S. Fryska

Institute of Materials Science and Engineering, West Pomeranian University of Technology, 70-310 Szczecin, al. Piastow 19, Poland

S-phase is a metastable phase with very high hardness and good corrosion resistance which demonstrates a large potential for many practical applications. This phase can be obtained using various methods, including gas and plasma nitriding of austenitic stainless steel as the most common ones. However, layers produced at such conditions have a gradient structure, which makes it difficult to characterise properties of layers as a function of nitrogen content. The S-phase coating obtained by magnetron sputter deposition are homogeneous in a bulk and can be produced in an effective way even at a very low temperature (<300°C). The paper presents the results of the investigations of S-phase coatings obtained by reactive unbalanced magnetron sputter deposition. A special attention is paid to deposition parameters such as substrate temperature and gas pressure. The phase composition was evaluated using X-ray diffraction (XRD and GXRD). EMPA (EDS and EDS) and GDOS techniques were used to study element composition of the layers. Microstructure was investigated by means of light and electron microscopy. Mechanical properties were measured by nanoindentation.

P-Tu-12

Synthesis of bismuth oxide solid electrolyte thin films deposited by reactive magnetron sputtering

Aleksandras Iljinas[1)], *Saulius Burinskas*[1)], *Julius Dudonis*[1)], *Darius Milčius*[2)]

[1)] *Departament of Physics, Kaunas University of Technology, Studentų 50, LT–51368, Kaunas, Lithuania*
[2)] *Center for Hydrogen Energy Technologies, Lithuania Energy Institute, Kaunas, Lithuania*

In this work Bi_2O_3 thin films were deposited onto Si (100) and soda lime glass substrates by reactive direct current magnetron sputtering system using pure Bi as sputtering target. The dependencies of electro-optical characteristics of the films on the sputtering pressure, Ar/O_2 working gas flow ratio, the discharge power and substrate temperature were investigated. X-ray diffraction (XRD), scanning electron microscopy (SEM) techniques and a surface profilometer were applied to characterize the structure, phase components and morphology of thin films. Transmittance and reflectance of the Bi_2O_3 films were measured with ultraviolet and visible light spectrometer (UV-VIS). Thickness and refractive index of the deposited films were measured by laser ellipsometer. Energy band gap was determined using Tauc method.

It was found that the substrate temperature during deposition has a very strong influence on the phase components of the thin films. The different temperatures of annealing can also cause the transformation between monoclinic phase and tetragonal phase of bismuth oxides.

P-Tu-13

Enhanced capacitance of porous carbon electrodes through deposition of small amounts of NiO_2

Zydrunas Kavaliauskas[1,3], *Liutauras Marcinauskas*[1,2], *Liudvikas Pranevicius*[3], *Pranas Valatkevicius*[1]

[1] *Lithuanian Energy Institute, Breslaujos 3, LT-4440, Kaunas, Lithuania.*
[2] *Kaunas University of Technology, Studentu 50, LT-51368, Kaunas, Lithuania.*
[3] *Vytautas Magnus University, Vileikos st. 8, LT-44404 Kaunas, Lithuania*

In recent years, a great deal of attention has been devoted to the research of supercapacitors since they exhibit some excellent properties: extremely large capacity (up to 780 F/g), high power density and high efficiency of discharge. The surface topography of carbon electrodes is the main criterion of a double electrical layer with high capacity and charge exchange kinetics [1].

In the present work, the carbon electrodes employing atmospheric plasma in the mixture of argon/acetylene gases torch technology have been deposited on the conductive substrates. Argon was used as gas carrier (the flow rate – 6.6 l/min) and acetylene - as precursor (the flow rates – 0.12 l/min, 0.165 l/min, and 0.236 l/min). The power of plasma generator – 750 W, the distance between the exit from plasma source and substrate – 5 mm, and the duration of deposition – 150 s. Small amounts corresponding to film thickness of 72 nm of nickel oxide (NiO) have been deposited on the top of carbon layer by reactive magnetron sputtering of Ni in the presence of oxygen. The magnetron discharge current – 1 A, voltage – 280 V. The structure and surface topography of the fabricated electrodes has been investigated by Raman scattering spectroscopy (RS), X-ray diffraction (XRD), and SEM techniques.

SEM results indicated that the deposition of nickel oxide changes the surface structure of the carbon electrode from fuzzy and snowflake-like to mesh-like structure. The capacitance of fabricated supercapacitors has been measured. The capacitance increases from 1 to 5.4 mF as the Ar/C_2H_2 ratio increases. Meanwhile, the hundredfold increase of capacitance (up to 110 mF) has been registered after the deposition of NiO_2 on the carbon.

References

[1] Pandolfo A, Hollenkamp A, Journal of Power Sources 2006;157:11.

P-Tu-14

The utilization of molecular ions for implantation purposes

K. Kiszczak[1)], D. Mączka[2)], B. Słowiński[2)] and J. Zubrzycki[3)]

[1)] *UMCS, Lublin, Poland*
[2)] *Institute of Atomic Energy POLATOM, Świerk, Poland*
[3)] *Lublin University of Technology*

It is commonly known that the implantation with ions of different kind and energy into solids to change their properties has been using successfully for years. For these purposes there are applied not only specific implanters but also cyclotrons, especially for high energy implantation, and even electromagnetic separators of isotopes having usually acceleration tension not exceeding 30-70 kV. Moreover, for very low energy ion implantation it is appropriate to use molecular ions (mostly diatomic molecules) because striking a solid surface they decay into their components with lower energies. In addition, the use of molecular beams has also other advantages, in particular, the time of implantation is abbreviated owing to larger mass of an ion carried into a target. Finally, in several cases the use of compounds of implanted element is more efficient from the viewpoint of the operation of ion source.

In the work we have described the process of generation of ions of diatomic molecules [1]. These ions have been created in the ion source of magnetron type which various kinds are using in electromagnetic mass-separators both in the JINR (Dubna) [2] and UMCS (Lublin) [3]. As an example of achieved results Table 1 shows the comparison of values of ions currents for different chemical compounds.

Table 1. The values of ions currents for different chemical compounds

Ion	Chemical compound	Ion source temperature (^oC)	Ion current (μA)	Implantatin time at $D=10^{14}cm^{-2}$ (sec)
H_2^+	H_2	-	180	3
Li_2^+	$LiCl+H_2O$	400	1,2	400
B_2^+	B	1900	0,5	961
N_2^+	N_2	-	60	8
Na_2^+	NaCl	400	0,15	3200
Al_2^+	Al	1000	0,15	3200
Al_2^+	$Al+CCl_4$	900	12	40
P_2^+		250	4,4	109
Cl_2^+	NaCl	500	18	28
Ar_2^+	Ar	-	1,5	320
Ga_2^+	Ga	800	0,9	538
As_2^+	As	250	4	120
Se_2^+	Se	350	0,2	2400
Ag_2^+	$Ag+CCl_4$	800	3	641

References

[1] Y.A.Vaganov, D.Mączka, B.Słowiński, Y.V.Yushkevitch and J.Zubrzycki. JINR communication, P13-2009-117. Dubna, 2009.
[2] V.G. Kalinnikov, K. Yu. Gromov, M. Janicki, S.V. Evtisov, Nucl. Inst. Meth. B 1992, V70, p. 62.
[3] D. Mączka, A. Latuszyński, R. Kuduk, J. Partyka, Nucl. Inst. Meth. B 1987, V21, p. 512.

P-Tu-15

The features of real part of admittance in the nanocomposites $(Fe_{45}Co_{45}Zr_{10})_x(Al_2O_3)_{(100-x)}$ manufactured by ion-beam sputtering technique with Ar ions

Tomasz N. Koltunowicz[1)], Pawel Zhukowski[1)], Vera V. Fedotova[2)], Anis M. Saad[3)], Alexander K. Fedotov[4)]

[1)] *Lublin University of Technology, Lublin, Poland*
[2)] *Scientific-Practical Material Research Centre NAS of Belarus, Minsk, Belarus*
[3)] *Al-Balqa Applied University, Salt, Jordan*
[4)] *Belarusian State University, Minsk, Belarus*

The present paper investigate the electron transport mechanisms around the percolation threshold in granular nanocomposites consisting of the nanoparticles of soft amorphous ferromagnetic $Fe_{45}Co_{45}Zr_{10}$ alloy embedded into amorphous dielectric alumina matrix using AC conductance measurements at different temperatures.

Temperature and frequency dependences of the real part of admittance $\sigma(T, f)$ in the range of $77 - 300$ K and $5 \cdot 10^1 - 10^6$ Hz in granular $(Fe_{45}Co_{45}Zr_{10})_x(Al_2O_3)_{100-x}$ nanocomposite films around the percolation threshold x_C have been studied. The films of $3 - 6$ μm thickness were deposited using Ar ion-beam sputtering of complicated target containing $Fe_{45}Co_{45}Zr_{10}$ alloy and alumina stripes. The behavior of $\sigma(T, f)$ dependences for the samples studied displayed the predominance of activation (hopping) conductance mechanism with $(d\sigma/dT) > 0$ for the samples below the percolation threshold determined as $x_C \approx 54 \pm 2$ at.%. Beyond the x_C the samples shown a metallic behavior with nearly linear $\sigma(T)$ and $(d\sigma/dT) < 0$.

The features of $\sigma(T, f)$ dependences confirm hopping of electrons by tunneling over the dielectric barriers between the closest neighbouring metallic nanoparticles. These $\sigma(T, f)$ curves allowed to estimate the mean hopping ranges d (between 7 and 1 nm depending on concentration x and nanoparticles diameters D) and the rate of wave function falling $\alpha_H \approx 1.06 \pm 0.25$ nm^{-1} of the hopped electrons for different metallic phase content 30 at.% $< x <$ 100 at.%. On metallic side of MIT ($x < x_C$), resistivity of nanocomposite samples increases practically linear with T and temperature coefficients of real part of impedance $\alpha_\rho = 4.0 \cdot 10^{-4}$ K^{-1} for $x = 64.1$ at.% and $3.2 \cdot 10^{-4}$ K^{-1} for $x = 100$ at.% are characteristic for metallic substances.

The work was partially supported from Fundation for Polish Science.

P-Tu-16

Hopping conductance in nanocomposites $(Fe_{45}Co_{45}Zr_{10})_x(Al_2O_3)_{100-x}$ manufactured by ion-beam sputtering of complicated target in $Ar+O_2$ ambient

T.N. Koltunowicz[1)], P. Zhukowski[1)], V.V. Fedotova[2)], A.M. Saad[3)], A.K. Fedotov[4)]

[1)] *Lublin University of Technology, Lublin Poland*
[2)] *Scientific-Practical Material Research Centre NAS of Belarus, Minsk, Belarus*
[3)] *Al-Balqa Applied University, Salt, Jordan*
[4)] *Belarusian State University, Minsk, Belarus*

The present paper investigate the regions of dielectric (hopping) and metallic conductance around the percolation threshold $x_C \approx 76 \pm 5$ at.% in granular nanocomposites $(Fe_{45}Co_{45}Zr_{10})_x(Al_2O_3)_{100-x}$ manufactured in $Ar+O_2$ atmosphere by ion-beam sputtering of target containing $Fe_{45}Co_{45}Zr_{10}$ and alumina stripes. Hopping transport has been studied by temperature T and frequency f dependences of the real part of admittance $\sigma(T,f)$ in the range of 77-300 K and $5 \cdot 10^1$-10^6 Hz. The shift of the x_C to the higher concentrations of metallic phase as comparing with the nanocomposites manufactured in pure Ar gas ($x_C \approx 54 \pm 2$ at.%) is due to the presence of oxide shells at the surfaces of metallic nanoparticles. The analysis of $\sigma(T,f,x)$ dependences for the samples studied displayed the predominance of activation (hopping) conductance mechanism with $(d\sigma/dT)>0$ for the samples below the percolation threshold determined as $x_C \approx 54 \pm 2$ at.%. Beyond the x_C the samples shown a metallic behavior with nearly linear $\sigma(T)$ and $(d\sigma/dT)<0$. The features of $\sigma(T,f)$ dependences confirm hopping of electrons by tunneling over the dielectric barriers between the closest neighbouring metallic nanoparticles. The observed $\sigma(T,f)$ dependences allowed to estimate, using the developed model and formula $\sigma \sim \exp(-2\alpha_H d)$ for $x<x_C$, the mean hopping ranges $d(x,\text{at.}\%) \approx 0.049$-$0.36$ (in nm), the rate constant of wave function falling $\alpha_H \approx 1.05 \pm 0.15$ nm^{-1} for the electrons tunneling between metallic nanoparticles and also $\tau(T)$ for time between two jumps of the electron. On the base of earlier models for hopping AC conductance, we have made computer simulation of the frequency coefficient α_f of hopping conductance in formula $\sigma \sim f^{\alpha}$ depending on the probability p of jump, frequency f and also shape of $\sigma(f)$. The experimental and simulation results has shown their good agreement.

The work was partially supported from Fundation for Polish Science.

P-Tu-17

Peculiarities of swift proton transmission through tapered glass capillaries

F.F. Komarov, A.S. Kamyshan

Institute of Applied Physics Problems, Belarusian State University, 7 Kurchatov Street, 220108 Minsk, Belarus

The purpose of this study was to examine energy, angle and time distributions of 190 to 320 keV protons transmitted through tapered capillaries made of the borosilicate glass. Capillaries with different taper angles, as well as different inlet and outlet diameters have been used. The energy spectrum of transmitter protons was measured directly using a mobile silicon surface barrier detector with an energy resolution of 17 keV. It was experimentally observed:

- an increase in the ion current at the output of the capillary versus the ion current at the input of the capillary behaves a nonlinear character, with a higher steepness up to 5×10^{-15} A inlet currents, and the linear dependence at higher currents. It demonstrated the effect of charging of capillary inner surface on the transparency coefficient;
- when the caper angle is decreased from 2.2° to 0.9°, the transparency coefficient is increased more than one order of magnitude for the identical outlet diameters;
- a total angular width in an angular dependence for 320 keV protons transmitted through the capillary with an taper angle of 0.9° is less than 0.14° just as the proton beams angular distribution at the inlet of the capillary amounts to 0.26°;
- during the guiding in the tapered capillary the 320 keV ions are gently defected, therefore, the transmitted protons suffer practically no energy loss (less than 3 keV in the direction of lower energies).

P-Tu-18

Comprehensive analysis of ion beam induced stainless steel surface morphology

Zbigniew W. Kowalski

Wrocław University of Technology, Wybrzeże Wyspiańskiego 27, 50-370 Wrocław, Poland

It is well known that ion bombardment of solid surface modifies its physical and chemical properties, among others surface morphology. Two aspects of the morphology in question are well known and studied, i.e. surface topography and surface roughness with about 30 parameters, distributions and functions. The paper presents two other aspects that seem to be important in comprehensive analysis of surface morphology modified by various technologies (chemical, mechanical, physical, e.g. with the use of ion beam bombardment), i.e. (a) surface profile variability, and (b) surface morphology arrangement.

Surface topographies (in micro- and nanometre range) were observed by means of scanning electron and near-field microscopes. The second aspect, i.e. surface roughness, was measured with the use of high quality profilograph and atomic force microscope. To describe that surface feature properly, a surface profile must be known well. A significant drawback of this method is that one can find profiles with the same values of roughness parameters but with different profile shapes – that could mean various physical properties of the surface in question. To detect any ion beam induced profile shape alteration fractal analysis was used, and especially fractal dimension D that can give information about rate of profile shape variability (e.g. D = const means that the shape of the profile in question does not change / does not depend on time of ion irradiation). The last aspect – surface morphology arrangement, i.e. a question whether it is undefined (random) or defined (determined), was studied with the use of frequency plots resulting from harmonic analysis of profiles – the wider frequency band the more random surface morphology and, on the contrary, the narrower frequency band the more determined surface morphology.

Surface topographies, selected roughness parameters, fractal dimensions and frequency plots were studied relating to stainless steel of 1H18N9T (made in Poland) bombarded with perpendicular and inclined ion beam. Low energy (800 eV) broad argon as well as neutralized narrow (up to 6 keV) argon or krypton ion beams were utilized in the experiments.

a) 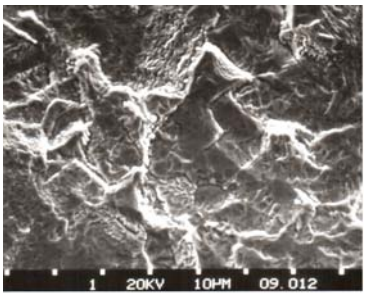

b) 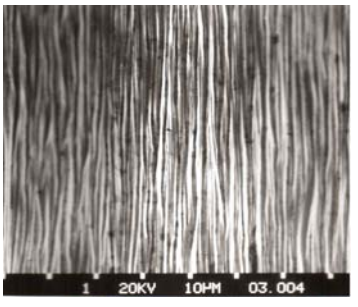

SEM images of stainless steel surface after: a) normal and b) oblique (Θ = 85°) narrow ion beam irradiation

The main aim of the work is to give relatively full picture of stainless steel surface morphology modification induced by ion beam. Comprehensive analysis include four aspects of the morphology in question: (a) topography, (b) roughness, (c) profile variability, and (d) morphology arrangement.

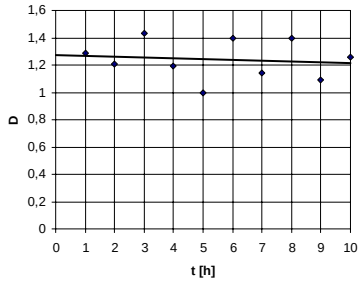

a)

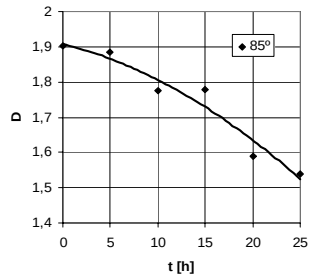

b)

Fractal dimension D calculated for stainless steel after: a) normal and b) oblique broad ion beam irradiation

P-Tu-19

Numerical modelling of the charged particles flow at the variable gas pressure

Michał Krysztof, Witold Słówko

Faculty of Microsystem Electronics and Photonics, Wrocław University of Technology, Janiszewskiego 11/17, 50-372 Wrocław, Poland

Variable Pressure / Environmental SEM (VP/E SEM) is commonly used to study insulator specimens or those with high vapour pressure constituents. It overcomes limitations of standard high vacuum SEM thanks to gas filling the sample chamber at the pressure suited to the sample features, while the electron optical column is maintained at high vacuum. These gaseous conditions in the sample chamber, are advantageous for the sample itself, but gas disturbs flow of electrons both in the scanning beam and the electron signal generated from the sample, because of frequent elastic and inelastic collisions with gas molecules. There are not many tools for analysis of the charged particle flow in a wide range of gas pressures characteristic for this instrument, i.e. from high vacuum to pressures exceeding 10 mbar [1]. There, electrons and ions go along trajectories shaped both by electric field and collisions of many types, and may produce a cascade of secondary electrons and ions.

A solution to the problem may be a computer programme prepared by the authors for simulations of electron flow in various gas conditions. The computer programme combines commercially available programme SIMION 3D V7 [2], destined for computations of trajectories of charged particles in electric and magnetic fields, and a Monte Carlo code written in the SIMION internal language. The MC programme simulates the process of electron scattering and multiplication for several types of their collisions with gas molecules, but tracing of the electron and ion trajectories between successive collisions is the SIMION task. The MC-SIMION packet classifies and memorizes most interesting phenomena in selected areas, which enables quantitative analysis of the particles flow process in all important sectors of the designed instrument, for any assumed gas pressure distribution in the investigated space.

References

[1] Krysztof M, Słówko W, Vacuum 2008;82:1075.
[2] Dahl D, SIMION 3D V7.0, Bechtel, Idaho Falls 2000.

P-Tu-20

The influence of technological parameters on the zirconium and cerium based thin films properties

Giedrius Laukaitis[1)], *Darius Virbukas*[1)], *Julius Dudonis*[1)], *Oresta Katkauske*[1)], *Darius Milcius*[2)]

[1)] *Physics Department, Kaunas University of Technology, 50 Studentu str., LT-51368 Kaunas, Lithuania; E-mail: gielauk@ktu.lt*

[2)] *Laboratory of Materials Testing and Research, Lithuania Energy Institute, 3 Breslaujos str., LT-44403 Kaunas, Lithuania; E-mail: milcius@mail.lei.lt*

New types of oxygen ion conducting materials are currently under investigation to overcome the problems which SOFC face at high temperatures. Zirconium and cerium based oxides are used as electrolyte materials in SOFCs. The efficiency of SOFC is influenced by initial electrolyte material, formed microstructure, thickness, working temperature and crystallite size, also.

Optical quartz (SiO_2) and Fe-Ni-Cr alloy (Alloy 600) were the two types of substrates chosen onto which zirconium and cerium based thin films were deposited by e-beam evaporation technique. The influence of deposition rate and particle size of the initial powder material on formed thin films microstructure and other properties were studied. The additional ion bombardment was used to change the microstructure of formed thin films.

The formed thin ceramic films were studied by X-ray diffraction (XRD), atomic force microscope (AFM) and Dynamic ultra-micro harness tester (DUH-211S). The ionic conductivity of the formed thin films was determined by impedance spectroscopy.

The formed thin films repeat the crystallographic orientation of the initial powder material and do not depends on the powder grain size. It was determined that the deposition rate has influence on the crystallite size. The ionic conductivity of formed films depends on the grain size of initial powder.

P-Tu-21

Mechanical properties of nitrogen ion implanted near-surface layers on NiTi Shape Memory Alloy

N. Levintant-Zayonts, S. Kucharski

Institute of Fundamental Technological Research Polish Academy of Sciences, Pawińskiego 5B, 02-106, Warszawa, Poland

In this paper, the recent progress made in our laboratory on NiTi surface modification by ion implantation method are described. The ion implantation is an effective technique to modify the surface properties of materials [1], [2], [3]. We have recently investigated the use of nitrogen ion implantation to improve of NiTi surface wear resistance and good results have been obtained [4]. The purpose of presented paper is investigation of near-surface layer mechanical properties on NiTi shape memory alloy. In order to improve mechanical properties of Nitinol, its surface has been modified by nitrogen ion beam at several fluences: $1x10^{17}cm^{-2}$, $1x10^{18}cm^{-2}$, $2x10^{18}cm^{-2}$ at the energy 50 keV. The effect of ion implantation on mechanical properties such as hardness and elastic modulus was studied using ultra-low load indentation testing. Differential scanning calorimetry (DSC) was used to characterize the transformation sequence and transformation temperatures for the non-implanted and surface-modified NiTi material. The experimental results have shown how the ion implantation treatment can change the original surface properties: reduction of Ni content in a thin layer and increase of its hardness. Furthermore, the hardness increase is observed in regions much deeper than the depth of ion penetration. Such regions has been observed in the cross-section TEM images of implanted NiTi samples. The experimental results of surface treatment parameters and mechanical properties of the modified NiTi alloys are compared, analyzed and discussed in this paper.

References

[1] Hirvonen J.K, ION IMPLANTATION, Academic Press, 1980
[2] Zhao X, Wei Cai, Zhao L, Surf. and Coat. Techn., 2002; 155: 236.
[3] Mandl S, Surf. and Coat. Techn., 2007; 201: 6833.
[4] Levintant-Zayonts N, Kucharski S, Vacuum,2009; 83,: S220.
[5] Cheng F.T, J. Mater. Sci. Techn, 2004; 20: 700.

P-Tu-22

Influence of high dose nitrogen ion implantation into pseudoelastic behavior of NiTi Shape Memory Alloy

S. Kucharski, N. Levintant-Zayonts

Institute of Fundamental Technological Research Polish Academy of Sciences, Pawińskiego 5B, 02-106, Warzsawa, Poland

Publications in recent years show and confirm that alloys with NiTi-matrix belong to the best of shape memory materials (SMAs) [1], [2]. It is well known that this materials exhibit extraordinary shape memory and superelastic properties, which commonly referred to as Shape Memory Effect (SME) and pseudoelastic effect (PE). These properties are a result of reversible martensitic transformation in this class materials [3], [4]. Wide range of their applications in medicine and technology lead to increase of role of their surface. Problem of NiTi alloy surface modification (in the context of improving its characteristics) – on the one hand, and maintenance of functional properties (shape memory effect and superelasticity) on the other hand – is a subject of research and development [5], [6]. In the proposed paper it is shown an attempt of evaluation of changes of mechanical properties of implanted with nitrogen ($1x10^{17}$-$3x10^{18}$j/cm^2) NiTi alloy (in austenitic form). The presented work is focused on investigation of superelastic properties of an equiatomic shape memory NiTi alloy with a surface layer generated by means of nitrogen ion implantation. We applied the spherical indentation (Microindentation test) test for study of the superelastic phenomenon. The results of investigation of selected functional characteristics, i.e. changes of permanent and recovered deformation in a room and elevated temperatures, characteristic temperatures of implanted and non-implanted NiTi alloy are presented.

References:

[1] Machado L, Savi M, J. Of Medical and Biological Research 2003;36:683.
[2] Jan van Humbeeck, Mater. Sci. & Eng.1999;A273-275:134.
[3] Ziolkowski A, Raniecki B, Miyazaki S, Mater. Sci. & Eng. 2004;A378:86.
[4] Naval Research Laboratory website: http://mstd.nrl.navy.mil.
[5] Shabalovskaya S, Anderegg J, J.Van Humbeeck, Acta Biomat. 2008;4: 447.
[6] Levintant N, VACUUM 2007;81:1283.

P-Tu-23

Structural evolution of near-surface layers in NiTi alloy caused by an ion implantation

Z. Swiatek[1)], M. Michalec[2)], N. Levintant-Zayonts[3)], A. Budziak[4)], O. Bonchyk[5)], G. Savitskij[5)]

[1)] *Institute of Metallurgy and Materials Science PASc., Reymonta 25, 30-059, Kraków, Poland*
[2)] *Jagiellonian University, Ingardena, 30-069 Kraków, Poland*
[3)] *Institute of Fundamental Technological Research PASc., Pawińskiego 5B, 02-106,Warszawa, Poland*
[4)] *The Niewodniczanski Institute of Nuclear Physics, PASc., Radzikowskiego 152, 31-342 Kraków, Poland*
[5)] *Institute for Applied Problems of Mechanics and Mathematics NASU, Naukova 5, 79-601 Lviv, Ukraine*

It was reported, that the martensitic transformation temperatures and the mechanical properties of NiTi could be changes by ion implantation [1], [2] as a result of formation of inhomogeneous structure in near-surface layers after ion irradiation [3]. Results of X-ray diffraction studies on structural changes in near-surface layers in equiatomic NiTi alloy caused by nitrogen-ion implantation with the energy 50 keV and dose 10^{18}cm^{-2} have been presented. X-ray diffractometry, using the Philips diffractometer type X'Pert in the Bragg-Brentano geometry, was used to identify the phase composition of NiTi alloy in both conditions: unimplanted and after nitrogen ion implantation. For layer by layer analysis of structural changes in near-surface-layers, the D8 Discover Bruker diffractometer with polycapilar beam optics was used. From the analysis of the X-ray diffraction patterns, it is evident that the implanted NiTi alloy in near-surface-layer exhibits five phases: the dominating austenite phase with a cubic structure, two martensitic phases with a monoclinic one and a small amount of the Ni_4Ti_3 and NTi phases. Along with the decreasing the thickness of near-surface-layer investigated in material an increasing fraction of the Ni_4Ti_3 and NTi phases was observed. For the thickness of this layer about 340 nm, beside still existing the austenite, Ni_4Ti_3 and NTi phases, only one martensitic phase is present in the alloy. Further decrease of the thickness of near-surface-layer to about 170 nm leads to an intensity drop of diffraction lines for the martensitic phase. Simultaneously, an increasing fraction of the Ni_4Ti_3 and NTi phases take place. On the base of results obtained the model of structure changes in ion-implanted region of NiTi alloy is presented.

References

[1] Ikenaga N, Kichi Y, Yajima Z, Sakudo N, Nucl.Inst. and Meth. 2009; B267:1509.
[2] Mandl S, Surface and Coatings Technology 2007; 201: 6833.
[3] Liu X, Shuilin Wu, Materials Science and Engineering 2007;A 444: 192.

P-Tu-24

Studies of Ga+ ions irradiated magnetic Pt/Co/Pt nanostructures

P. Mazalski[1)], A. Maziewski[1)], B. Liedke[2)], M.O. Liedke[2)], J. Fassbender[2)]

[1)] *University of Bialystok, Lipowa 41, 15-424 Białystok, Poland*
[2)] *Forschungszentrum Dresden-Rossendorf, BautznerLandstr. 400, 01328 Dresden, Germany*

Ion irradiation is known as an elegant tool to tune the magnetic properties of ultrathin films, in which the perpendicular anisotropy is mainly of interfacial origin [1-3]. New effect has been recently reported [3] – double spin reorientation (from in-plane to out-of-plane) increasing fluence of 30keV Ga^+ ions irradiating Pt(4.5nm)/Co(2.6nm)/Pt(3.5nm) films. We used TRIDYN software to investigate in these films the dependence of the elements changes and sputtering yields on the applied ion fluence from the range of $1*10^{13}$ to $1*10^{15}$ Ga + ions/cm^2. We have determined the fluence driven changes of: (i) spatial distribution of Co, Pt and Ga ions, (ii) sputtering yield, (iii) distribution of Ga+ ions energy loses. $Co_{1-x}Pt_x$ alloys are known as systems with high uniaxial magnetic anisotropy [4] dependent on the composition parameter x. Spatial distribution of Co-Pt ions, obtained from simulations are used to discuss observed creation of magnetic anisotropy considering magnetic properties of $Co_{1-x}Pt_x$ alloys [4].

This work was in part supported by PPP Polish-Geramny project

References

[1] J. Ferré et al., in Handbook on Magnetism and Advanced Materials. Eds H. Kronmüller and S. Parkin Vol. 3, 1710 (2007).
[2] J. Fassbender and J. McCord, J. Magn. Magn. Mat. 320 (2008).
[3] J. Jaworowicz, et al., Appl.Phys.Lett., 95, 022502 (2009).
[4] D. Weller, H. Brändle, and C. Chappert, J. Magn. Magn. Mater. 121, 461(1993).

P-Tu-25

Electronic sputtering of $Gd_3Ga_5O_{12}$ and $Y_3Fe_5O_{12}$ garnets: yield, stoichiometry and comparison to track formation

A. Meftah[1)], W. Assmann[2)], N. Khalfaoui[3)], F. Studer[4)], M. Toulemonde[3)], C. Trautmann[5)], and K.-O. Voss[5)]

[1)] *LRPCSI, Université 20 août 1955, BP 26, Route d'El-Hadaiek, 21000 Skikda, Algeria*
[2)] *Sektion Physik, LMU München, 85748 Garching , Germany*
[3)] *CIMAP, (CEA-CNRS-ENSICAEN-Univ. Caen), BP5133, 14070 Caen Cedex 5, France*
[4)] *CRISMAT, Université de Caen, 14032 Caen Cedex, France*
[5)] *Gesellschaft für Schwerionenforschung, Planckstr. 1, 64291 Darmstadt, Germany*

Keywords: Sputtering, swift heavy ions, electronic stopping power, garnets.

Previous work [1] has shown that sputtering of yttrium iron garnet ($Y_3Fe_5O_{12}$) under swift heavy ions in the electronic energy loss regime is non-stoichiometric. Here we are presenting additional experimental results for gadolinium gallium garnet ($Gd_3Ga_5O_{12}$) as target. The irradiations were performed with different ions in equilibrium charge states (^{50}Cr (589 MeV), ^{86}Kr (195 MeV), ^{181}Ta (400 MeV), and ^{238}U (150 MeV)). As earlier, the sputtering yield was determined by collecting the emitted gadolinium and gallium atoms on a thin aluminium foil, placed upstream above the target [1] and analyzing the Al catcher by Rutherford backscattering. Also for $Gd_3Ga_5O_{12}$, the emission of Gd and Ga is non-stoichiometric. Sputtering appears above a critical electronic stopping power of S_{th}=10±2 keV/nm, which is larger than the threshold for track formation [2], in agreement with other amorphisable materials [1, 3]. In addition, the angular distribution of the sputtered species was measured for $Y_3Fe_5O_{12}$ and $Gd_3Ga_5O_{12}$ using 200-MeV Au ions (equilibrium charge state). For the two garnets we observe a significantly increased yield (jet) perpendicular to the sample surface superimposed to an isotropic angular distribution. The stoichiometry of Y/Fe (and Gd/Ga) is preserved exclusively in the jet, whereas no Y and Gd species could be detected at large angles within the experimental errors. Such an angular dependence of the stoichiometry suggests a combination of two different sputtering mechanisms.

References

[1] A. Meftah, J.M. Costantini, M. Djebara, J.P. Stoquert, F. Studer, and M. Toulemonde, Nucl. Instr. Meth. B 107 (1996) 242.
[2] A. Meftah, J.M. Costantini, N. Khalfaoui, S. Boudjadar, J.P. Stoquert, F. Studer, and M. Toulemonde, Nucl. Instr. Meth. B 237 (2005) 563.
[3] M. Toulemonde, W. Assmann, C. Trautmann, F. Grüner, Phys. Rev. Lett. 88 (2002) 57602.

P-Tu-26

Phase transformation of Fe-based thin films after ion irradiation

R. Brzozowski, K. Dolecki, B. Pawłowski and M. Moneta

Uniwersytet Łódzki, Wydział Fizyki i Informatyki Stosowanej, Katedra Fizyki Ciała Stałego, Pomorska 149, PL 90-236 Łódź, Poland

It is known that heating reconstructs imperfect structures, whereas heavy ion irradiation makes crystalline sample, at lest locally amorphous. However, especially prepared alloys, initially amorphous alloys, and thus far from thermodynamic equilibrium, undergo partial crystallisation, if some amount of energy is supplied [1,2]. During slowing down of a fast particle its energy lost is deposited to the material mainly through electronic excitations. The both: pulse of heat and shock wave can cause rearrangement of target atoms and introduce or relax internal stress. Recently [3], crystallization induced by 5 GeV Pb ions at low fluence in amorphous Finemet alloys, which exhibit two steps thermal crystallisation was reported, against absence of the crystallisation induced by the ions in case of other materials suffering only a single step thermal crystallisation. Only secondary (without primary) crystallisation was observed, probably in some correlation with absence of Cu. It was reported that crystallites of 1-4 nm size were formed around amorphous ion track of 6-8 nm diameter, thus a single ion converts material from amorphous to crystalline structure roughly within 100 nm^2 area.

In this work properties of 10÷200 nm Fe-based thin films (Fe and Fe_3Si) of initially nano-crystalline or amorphous metal alloys were analysed with conversion electrons Mössbauer spectroscopy (CEMS), γ-ray backscatering Mössbauer spectroscopy (BMS), transmission electron microscopy (TEM) and Rutherford's backsacttering spectrometry (RBS). With the use of physical vapor deposition (PVD) technique, the films were electron beam evaporated in high vacuum on Al/Si(100) substrates maintained in LN_2 temperature. After primary measurements the films were irradiated, also at LN_2 temperature, with a controlled dose of MeV/amu light ion beam and subjected to secondary CEMS, BMS, TEM and RBS measurements. We looked for change of structural and magnetic properties induced in the film at the points of ion incidence.

References

[1] G.Herzer, IEEE Trans. Magn. 1990; 26, 1397.
[2] R.Brzozowski, M.Wasiak, H.Piekarski, P.Uznański, P.Sovak, M. Moneta, J. Alloys and Comp. 2009; 470, 5.
[3] A.Dunlop,G.Jaskierowicz, G.Rizza and M.Kopcewicz, Phys. Rev. Lett. 2003; 90, 015503-1.

P-Tu-27

Role of Ta replacing Nb in Finemet™

A. Puszkarz and M. Moneta

Uniwersytet Łódzki, Wydział Fizyki i Informatyki Stosowanej, Katedra Fizyki Ciała Stałego, Pomorska 149, PL 90-236 Łódź, Poland

The metal alloys, like $Fe_{73.5}Cu_1Si_{13}.5B_9Nb_3$ Finemet, consist primarily of amorphous-magnetic phase which, after appropriate thermal or mechanical treatment, are transformed into the phase in which iron-silicides and borides magnetic nano-crystals are embedded in an amorphous residual matrix [1]. An important task is to keep size of the nano-crystals smaller than the exchange-correlation length.

So far many different modifications of the basic FeSiB compositions were analysed in search for better technical properties. In this work selected properties of Finemet with Ta successively substituted for Nb, were analysed. It can be expected that heavier, but belonging to the same Va group Ta would more than Nb retard nano-crystal growth due to larger atomic size and weaker diffusion. Properties of Fineme alloys $Fe_{73.5}Cu_1Si_{13}.5B_9Nb_{3-x}xTa_{x=0,1,2,3}$ with Nb successively replaced by Ta were studied experimentally using γ-rays and x-rays and e^--beam. Scanning electron microscopy (SEM), energy disperse X-rays (EDX), differential scanning callorimetry (DSC), transmission Mössbauer spectroscopy (TMS) and X-ray diffraction (XRD) were used for analysis.

EDX show agreement between nominal and measured atomic content for all alloys. TMS spectra reveal typical hyperfine structure of annealed nano-crystalline phase embedded in amorphous reminder. XRD scans of annealed alloys show crystalline phases, corresponding to that for pure Finemet™.

References

[1] G.Herzer, IEEE Trans. Magn. 1990; 26, 1397.
[2] R.Brzozowski, M.Wasiak, H.Piekarski, P.Uznański, P.Sovak, M. Moneta, J.Alloys and Comp. 2009; 470,5.

P-Tu-28

Aluminium morphological modification by nitrogen-argon mixture PIII

A.E. Muñoz-Castro[1)], *R. López-Callejas*[1,2)], *R. Valencia Alvarado*[1)], *R. Peña-Eguiluz*[1)], *A. Mercado-Cabrera*[1)], *S.R. Barocio*[1)], *B.G. Rodríguez-Méndez*[1)], *A. de la Piedad-Beneitez*[2)]

[1)] *Instituto Nacional de Investigaciones Nucleares, AP 18-1027, 11801, Mexico DF*
[2)] *Instituto Tecnológico de Toluca, AP 890, Toluca, Estado de México, Mexico*

With incident fluencies of ~10^{18} atoms/cm^2 aluminium samples have been PIII implanted with either pure nitrogen or argon/nitrogen mixtures at temperatures around 400|°C. X ray diffraction studies have validated the formation of the cubic phase of AlN, in samples treated with both the gas mixtures and pure nitrogen. Likewise, the presence of the hexagonal phase of AlN has been detected when either pure nitrogen or the 50% mixture have been used. The signature peak of AlN has also been confirmed by Raman spectroscopy. The maximal microhardness values were found in samples treated with the equal part mixture. The maximal roughness was achieved with this gas mixture in all cases, although increasing with the implantation pulse width up to a 350 nm peak at 150 μs. The latter critical value remains invariant under the pure nitrogen plasma treatment, provided that implantation periods in the order of 4.5 hour are carried out.

P-Tu-29

Investigation of direct current discharge plasma in a coaxial structure

A.R. Niknam, S. Abdi, A.R. Rastkar

Laser and Plasma Research Institute, Shahid Beheshti University, G.C., Evin, 1983963113, Tehran, Iran

It is well known that the direct current discharges are used widely in the material processing industry for thin film deposition. Therefore, the modeling of the direct current discharge plasma at low pressure in a coaxial structure is presented. This structure consists of three media: plasma, dielectric and air. A metallic rod is placed in the axis of the setup and a metallic cylinder shields the whole system. A direct current voltage is applied to these two metals. Considering the diffusion regime in the plasma bulk and using the diffusion equation, we obtain the radial electron density profile in the plasma region. Furthermore, the model is based on the solving of the Laplace's and Poisson's equations. The radial distributions of the direct current electric field and potential are shown by using the appropriate boundary conditions on electric field and electric displacement vector at plasma boundaries and dielectric-air boundary.

P-Tu-30

Physical-chemical, mechanical, thermal, and radiation resistance of hard and super-hard nano-structured coatings

Alexander D. Pogrebnjak[1,2], Mannab Tashmetov[3], Maxim Il'yashenko[1,2], Nemat A. Makhmudov[4], Vyacheslav M. Beresnev[5], Oleksey Borysenko[1], Igor Kulik[1], Mikhail Kaverin[1,2], Ivan Yakuschenko[1,2], Janusz Partyka[6], Bogdan Postolnyi[1,2]

[1] *Sumy State University, Department of Electron Techniques and Physics, 40007 Sumy, Ukraine, apogrebnjak@simp.sumy.ua*
[2] *Sumy Institute for Surface Modification, P.O.Box 163, 40030 Sumy, Ukraine, e-mail;alexp@i.ua*
[3] *Institute of Nuclear Physics, NAS of Uzbekistan, Tashkent, Uzbekistan*
[4] *Samarkand Branch of Tashkent State University of Information, Samarkand, Uzbekistan*
[5] *Kharkov National University, Kharkov, Ukraine*
[6] *Lublin University of Technology, Lublin, Poland*

The report deals with investigation results on structure and properties of hard Zr-Si-N, Zr-Ti-N, and super-hard Zr-Ti-Si-N coatings of 1.8 to 3.2μm thickness. Coated samples were γ-irradiated during several months in a reactor and cobalt gun. Hardness of Zr-Si-N coatings was 28 to 32GPa, that of Zr-Ti-N reached 35 ±2.6GPa, and hardness of Zr-Ti-Si-N was 40 to 48GPa.

Thermal annealing of coated samples to 550^{o}C increased their hardness to 53GPa, and subsequent γ-quantum-irradiation under 10^8 to 10^9Grey essentially decreased their hardness. Nano-grain sizes increased as a result of annealing and subsequent γ-quantum-irradiation. Inter-layers of amorphous phase (α-Si_3N_4) surrounding nano-grains (Zr, N)-*nc*, ….(Zr, Ti)N-*nc* increased by several per cent, which seemed to be related to enhanced processes of relaxation-accelerated diffusion γ-quantum-irradiation of samples with super-hard coatings till high-temperature annealing resulted in a shift of hardness maximum to 150^{o}C (as a result of subsequent annealing in vacuum) closer to the beginning of temperature interval.

The work was funded within the framework of project "Nano-Systems, Nano-Composite Coatings, and Nano-Materials" of National Academy of Science of Ukraine.

Key words: Hardness, γ-quantum-irradiation, nanocomposite, annealing, structure.

P-Tu-31

Structure and mechanical properties of superhard nanocomposite coatings on Hf-Ti-Si-N base

A.D. Pogrebnjak[1,2], V.M. Beresnev[3], M.V. Kaverin[1,2], Cz. Karvat[4], N.A. Makhmudov[5], M.V. Il'yashenko[1,2], O.V. Sobol[5], A.P. Pshyk[1], V.A. Baidak[1], A.A. Dem'yanenko[1]

[1] *Sumy State University, 40007 Sumy, Ukraine*
[2] *Sumy Institute for Surface Modification, P.O.Box 163, 40030 Sumy, Ukraine*
[3] *Kharkov National University, Kharkov, Ukraine*
[4] *Lublin University of Technology,Lublin,Poland*
[5] *Kharkov Technical University (KhPI), Kharkov, Ukraine*
[6] *Samarkand Branch of Tashkent University of Information, Samarkand, Uzbekistan*

Using vacuum-arc deposition with HF discharge, superhard coatings Hf-Ti-Si-N of 3.2 to 4μm thickness, 46 to 62GPa hardness, and high values of elastic modulus reaching 480 to 630GPa, were fabricated. For coating deposition, we employed a composite sintered cathode Hf-Ti-Si, leaking-in N into the source chamber.

We found that multiple changes of physical-chemical and mechanical properties depended essentially on potential, which was fed to a substrate, rather than pressure of Ar/N mixture fed to reaction chamber.

Using RBS, EDS with SEM, XRD, X-ray tensometry (α-$\sin^2\psi$-method), AFM, STM, measurements of nanohardness and cylinder-plane wear tests, we investigated structure, properties, and stress of the coatings.

Grain size of nanocomposite coatings was determined using XRD and TEM, which demonstrated 6.8 to 15.6nm range. Phase composition of the coating was determined using X-ray diffraction and transmission electron diffraction and was the following nc-(Ti,N), nc-(Hf, Ti)N, and α-Si_3N_4. Hf, Ti, and Si concentration varied depending on condensation (deposition) conditions.

Keywords: superhard nanocomposite coatings, wear, structure, properties, Hf-Ti-Si-N.

P-Tu-32

Multilayers nanocomposite coatings Ti-N-Al/Ti-N/Al_2O_3/substrate, their structure and properties

A.D. Pogrebnjak[1,2], V.M. Bersnev[1,2], M.V. Il'yashenko[1,2], M.K. Kylyshkanov[3], A.P. Shypilenko[1,2], M.V. Kaverin[1,2], N.K. Erdybaeva[3], P.V. Zukovski[5], F.F. Komarov[4], Yu.Zh. Tuleushev[6]

[1] *Sumy Institute for Surface Modification, PO BOX 163, 40030 Sumy, Ukraine*
[2] *Sumy State University, R-Korsakov-2, Sumy 40007, Ukraine*
[3] *East-Kazahstan State Technical University, Ust'-Kamenogorsk, Kazahstan*
[4] *Belarus State University, Minsk, Belarus*
[5] *Lublin University of Technology, Lublin, Poland*
[6] *Nuclear Physics Institute, NNC, Almaty Kazahstan*

The works presents first results on formation and investigation of structure and properties of nanocomposite combined coatings. Modeling the deposition processes (deposition conditions, current density-discharge, plasma composition and density, voltage) we formed the three-layer nanocomposite coatings of Ti-N-Al/Ti-N/Al_2O_3/.The coating composition, structure and properties were studied using physical and nuclear-physical methods. We applied the Rutherford proton and helium ion back scattering (RBS), Scanning Electron Microscopy with microanalysis

(SEM with EDS and WDS),X-Ray diffraction (XRD) including a sliding beam to 0.5^o, as well as nanohardness tests(hardness),Measurements of wear resistance, corrosion resistance in NaCl, HCl and H_2SO_4 solution. Also we measured such characteristics as H(hardness), elastic modulusE:H3/E2 etc. It was demonstrated that the formed many-layered(three-layer) nanocomposite coating had hardness 32 to 36GPA,328+- 18 to 364+ -14 GPa elastic modulus.

Its wear resistance (cylinder-surface friction) increased by a factor of 17 to 25 in comparison to the substrate(stainless steel). The layers thickness was 56- 120 mkm.

The work was funded by the Project NAS Ukraine and ISTC K-1198.

Keywords: structure and properties of nanocomposite combined coatings, wear, corrosion resistance

P-Tu-33

Phase composition, thermal stability, and properties of hard ZrN and superhard on base Zr-Ti-Si-N nanocomposite coatings

A.D. Pogrebnjak[1,2], O.V. Sobol[3], V.M. Beresnev[4], M. Kozak[5], N.A. Makhmudov[1,6], M.V. Il'yashenko[1], A.P. Shypylenko[1,2], M.V. Kaverin[2], M.Yu. Tashmetov[7], V. Rogoz[1,2], A.V. Pshyk[1,2]

[1] *Sumy Institute for Surface Modification, P.O.Box 163, 40030 Sumy, Ukraine, E-mail: apogrebnjak@simp.sumy.ua*
[2] *Sumy State University, 40021 Sumy, Ukraine, alexp@i.ua*
[3] *National Technical University, Kharkov, Ukraine*
[4] *Science Center for Physics and Technology, Kharkov, Ukraine*
[5] *Lublin University of Technology, Lublin, Poland*
[6] *Samarkand Branch of Tashkent Information Technology University, Samarkand, Uzbekistan*
[7] *Institute of Nuclear Physics, UAS, Tashkent, Usbekistan*

Zr-Ti -Si-N coating had high thermal stability of phase composition and remained structure state under thermal annealing temperatures reached 1180°C in vacuum and 830°C in air. Effect of isochronous annealing on phase composition, structure, and stress state of Zr-Ti-Si-N- ion-plasma deposited coatings (nanocomposite coatings) was reported. Below 1000°C annealing temperature in vacuum, changing of phase composition is determined by appearing of siliconitride crystallites (B-Si_3N_4) with hexagonal crystalline lattice and by formation of ZrO_2oxide crystallites. Formation of the latter did not result in decay of solid solution (ZrTi)N but increased in it a specific content of Ti-component. Vacuum annealing increased sizes of solid solution nanocrystallites from (12 to 15) in as-deposited coatings to 25nm after annealing temperature reached 1180°C. One could also find macro- and microrelaxations, which were accompanied by formation of deformation defects, which values reached 15.5 vol.%.Under 530°C annealing in vacuum or in air, nanocomposite coating hardness increased, demonstrating, however, high spread in values from 29 to 54GPa (first series of samples). When Ti and Si concentration increased (second series) and three phases nc-ZrN, (Zr, Ti)N-nc, and α-Si_3N_4 were formed, average hardness increased to 40,8 ± 4GPa.(second series of samples). Annealing to 500°C increased hardness and demonstrated lower spread in values H = 48 ± 6GPa and E = (456 ± 78)GPa.

P-Tu-34

Computation of diffusion processes in nanoscale thin films system based on Fe and Cr

Serhiy Protsenko[1)], *Helena Fedchenko*[1)], *Marta Marszalek*[2)], *Pawel Zukowski*[3)]

[1)] *Sumy State University, R.-Corsakova str.2, 40007, Sumy, Ukraine*
[2)] *The Institute of Nuclear Physics Polish Academy of Science, Radzikowskiego 152, 31-342, Kraków, Poland*
[3)] *Lublin University of Technology, Nadbystrzycka 36B, 20-618, Lublin, Poland*

Wide usage of nanocrystalline multilayer film systems in microelectronics constantly stimulates research of various phenomena, including diffusion. In this work, an Auger electron spectroscopy (AES) (one of the most widely used modern technique for the surface analysis of solids) has been performed and the condensation-induced diffusion in nanoscale film systems Fe/Cr/Si and Cr/Fe/Si has been investigated. Auger spectrum for these structures was obtained on each step of increasing the top layer thickness on 0.5nm.

Then values of elemental sensitivity were used for interpretation of the experimental data and for concentration profile calculation. According to these results the effective condensation-induced diffusion coefficients were determined with help of different computational models: Fourier analysis, Sudzuoki and Matano methods, Gaussian error function, the method for double-layer thin films (H. Zefakis, I. Gain) and estimation formula [1]. The results are given in Table 1.

Table 1. Computational results for effective condensation-induced diffusion coefficient $D \cdot 10^{-19}$(m/sec^2) of nanoscale film systems Fe/Cr/Si and Cr/Fe/Si.

Calculation model	Fourier analysis	Sudzuoki method	Matano method	Gaussian erfc	Zefakis method	Estimation formula
Cr→Fe	0,61	0,95	0,52	0,64	0,74	≤ 0,9
Fe→Cr	0,24	0,18	0,14	0,22	0,25	≤ 0,5

As we can see from the table above the most correct method for the description of diffusion process in nanoscale film systems is Sudzuoki method.

Reference

[1] Wang J., Mittemeijer E., Material Research 2004; 19:33.

P-Tu-35

Application of Raman microspectroscopy to the studies of carbon-silver coatings formed by DB IBAD on polyurethane substrate

B. Rajchel, J. Kwiatkowska

Institute of Nuclear Physics Polish Academy of Sciences, 31-342 Kraków, Radzikowskiego 152, Poland

The polyurethane parts of artificial heart can be modified by covering them with a thin coating with biocompatible and bioactive properties. The carbon-silver layer is a good candidate to improve bioactivity of polyurethane surface, however, only coatings with excellent adhesion to the substrate can be accepted. For this reason the dual beam IBAD method was applied to create the carbon-sliver coatings. The polyurethane-coating system was studied by confocal, dispersive Raman microspectroscopy to determine the type and depth distribution of chemical bonds formed in the process.

The adhesion and stability of the coatings were also tested by recording the Raman spectra at elevated temperatures.

This work was partly supported by the project “Polish Artificial Heart”.

P-Tu-36

Martensite γ→α transformation in deformable stainless steels irradiated with ions and pulse electron flows

A.V. Russakova, D.T. Berdaliev, O.P. Maksimkin, K.V. Tsay

Institute of Nuclear Physics NNC RK, Almaty

It was revealed earlier that intensive influence of high energy particles can lead to formation of thin ferromagnetic layers on surface of austenitic stainless steels/1/. Along with that it is noticed that occurrence of a ferromagnetic layer took place at evaporation of easy volatile components (Cr, Mn) from paramagnetic material /2/.

It is not excluded that the favorable conditions (temperature, an irradiation) for this effect can develop on surfaces of constructional materials of the first wall of thermonuclear facilities in the conditions of their operation. Thus formation of magnetic layers can be promoted by the blistering phenomenon, and also by the martensite γ→α transformation.

Thereupon in the present work the influence of irradiation with light (C, N, Ti) and heavy (WC, ^{84}Kr) particles, and also with pulse electron flow (E=200-500 keV, g=10^7-10^{10} W/cm^2) on characteristics of durability and plasticity at stretching and fatigue tests, and also regularities of non-diffusive γ→α transition in a corrosion-proof industrial steel 12Cr18Ni10Ti and austenitic nickel less steels Cr15Mn14 were investigated.

By means of transmission electronic microscopy and magnetometry methods the dislocation structure and phase structure of the near-surface layers modified by an irradiation was investigated.

In particular, it was established that as a result of influence on materials of pulse electronic beams in deep layers of 12Cr18Ni10Ti steel the dislocation structure, typical for strongly deformed material with low energy of packing defect is formed. The increase of power density over $5\cdot10^8$ W/cm^2 has led to the formation of developed cellular dislocation structure which evolution comes to the end with origin and development of martensite α - phase.

For 12Cr18Ni10Ti steel, implanted by C and N ions, durability at low-cycled fatigue tests was defined, vicissitude of destruction process was revealed and the important role of γ→α transformation kinetics in formation of fatigue properties of the metastable steel was shown. As a result of the steel irradiation with heavy ^{84}Kr ions with energy E=1.56 MeV /nucleon and fluence 1x10^{15} particles/cm^2 in the near-surface layer according to electronic- microscope researches so-called α – «irradiation martensite» is formed.

Bombardment of the deformed samples of Cr15Mn14 steel by WC ions with energy of 50 KeV has led to the appreciable change of their magnetization which is connected with formation of so-called «elastic α - martensite» which content changed as a result of loading removal and repeated loading of plastically deformed steel.

References

[1] V.K.Shamardin, Z.E.Ostrovsky, A.M. Pecherin, V.M.Kosnkov, V.V. Jakovlev, F.V.Risovannaja. Research of screen assemblage e-26 cover after 22-year-old exploitation in BOR-60 reactor. In the

book “Collection of reports of the fifth interbranch conference on reactor material science”. Vol.2.part2., Dmitrovgrad 1998.,p.25-40;
[2] G.S.Krinchik, L.V.Nikitin, L.I.Ivanov, G.G.Bondarenko, G.M.Fedichkin “Magnet-optical method of the first wall of thermonuclear reactor material research”, given by academician B.B.Kadomtsev 20 V II 1987, p. 839-841.

P-Tu-37

Diagnosis and investigation strategies in the Coptic mural paintings in Upper Egypt

A. Sallam[1)], M. Fouad[2)], B. Ismail[3)], S. Abd El Aal[4)]

[1)] *Conservation Department, Faculty of Archaeology, South Vaelly University, Qena, Egypt, E-mail: sallam90@hotmail.com*
[2)] *Conservation Department, Faculty of Archaeology, Cairo University, Egypt*
[3)] *Conservation Department, Faculty of Archaeology, South Vaelly University, Egypt*
[4)] *Conservation Department, Faculty of Archaeology, Fayoum University, Egypt*

The Monasteries in Upper Egypt suffer from many manifestations of the damage which associated with the complex mechanisms of weathering. Many of natural and anthropological,we find that the human damage is one of the most important mechanisms of damage to those monasteries also find that known as wall painting multi-layered (Over Painting).Diagnosis and investigation strategies PhaseI: Studies Status:This phase includes studies of the impact of the current situation and documentation, studies. PhaseII:laboratory tests of materials by SEM, PL, XRD, XRF, EDX, FTIR and Raman. PhaseIII:the restoration project: restoration plan to reach the best results through the restoration workshop to reach sound decisions and to avoid quick decisions that may affect negatively on the work itself, and in this way be reduced to unforeseen events, which increase the risk and cost.The study proved that the technique performed duties in Coptic wall painting is Semi Fresco and is not common to all Coptic wall painting executing in Fresco but Semi Fresco, through analysis by infrared IR & FTIR been identified one medium which is Arabic gum that was used by Coptic artist with pigments.

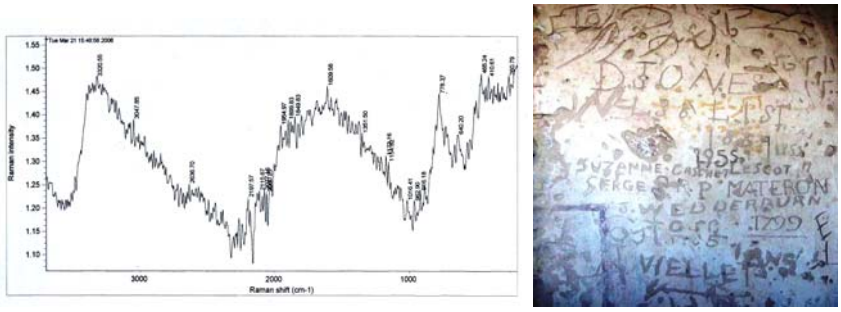

Fig. 1. A view of multiple flakes for pigment of red analysis by Raman

P-Tu-38

Comparative study of the Stratagraphic Composition of mural painting in Qubbet el Hawa Monastery and Anba Hidra Monastery in the eastern bank in Aswan

A. Sallam[1)], *M. Fouad*[2)], *B. Ismail*[3)]

[1)] *Conservation Department, Faculty of Archaeology, South Valley University, Egypt*
[2)] *Conservation Department, Faculty of Archaeology, Cairo University, Egypt*
[3)] *Conservation Department, Faculty of Archaeology, South Valley University, Egypt*

In Monasteries of Upper Egypt, the Coptic artist usually applied several plaster layers over old ones, a common application at that time which is now known as multi-layered wall painting (over painting). Deir Oubbet El-Hawa in Aswan was built with Nubian sandstone blocks, and mud bricks were used for supporting purpose in various regions. The stone support was prepared in order to fill the gaps, and this step involved covering the support with a thin layer of rough plaster, approximately 4 mm thick. A second layer of rough plaster about 3 mm thick was applied. In this case, rough plaster is a mixture of kaolinite, sand, and anhydrite minerals. There is also a third layer about 1-2 mm thick made from white-thin lime and very fine sand. This former layer is known as the ground layer, and it was probably made for painting purpose. Studies have revealed the presence of another rough plaster layer, approximately 0.6-0.9 mm thick. This layer is a mixture of sand, clay minerals, and calcium carbonate as a binder. Perhaps this layer was made to cover the murals located below it. This was followed by a fine sand and lime layer about 4 mm thick. Thus, the total thickness here is about 2 cm. In Deir Anba Hidra found in Aswan, the support is covered with a layer of plaster made from a mixture of coarse sand and clay minerals. Its thickness is no more than 5 mm. On top, there is a layer of plaster about 2 mm thick made from soft lime and proportions of gypsum and sand. A yellow colored preparatory layer was also noted and it is about 0.5 mm thick. This study explores a new technique for historical Coptic Monasteries.

photo showing the general view of the Dome of the top al-Hawa in Aswan tombs of nobles

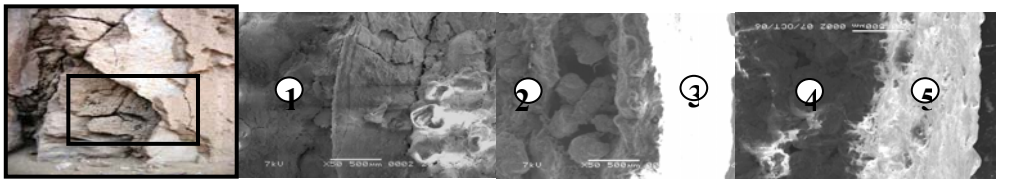

Picture by SEM show the composition of Stratagraphic the Monastery of the Dome Hawa in Aswan X50

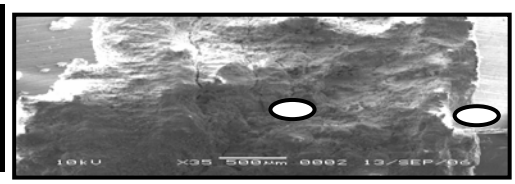

Picture by SEM show the composition of the Stratagraphic Monastery of the Anba Hidra in Aswan X50

P-Tu-39

Structure and composition of scales formed on AISI 316 L steel alloyed with Ce/La using high intensity plasma pulses after oxidation in 1000°C

Bożena Sartowska[1)], Jerzy Piekoszewski[1,2)], Lech Waliś[1)], Marek Barlak[1,2)], Wojciech Starosta[1)], Cezary Pochrybniak[2)], Katarzyna Bocheńska[2)]

[1)] Institute of Nuclear Chemistry and Technology, Dorodna 16, 03-195 Warszawa, Poland
[2)] The Andrzej Sołtan Institute for Nuclear Studies, 05-400 Otwock/Świerk, Poland

The beneficial effect of active elements with high oxygen affinity, such as yttrium, cerium, lanthanum and other rare earths elements (REE) on high temperature oxidation resistance of austenitic stainless steel is well documented.

In order to introduce Ce and La into austenitic stainless steel AISI 316L surface, the high intensity plasma pulses (HIPP) were used. The plasma pulses contain both ions/atoms of Ce and La and those of the working gas. The pulse energy densities with their duration in μs range were sufficient to melt the near surface layer of the substrate and hence introduce those elements into the surface layer of steels.

Modified samples were oxidized at 1000ºC for 100 h in air at atmospheric pressure. The obtained effects were: oxide scales formed on the HIPP treated samples were more fine-grained, compact and adhered better that those formed on the un-treated samples.

In the present work we report the results of examination of scales structure and their composition. Surface distribution of elements present in investigated materials, mainly Fe, Cr and REE was determined. Structure of grains observed at the oxidized surfaces was also determined.

Structure and properties of nanocomposite coating based on Ti-Si-N/WCCo-Cr

A.D. Pogrebnjak[1,2], V.M. Beresnev[3], M.V. Il'yashenko[2], A.P. Shypylenko[1,2], M.V. Kaverin[1,2], P.V. Zukovski[7], Yu.A. Kunitskyi[4], O.V. Kolisnichenko[5], N.A. Makhmudov[6]

[1] *G.V. Kurdyumov Institute for Metal Physics, NAS Ukraine, Sumy, Ukraine*
[2] *Sumy Institute for Surface Modification, PO BOX 163, Sumy, Ukraine*
[3] *Science Center for Physics and Technology, Kharkov, Ukraine*
[4] *Institute of Metal Physics, G.V.Kurdyumova NAS of Ukraine, Kiev, Ukraine*
[5] *O.E. Paton Welding Institute, NAS of Ukraine, Kiev, Ukraine*
[6] *Samarkand State University, Samarkand, Uzbekistan*
[7] *Lublin Technical University, Lublin, Poland*

Using two technologies: a plasma-detonation and a vacuum-arc deposition, we fabricated two types of coatings: Ti-Si-N/WC-Co-Cr/steel and Ti-Si-N/steel. We found that an top coating of Ti-Si-N was a nanostructured one, with 12 to 15 nm grain dimensions and 30 to 38 GPa hardness. A thick coating which was deposited using a pulsed plasma jet, demonstrated 11 to 15.3 GPA hardness, an elastic modulus changing within 176 to 240 GPa, and tungsten carbide grain dimensions varying from 150 to 350 nm to several microns.

An XRD analysis shows that the coating has the following phase composition: (Ti,Si)N solid solution, WC, W_2C tungsten carbides. An element analysis was performed using EDS (a microanalysis) and SEM, as well as a Rutherford back-scattering RBS of $^{+}He^{4}$ ion and AES.

A surface morphology and structure were analyzed using SEM (scanning electron microscopy) and a scanning tunnel microscopy. Tests for friction and resistance (cylinder-plane) demonstrated an essential resistance to an abrasive wear and to corrosion in a solution.

A decrease of grain dimensions ≤10 nm occurring in the top Ti-Si-N coating layer increased the sample hardness to 42±2.7 GPa under Ti_{72}-Si_8-N_{20} at.% concentration.

The work was performed within the framework of a project: Nanotechnologies, nanocoatings and nanosystems "Production of nanocomposite materials and coatings using ion, plasma and electron beams " NAS of Ukraine.

References

[1] A. D. Pogrebnjak, A. P. Shpak, N. A. Azarenkov, V. M. Beresnev. Usp.Phys. 2009 179. 1. P. 35-64.
[2] Sh. Hao, B. Delley, S. Veprek, Cath. Stampl. Phys. Rev. Lett. 2006. V. 97. 086102. P. 1-4.
[3] V. M. Beresnev, A. D. Pogrebnjak, N. A. Azarenkov, G. V. Kirik, N.K.Erdybaeva, V. V. Ponaryadov. Progress in Physics of Metals. 2007. V. 8. N. 3. P. 172-246.

Environmental equipment for a classic SEM enabling investigations of dielectric and wet surfaces

Witold Słówko and Michał Krysztof

Faculty of Microsystem Electronics and Photonics, Wroclaw University of Technology, Janiszewskiego 11/17, 50-372 Wrocław, Poland

Classic Scanning Electron Microscopes (SEM) are vacuum instruments, which disqualify insulator specimens or those with high vapour constituents like water. These limitations can be overcome in Variable Pressure or Environmental SEM (VP/E SEM) operating at elevated pressure in the sample chamber while the electron optical column is maintained at high vacuum [1]. This implies differential pumping of the two regions which have to be separated by an intermediate chamber with vacuum of order of 10^{-2}mbar, limited by two pinhole throttling apertures preventing intensive gas flow from the sample chamber to the high vacuum side. A second peculiarity of the VP/E SEM is an electron detection system which must work at the elevated gas pressure.

To extend capabilities of the classic instrument toward the VP/E technique, authors supplemented it with the two mentioned units [2], designed in the form of a simple attachment, which can be mounted to a classic SEM, without changes in its original structure. The main part of the system is the vacuum and detection head, combining the intermediate chamber and electron detectors of chosen kinds. The low vacuum secondary electron (SE) detector extracts electrons through the lower throttling aperture and is designed in the form of an unipotential electrostatic lens with the anode covered with scintillator. It can work from pressures exceeding 10 mbar to high vacuum, i.e. in the whole range of the SEM applications for almost all possible samples. Ions generated in electron collisions with gas molecules recombine with electrons deposited by the scanning beam on non conducting surfaces which enables investigations of dielectric samples without conductive coatings. On the other hand, samples containing liquid water like suspensions and slurries or biological samples can be observed on the Peltier stage cooled to ~ 0 ^{o}C. This reduces the water vapour pressure necessary to keep the sample in a natural state to ~ 5 mbar, and facilitates imaging of light samples at low accelerating voltages.

References

[1] Danilatos G, Advances in Electronics & Electron Physics,1988;71: A.P. London.
[2] Słówko W, Krysztof M, Proc. Microscopy Conf. MC2009 Graz; V.1:227.

Vacuum system of the thermostat TS-3000K

C. Oprea[1)], G. Mateescu[2)], Zh.A. Kozlov[1)], I.A. Oprea[1)], V.A. Semenov[3)], I. Padureanu[2)], M. Ion[2)], L. Craciun[2)], P.J. Szalanski[4)], M. Curuia[5)], I. Stefanescu[5)]

[1)] *Joint Institute for Nuclear Research, 141980 Dubna, Russia, E-mail: coprea2007@yahoo.co.uk*
[2)] *"HORIA HULUBEI" – National Institute for Physics and Nuclear Engineering, Bucharest, RO-077125, Romania*
[3)] *Institute for Physics and Power Engineering, Obninsk, Russian Federation*
[4)] *Faculty of Physics and Applied Informatics, Łódź University, Łódź, Poland*
[5)] *Institute of Cryogenic and Isotopic Technologies, 1000 Ramnicu Valcea, Romania*

A high temperature thermostat TS-3000K has been designed for investigation of structure and dynamics in condensed matter by scattering neutron methods. It allowed measurements of large targets at temperatures up to 2500K. The thermostat TS-3000K is operating at the DIN-2π spectrometer installed on the channel two of the IBR-2 reactor.

The thermostat TS-3000K is a complex installation which contains mechanical, electric, pneumatic and vacuum equipments, organized in 5 separated sub-units as the furnace itself, the vacuum system, the cooling system, the electrical and power supply system and respectively, the control panel of the thermostat. The main characteristics of the facility are the followings: the power 60 KVA, pressure in technologic area during heating of ~ 10^{-6}mbar, sample temperature adjustable in the range 200-~2700^{0}C.

References

[1] Balasko, M., E. Svab, G. Endrczy. 2005. Comparison of neutron radiography with other nondestructive methods. IEEE Transactions on Nuclear Science 52 1:330.
[2] Tohru, Gemma and Kazuyoshi, Ogino. 1989. Thermostat for Dynamic Light Scattering Measurements at High Temperatures. Jpn. J. Appl. Phys. 28:916.

The method of perturbed angular correlations used to study the molecular dynamics in Satureia hortensis vegetal oil

C. Oprea[1)], A.I. Velichkov[1)], D.V. Filossofov[1)], I.A. Oprea[1,2)], P.J. Szalanski[3)], A. Mihul[2)]

[1)] *Joint Institute for Nuclear Research, 141980 Dubna, Russia*
[2)] *Bucharest State University, 76900 Bucharest, Romania*
[3)] *Faculty of Physics and Applied Informatics, Łódź University, Łódź, Poland*

The perturbed angular γγ-correlations method (γγ-PAC) technique has been employed to study the parameters of hyperfine interactions in aqueous solutions of vegetal oils, using ^{154}Eu isotope as a probe nucleus. The measurements were carried out by means of a four-detector perturbed angular γγ-correlations spectrometer. The perturbation factors $A_2G_2(t)$ in strongly mixed and centrifuged liquid and solid solutions of vegetal oil in the presence of a reactivant (as 2–ethilexil–ortho-phosphorus acid) and a metal were measured. The spectrum data suggest a high degree of local flexibility of the europium label. The attenuation is more pronounced with increasing concentration of the metal. The relaxation constant increases with increasing concentration of the solution.

References

[1] Akselrod, Z.Z., D.V. Filossofov, et al. 2000. Z. Naturforsch. 55a:151.
[2] Brudanin, V.B., D.V. Filossofov, O.I. Kochetov, N.A. Korolev, et al. 2005. Nucl. Instrum. Meth. in Phys. Res. A 547:389.
[3] Hemmingsen, L., T. Butz, 2008. Encyclopedia of Inorganic Chemistry, DOI: 10.1002/0470862106.ia322.
[4] Hickman, G.D., M.L. Wiedenbeck, 1958. Phys. Rev. 111 2:539.
[5] Ivanov, E., Vata, I., Dudu, D., Rusen, I, et al., 2008. Appl. Surf. Sci. 225:179
[6] Tsvyashchenko, A.V., L.N. Fomicheva, M.V. Magnitskaya, E.N. Shirani, et al. 2001. Solid state Commun. 119(3):153.
[7] Wolf, A., C. Chung, W.B. Walters, G. Peaslee, et al. 1983. Nucl. Instrum. Meth. 206:397.

P-Tu-44

TEM and AFM investigation of obliquely evaporated thin cobalt films

Witold Szmaja[1)], *Michał Cichomski*[2)], *Katarzyna Kośla*[2)], *and Józef Balcerski*[1)]

[1)] *Department of Solid State Physics, University of Łódź, Pomorska 149/153, 90-236 Łódź, Poland*
[2)] *Department of Chemical Technology and Environmental Protection, University of Łódź, Pomorska 163, 90-236 Łódź, Poland*

Cobalt films 100 nm thick were thermally evaporated on NaCl crystals at an incidence angle of 45° (with respect to the surface normal) in a vacuum of approximately 10^{-5} mbar. The magnetic structure of the films was made visible by the Fresnel mode of transmission electron microscopy (TEM), their morphological structure was observed with atomic force microscopy (AFM), and their crystallographic structure was revealed by electron diffraction of TEM. The magnetic structure was composed of domains running predominantly in the direction parallel to the incidence plane. The domains were a few micrometers in size and were substantially magnetized in the plane of the film. The morphological structure consisted of nanocrystalline grains. The films were mainly composed of the hexagonal close-packed (HCP) phase of cobalt.

P-Tu-45

Effect of argon plasma on the glass surface

Marek Tuleta

Institute of Physics, Technical University of Cracow, Podchorążych 1, 30-084 Kraków, Poland

The effect of argon plasma on the glass surface was studied using samples of commercial float glass. This glass is one of the most important kinds of commercial glass widely used in modern architecture, automotive industry and optoelectronics [1]. The float glass is flat, multicomponent oxide glass manufactured in the float process, in which the molten glass material floats on the bath of molten tin in a hot reducing atmosphere. Therefore, the float glass has two characteristic surfaces (the bottom and top surfaces) differing in the chemical composition and structure from those of the bulk.

Both surfaces were treated simultaneously by the low-temperature argon plasma generated by an inductively coupled rf power supply. The influence of plasma treatment on the outer surface composition of both sides of the glass was analysed by means of the ion scattering spectroscopy (ISS) technique.

The observed recomposition of the outer surface atoms was explained basing on the thermal and electric fields created by the plasma.

References

[1] Takeda S, Akiyama R, Hosono H, J. Non-Cryst. Solids 2002;311:273.

P-Tu-46

Ionization efficiency of a source with a spherical ionizer

Marcin Turek

Institute of Physics, Maria Curie Sklodowska University, Lublin

Particular needs of various applications in fields of spectroscopy, material science, micro- and optoelectronics, isotope separation, medicine and many others resulted in a multitude of ion source constructions. One of them is a surface ionization source equipped with a hot cavity ionizer charcaterized by small dimensions and a simple design. Despite the fact the source was invented many years ago [1,2] it is still successfully used and developed [3,4], mostly due such their advantages as: the purity of obtained ion beam (free of multicharged and residual gas ions), high ionization efficiency as well as a low energy spread of extracted beam, the short time ions remain in the ionizer, which is a clue in the case of short-lived isotopes.

The paper presents a numerical model of ionization in a spherical ionizer. The code solves equation of motion for particles trapped inside the ionizer. It is assumed that neutral particles undergo ionization with some probability when touching a hot surface, as described by Saha-Langmuir formula [5]. This process is modelled using Monte Carlo methods to decide whether the particle was ionized/neutralized or not, as well as to determine a velocity for desorbed particle. Two kinds of a spherical ionizer geometry are considered. First of them (conf. A) resembles that used in experiments for both negative and positive ion production [6,7] In that case a hemispherical ionizer closed by a plate with extraction hole was used. Another configuration (B) we propose is a spherical cavity with a small extraction opening. It will be shown that such shape of the ionizer leads to source efficiency β_s higher than in the previous case, due to stronger effect of multiple collisions with hot walls (see figures below).

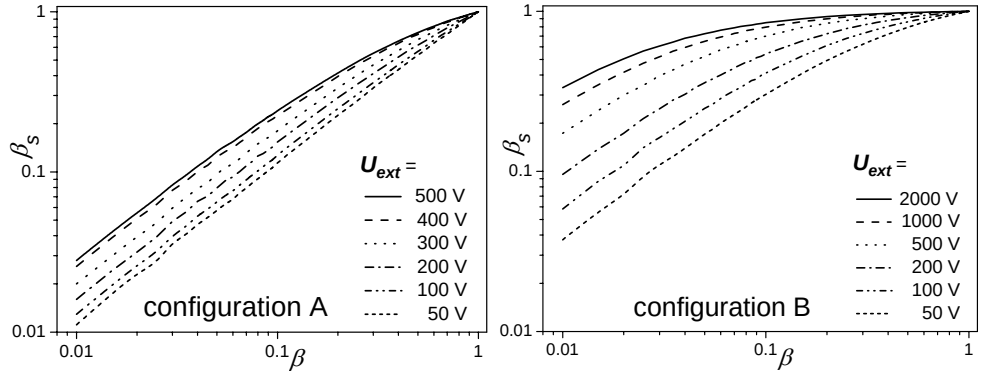

Influence of ionizer's temperature on ionization efficiency was under investigation for both cases. Changes caused by of extraction hole diameter adjusting are studied in order to find its optimal value. The role played by other factors, like the value of extraction voltage U_{ext}, the distance between the opening and extraction electrode will be studied in order to find the optimal configuration of the ionizer.

References

[1] G.J. Beyer, E. Herrmann, A. Piotrowski *et* al., Nucl. Instrum. Meth. 96 (1971) 347.

[2] P.G. Johnson, A. Bolson, C.M. Henderson, Nucl. Instrum. and Meth., 106 (1973) 83.
[3] V.N. Panteleev, Rev. Sci. Instr. 75 (2004) 1602.
[4] G. D. Alton, Y. Liu, D. W. Stracener, Rev. Sci. Instr. 77 (2006) 03A711.
[5] I.G. Brown (ed.), The Physics and Technology of Ion Sources,Wiley-VCH, Berlin, 2004.
[6] M. Menna, R. Catherall, J. Lettry, E. Noah, T. Stora, the ISOLDE collaboration, Nucl. Instrum. and Meth. B 266 (2008) 4391.
[7] G.D. Alton Y. Liu, H. Zaim and S. N. Murray, Nucl. Instr. and Meth. in Phys. Res. B 211 (2003) 425.

P-Tu-47

Phase and chemical composition of titanium surface layer simultaneously alloyed with chromium and molybdenum atoms

V.V. Uglov[1)], V.I. Shymanski[1)], N.N. Cherenda[1)], V.M. Astashynski[2)], P. Konarski[3)], A.V. Shashok[1)]

[1)] *Belarussian State University, Nezalezhnasci ave. 4, Minsk, Belarus*
[2)] *The B. I. Stepanov Institute of Physics, The National Academy of Sciences of Belarus, Nezalezhnasci ave. 68, Minsk, Belarus*
[3)] *Tele and Radio Research Institute, Ratuszowa 11, Warszawa, Poland*

Compression plasma flows (CPF) is a specific high energy influence allowing to modify the surface layer of different materials. The acting of the CPF on a complex coating-substrate system results in melting the surface layer with following its alloying by atoms of the coating and atoms of plasma formed gas. It gives a possibility to produce new materials with required properties.

A complex chromium-molybdenum coating (thickness about 1 μm) was deposited on the titanium substrate by means of arc-vacuum deposition method. The chromium and molybdenum were chosen as a alloying elements due to their different solubility in α- and β-phase of titanium. Then this system was treated by compressive plasma flows in nitrogen atmosphere with absorbed energy 10-30 J/cm^2.

The concentration of chromium and molybdenum atoms decreasing with increase of the absorbed energy density due to growth of deep of the melted layer. According to the SIMS results the content of nitrogen in the surface layer has the same dependence on the absorbed energy density and its maximum penetration depth is up to 2 μm.

The presence of chromium and molybdenum atoms in modified layer results in forming the high-temperature β-phase of titanium, their structure is being determined by the parameters of the compressive plasma flows.

P-Tu-48

The formation of noncoil-like inductance in nanocomposites $(Fe_{45}Co_{45}Zr_{10})_x(Al_2O_3)_{100-x}$ manufactured by ion-beam sputtering of complicated targets in $Ar+O_2$ atmosphere

Pawel Zhukowski[1)], Tomasz N. Koltunowicz[1)], Pawel Wegierek[1)], Julia A. Fedotova[2)], Alexander K. Fedotov[3)], Andrey V. Larkin[3)]

[1)] *Lublin University of Technology, Lublin, Poland*
[2)] *Scientific-Practical Material Research Centre NAS of Belarus, Minsk, Belarus*
[3)] *Belarusian State University, Minsk, Belarus*

The present paper investigate the inductive contribution into AC conductance below the percolation threshold $x_C \approx 54 \pm 2$ at.% in granular nanocomposites $(Fe_{45}Co_{45}Zr_{10})_x(Al_2O_3)_{100-x}$ subjected to annealing on air. The initial nanocomposites studied were manufactured in $Ar+O_2$ atmosphere by ion-beam sputtering of target containing $Fe_{45}Co_{45}Zr_{10}$ and alumina stripes, These samples before and after annealing procedure has been studied by temperature T and frequency f dependences of the real part of admittance $\sigma(T, f)$ in the range of 77-300K. The used setup allowed one to conduct measurements of current amplitude and phase angle θ in the frequency range of $5 \cdot 10^1$-10^6 Hz calculating then the real and imaginary parts of admittance in the studied samples.

The $\sigma(f)$ dependences displayed that for the samples below the percolation threshold high-temperature annealing resulted in the presence of a $\theta < 0$ in the region of low frequencies and a $\theta > 0$ at high frequencies (Fig. 1). The analysis of equivalent circuits corresponded to the observed $\sigma(f)$ dependences has shown that in the samples studied the series connection of capacity and noncoil-like inductance can be realized. So just for this case, capacitive properties of LC circuit with $-90 \le \theta_C < 0°$ are presented at low frequencies and its inductive properties with $0 \le \theta_L < 90°$ become apparent at high frequencies. The value f_c of critical frequency depends on metallic phase concentration x, measuring temperature T and annealing temperature T_a.

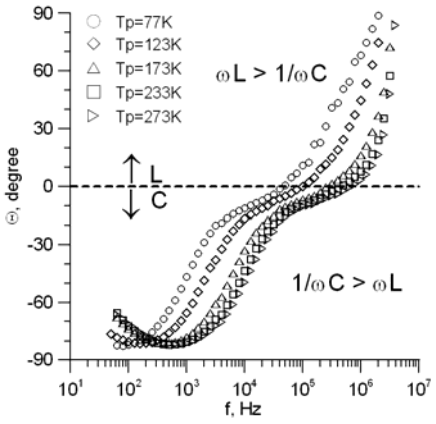

Fig. 1. Frequency dependences of phase angle θ.

The work was partially supported from Fundation for Polish Science.

POSTER PRESENTATIONS

Wednesday, June 16, 2010

P-We-1

Melanin complexes as a radiation bioprotector

I.I. Azarko[1)], A. Bakulin[2)], E.I. Kozlova[1)], V.P. Kurchenko[1)], L.V. Ajayeva[3)]

[1)] *Belorussian state university, Minsk, Republic of Belarus, azarko@bsu.by*
[2)] *"Bioingeneria" Center Russian Academy of Sciences, Moscow, Russia*
[3)] *4 Hospital, Minsk, Republic of Belarus*

A significant problem with most UV-visible radiation (photo-) protectors is phototoxic and photo allergic action they show in a varying extent. That is why it is important to search for some natural biopolymers, which efficiently absorb and dissipate the UV light energy. A special place in this aspect belongs to melanin pigments and their chitin complexes. Chitosan is non-toxic, has a high sorption capacity, and the potentialities of chitosan's chemical transformations can be applied to form a variety of new materials with different structure and properties.

The goal of the present study is to determine the best ratio of melanin and chitosan to prepare the most promising radiation safe melanin-chitosan complexes. Tinders and grapes were used as the source of melanin pigments to prepare the samples for the studies. The influence of UV-irradiation over the paramagnetic properties of melanin pigments and their chitosan compounds was studied by standard EPR method. All the samples show an intensive paramagnetic absorption line with g-factor of 2.0035. For the samples of pure chitosan, a similar signal is not detected. The studies of photo screening activity of the samples show that the investigated pigments absorbs radiation in all UV ranges.

The original melanins, like their chitosan complexes, show photo protective properties and participate the photochemical processes due to the presence in their molecules of such structures as free radicals, systems of poly-conjugated double bonds, highly reactive functional groups, capable of restorable oxidation. The photo induced paramagnetic centers appearing in the samples may be due to generation of anion- and cation-radical centers in the process of electrons transfer within the polymer granules. Moreover, the UV-irradiation is hard physical agent able to cause the polymer molecules lacing which may cause the reduction of the pigments capabilities of restorable oxidation.

The present studies show the effectiveness of the ESR-method to study both the initial melanin samples and their compounds with chitosan.

Investigation of defect structure of Mn-implanted GaSb

J. Bak-Misiuk[1)], P. Romanowski[1)], E. Dynowska[1)], J.Z. Domagala[1)], A. Barcz[1)], W. Caliebe[2)], A. Hallen[3)]

[1)] *Institute of Physics, PAS, Al. Lotników 32/46, PL-02668 Warszawa, Poland*
[2)] *HASYLAB at DESY, Notkestr. 85, D-22603 Hamburg, Germany*
[3)] *Rolay Institute of Electron Technology, Dept. of Microelectronics and Applied Physics, 164 40 Kista, Sweden*

Strong ferromagnetic behavior is achieved when hexagonal MnAs or MnSb clusters are formed in the GaAs or GaSb matrices. Both MnAs and MnSb materials indicate, at room temperature, the presence of the stable metallic magnetic phase of the NiAs-type structure. It has been demonstrated that, as an effect of high temperatures *(HT)* annealing of the GaMnAs layers or of the Mn-implanted GaAs crystals, ferromagnetic MnAs precipitates are fairly easily produced, yielding multi-phase materials. The Curie temperature for bulk MnAs is 310 K, while 580 K for MnSb. This suggests that granular GaSb:MnSb might be interesting candidate for increasing *Tc*. It has been stated that high temperature growth (550^{o}C) of GaMnSb on the GaAs (111)A or GaSb (001) substrates induces the formation of MnSb clusters in GaSb. The formation of Mn-based nanoclusters by ion implantation and subsequent annealing is a relatively simple technique compared to the growth of diluted magnetic semiconductors by epitaxial method with an advantage to control the relative Mn density. However, to our knowledge, there are no papers concerning Mn inclusion formed in GaSb by implantation. Therefore, it seems very promising to determine optimal conditions to prepare MnSb inclusions inside GaSb by Mn implantations. Two set of Mn^{+}-implanted GaSb crystals were investigated. The implantation was carried out at room temperature. The first group of samples was prepared by Mn implantation at energy E=150 keV and dose, D=1.7x10^{17}cm^{-2}, subsequent annealing in vacuum for 20 min. at 500^{o}C. Some samples were also capped with thin Si_3N_4 layers. The second set was prepared using E=350 keV and D=1.3x10^{17} cm^{-2}. After implantation the samples were annealed in Ar atmosphere for 5min. at 350^{o}C while the others – in vacuum, with Sb vapors, at 400^{o}C for 48 h and at 600^{o}C for 2 h.

Investigation of the defect structure was carried out using synchrotron radiation X-ray diffraction techniques. To determine the crystallographic orientation of nanoclusters with well-defined orientation in respect to the GaAs matrix, the 2θ-ω scans were performed. The phase analysis of the near surface layers was done using diffraction in the glancing incidence geometry *(*2θ scan). For the Mn-implanted samples (Mn^{+} lower energy), no polycrystalline phases were found before annealing, but, after annealing, the GaSb, Mn_2O_3 and Sb_2O_3 polycrystalline phases were observed. For all samples implanted at higher energy (before and after annealing) the diffraction peaks coming from polycrystalline GaSb were detected. For annealed samples, in dependence on the annealing conditions, the polycrystalline Sb or epitaxial grown Sb phases were also detected. In summary, no MnSb precipitates were formed in investigated samples. Annealing in Sb vapors results in re-introducing of Sb atoms but

only in the presence of oxygen, which is more reactive and bounds to Mn atoms. Therefore, most important problem concerns preventing, during implantation, of Sb atoms removal. Presented research may help in understanding the main problems concerning formation of MnSb inclusions inside the GaSb matrix.

Acknowledgements: This work was partially supported by national grant of Ministry of Science and High Education N202-052-32/1189 as well as by DESY/HASYLAB (EC support program: Transnational Access to Research Infrastructures).

P-We-3

Mass – spectrometric investigations of silver clusters

M. Szymanska-Chargot, A. Gruszecka, A. Smolira, K. Bederski

Institute of Physics, Maria Curie-Sklodowska University, 20-031 Lublin, Poland

Investigation of cluster formation by mass spectrometry tools has been an effective approach to gain valuable information on the ion-molecular reactions, ion-induced nucleation or stability and electronic properties of clusters. The past decades brought development of number of cluster production techniques. The most commonly used method of cluster produce is laser vaporization technique [1,2]. In this method, the metal vapors are generated by laser impulse and then vapor is expanded in presence of carrier gas. Another method involves metal vaporization by heating and then metal aggregation in presence of carrier gas [3]. Apart these methods, ion-bombardment or laser ablation of metals were also introduced [4-7].

The method applied, in this work, was direct formation of silver clusters from silver salts in laser desorption/ionization process connected with mass spectrometry. In addition we investigate influence of organic matrix on silver clusters formation (matrix assisted laser desorption/ionization). Recently, many of researchers have used both laser desorption/ionization method and matrix assisted laser desorption/ionization method incorporated to silver cluster formation from different silver salts [8].

Silver salts used for laser desorption/ionization were silver nitrate ($AgNO_3$), silver chloride (AgCl), silver carbonate (Ag_2CO_3), silver trifluoroacetate (AgTFA), silver benzoate (AgBz). The most prominent sliver clusters, Ag_n, formation was in the case of organic silver salts (AgTFA – $n < 11$, AgBz – $n < 45$).

Usage of organic matrix has strong impact on silver clusters formation. The results of silver clusters formation during matrix assisted laser desorption/ionization of silver salts are summarized in the Table 1.

Table1. The ions of the largest cluster sizes obtained in LDI and MALDI methods (dependence on the type of used silver salt).

Silver compound	Ag_n^+		Ag_n^-		Magic clusters
	MALDI	LDI	MALDI	LDI	(for positive ions only)
Silver nitrate	41	5	4	4	9, 21
Silver trifluoroacetate	59	11	6	5	9, 21, 35
Silver benzoate	72	45	53	2	9, 21, 35

References

[1] S.J. Riley, E.K. Parks, C.R. Mao, L.G. Pobo, S. Wexler, *J. Phys. Chem.* 86 (1982) 3911.
[2] R.E. Smalley, *Laser Chem.* 2 (1983) 167.
[3] W.A. de Heer, *Rev. Mod. Phys.,* 65 (1993) 611.
[4] C. Staudt, R. Heinrich, A. Wucher, *Nuc. Instr. And Meth. In Phys. Res. B* 164 – 165 (2000) 677.
[5] W. Begemann, S.Deihöfer, K. H. Meiwes-Broer, H. O. Lutz, *Z. Phys. D: At., Mol. Clusters* 3 (1986) 183.
[6] Ch. H. Bae, S. H. Nam, S. M. Park, *Applied Surface Science,* 197-198 (2002) 628.
[7] R. Brause, H. Möltgen, K. Kleinermanns, *Appl. Phys. B*, 75 (2002) 711.
[8] S. Keki, L.Sz. Szilagyi, J. Torok, G. Deak, M. Zsuga, *J. Phys. Chem. B* 107 (2003) 4818.

P-We-4

Effect of arsenium dose implanted in silicon substrate on titanium silicide growth during pulse photon processing

A.M. Chaplanov[1)], C. Karwat[3)], V.V. Kolos[1)], M.I. Markevich[1)], V.F. Stelmakh[2)]

[1)] *National Academy of Sciences of Belarus, Physical-Technical Institute, 10 Kuprevich St., 220141 Minsk, Belarus*
[2)] *Belarus State University, Minsk*
[3)] *Lublin University of Technology, Lublin, Poland*

The up-to-date GSI require multilevel metallization. Titanium disilicide is now widely used as ohmic contact material for silicon layers. The material has a low resistivity.

The silicon plates of КДБ 12 grade were implanted by $5 \cdot 10^{15}$, $3 \cdot 10^{15}$, $1 \cdot 10^{15}$ cm^{-2} doses of arsenium. In this work the formation of titanium silicide is a multistage process that involves silicon deposition with subsequent hardphase reaction in the area of titanium-silicon contact during pulse photon processing (PPP).

The hardphase reaction was carried using the method of pulse photon annealing that involved two stages done at 650°C and 850°C. On processing carried out at 650°C silicon atoms probably break off at the boundary with metal in energetically weak points; the $TiSi_x$ growth is determined by breaking of Ti-Si bond and intermediate $TiSi_x$ phases are formed. After completing the first annealing stage unreacted titanium is removed from the plate surface and the second thermal treatment is carried out to form a low-ohmic $TiSi_2$ (C54) phase. After titanium disilicide formation by means of the pulse photon annealing the distribution of elements was investigated throughout the plate depth using the method of secondary ion mass-spectrometry.

From the analysis of spectra is follows that the presence of a high concentration of arsenium is observed in them on synthesis of titanium disilicide layer. This affects the process of formation and subsequent growth of the layer. It is established that with the implantation dose equal to $5 \cdot 10^{15}$ cm^{-2} the thickness of titanium disilicide layer formed is ~ 50 nm and with that of $1 \cdot 10^{15}$ cm^{-2} it is ~ 68 nm.

The effect observed is of threshold nature and the implantation dose of 3.1015 cm^{-2} and under does not influence the thickness of the formed titanium disilicide layer. Therefore, in contrast to boron impurity that of arsenium has a substantial effect on the process of formation and growth of titanium disilicide layer.

P-We-5

Improved phase change recording systems using silicon nitride dielectric layers prepared by mixed gas plasma

W.L. Wang, H.W. Chien and G.M. Wu[*]

Advanced Materials Laboratory, Institute of Electro-Optical Engineering, Chang Gung University, Kweisan, Taoyuan 333, Taiwan R.O.C.

Multi-layer phase-change recording materials have been widely used in rewritable recording disks. Ge-In-Sb-Te alloys provided fast phase change by 650 nm laser and have served as the active layers. The demand for higher recording and writing speed inevitably increased the power. A high heat-conducting and optical-reflecting material such as silver was chosen to replace the conventional reflective layer. However, silver could react with sulfur when in contact with the traditional ZnS-SiO_2 dielectric layer. The novel silicon nitride has thus been investigated to replace the buffer material and upper dielectric layer. The silicon nitride layer was reactively sputtered using a mixed gas plasma of argon and nitrogen at 3 kW. The SiNx dielectric layer was created between the active Ge-In-Sb-Te layer and the silver reflective layer. The optical storage disks were then initialized by Hitachi POP120-8E to provide crystalline active layers before the dynamic tests. The initialization was conducted using 810 nm laser at 2300 mW while the disks were rotated at a constant linear velocity of 10 m/s. The optical properties were analyzed by Steag ETA-RT using 410-1010 nm wavelength. The results showed that the novel SiNx dielectric layer exhibited excellent and compatible electro-optical characteristics. The power margin window was improved by 50%. TEM micrographs showed improved laser mark profile on the active layer.

[*] Corresponding author e-mail: wu@mail.cgu.edu.tw

P-We-6

Investigation of the structure of fluoroalkylsilanes on alumina surface by XPS and ToF-SIMS

Michał Cichomski[1)], Katarzyna Kośla[1)], Witold Szmaja[2)], Witold Kozłowski[2)], Jacek Rogowski[3)]

[1)] *Department of Chemical Technology and Environmental Protection, University of Łódź, Pomorska 163, 90-236 Łódź, Poland*
[2)] *Department of Solid State Physics, University of Łódź, Pomorska 149/153, 90-236 Łódź, Poland*
[3)] *Institute of General and Ecological Chemistry, Technical University of Łódź, Żeromskiego 116, 90-924 Łódź, Poland*

With increasing miniaturization and advances in micro-/nanoelectromechanical systems (MEMS/NEMS), fluoroalkylsilanes on alumina surface are of interest for a wide range of applications. Fluoroalkylsilanes are formed by the chemical adsorption on an active solid surface and show good thermal and chemical stability. These compounds as a self-assembled monolayer (SAM) consist of three building groups: a head group that reacts with a substrate, a backbone molecular chain group and a terminal group that interacts with the outer surface of the film. In our work fluoroalkylsilanes films were grown on alumina surface by vapor phase deposition (VPD). The studied fluoroalkylsilanes had different amount of the reactive attachment groups. The films were characterized by means of a contact angle analyzer for hydrophobicity, time-of-flight secondary ion mass spectrometry (ToF–SIMS) and X-ray photoelectron spectroscopy (XPS) for identification of thin monolayers. The influence of the formed compounds on the nanotribological properties was measured by atomic force microscopy (AFM). Nanotribological measurements showed that fluoroalkylsilanes with three reactive groups have improved properties of the hydrophobicity and lowest friction coefficient.

This work was supported by the Polish Ministry of Science and Higher Education within Research Grant No. NN 507551538.

P-We-7

Influence of annealing on the electrical and structural properties of Cz Si wafers preliminary subjected to the hydrogen ion-beam treatment

A. Fedotov[1)*], *O. Korolik*[1)], *A. Mazanik*[1)], *N. Stas'kov*[2)], *T.N. Kołtunowicz*[3)], *P. Żukowski*[3)]

[1)] *Belarusian State University, Nezavisimosti, 4, 220050, Minsk, Belarus,*
[2)] *Mogilev State University, Kosmonavtov 1, Mogilev 212022, Belarus*
[3)] *Lublin University of Technology, 38, Nadbystrzycka St. 20-18 Lublin, Poland*

Standard commercial 0.5-40 Ω·cm both n- and p-type Cz Si wafers were subjected to hydrogen or argon ion-beam treatment at 25-350^{o}C. The ion energy was equal to 100-400 eV, ion current density – 0.1-0.15 mA/cm^2, duration of treatment – 5-40 min. The ion-treated samples were annealed in an inert ambient (argon) during 30 min at a temperature ranging from 200 to 900°C.

The structural properties of the near-surface region of the ion treated and annealed wafers were studied using the monochromatic (wavelength 632.8 nm) and spectral ellipsometry, as well as Auger spectroscopy combined with ion etching.

The measurements of DC and AC conductance, surface resistance, thermoEMF and photovoltage spectra for the ion beam treated and annealed wafers were used to examine their electrical properties.

The conducted studies have shown that the influence of annealing on the wafer properties strongly depends on the temperature of the ion beam treatment and the type of ions. The correlations between the ion-beam treatment conditions and the behavior of the ion treated wafers under annealing are discussed.

* fedotov@bsu.by

P-We-8

Formation of cone-shaped and crystallographically oriented defects on the Cz-Si wafer surface by the helium implantation and DC nitrogen plasma treatment

N.V. Frantskevich[1)], A.K. Fedotov[2)], A.V. Mazanik, A.V. Frantskevich[1)], T.N. Kołtunowicz[3)], P. Żukowski[3)]*

[1)] Belarusian National Technical University, Minsk, 220063 Belarus
[2)] Belarusian State University, Minsk, 220030 Belarus
[3)] Lublin University of Technology, 38, Nadbystzycka St. 20-18 Lublin, Poland

In work [1] we investigated the possibility to form the buried insulating Si_xN_y layers by a new method based on the nitrogen gettering onto buried defect layer created by helium implantation. One of the problems of this method is the formation of surface defects when the number of implantation-induced defects in the buried layer does not correspond to the number of introduced from plasma nitrogen atoms. The goal of this work is more detailed study of defects formed on the surface.

Standard 4.5 Ω·cm phosphorus doped Cz Si wafers were subjected to helium ion implantation at the room temperature with the energy of 300 keV and the fluences of $1 \cdot 10^{15}$, $5 \cdot 10^{15}$, $1 \cdot 10^{16}$ or $2 \cdot 10^{16}$ at/cm^2. Then the nitrogen was introduced into silicon from a DC plasma source at the temperature of 350°C. Finally, all samples we subjected to vacuum annealing at 800°C. The structural properties of the formed samples were studied by scaning electron microscopy.

The experiments have shown that the crystallographically oriented and cone-shaped defects are formed on the surface of the treated silicon wafer. The typical length of crystallographically oriented line defects equals to 1-2 μm. Base diameter of cone-shaped defects is equal to 200-2000 nm, the ratio of diameter to height is appr. 1:1. The X-ray microanalysis of cone-like defects does not reveal any chemical elements except silicon and nitrogen. Such defects have enhanced emission ability in comparison with silicon surface. Increase of helium implantation fluence leads to decrease of number of defects.

References

[1] N.V. Frantskevich, A.V. Frantskevich, A.K. Fedotov, A.V. Mazanik // Solid State Phenomena 156-158 (2010) 91

* a.frantskevich@rambler.ru, fedotov@bsu.by

P-We-9

Distribution of radiation defects on thickness of IV-VI thin films at α-irradiation

P. Żukowski, D. Freik, Ya. Saliy, N. Stefaniv, L. Mezhylovska

Vasyl Stefanyk Precarpathian National Universit, 57, Shevchenka, Str, Ivano-Frankivsk, 76026, Ukraine

Irradiation of materials by easy particles with energy 0.1-10 MeV plays an important role at creation of semiconductor devices. The decision of problem of control of semiconductor properties of material by α-irradiation is impossible without understanding of the mechanism of interaction of irradiation with a solid and influence of defects on his properties. Exactly defects in undoped films of lead chalcogenides and tin are responsible for their semiconductor properties.

At rather large energies of falling α-particles, when maximum of profile of damages is on a depth of few microns, for it analysis it is possible to use the method which is based on the change of electrical resistance of thin sample. Thus, to define the degree of damages with depth for weakening of flood foils of different thickness are putted.

The calculation of profiles of ionization loss and damages of crystalline lattice under the action of monoenergetic α-particle beam is actual for the tasks of modification of properties of semiconductor materials; for development, choice of the regimes of exploitation and radiation firmness of detectors of ionizing radiation.

An ionization loss of charged particles in semiconductor is mainly spent for formation electron-hole pairs. Knowledge of size of concentration of generating non-equilibrium charge carriers is necessary at use of semiconductors for the detectors of radiation. Also ionization loss are mainly determine free path of a charged particle.

For the purpose of reception of a primary information about the distribution of electrically active defects in samples is applied the method witch connected with measuring of bulk resistance of films of different thickness. The spatial distribution of ionization and nuclear loss of energy by fast α–particles in $A^{IV}B^{VI}$ semiconductors was calculated.

P-We-10

Scaling down the lateral dimensions of silicon nanopillars fabricated by RIE, using Au/Cr self-assembled clusters as an etch mask

R. Kaliasas[1)], M. Mikolajunas[1)], L. Jakucionis[2)], J. Baltrusaitis[3)], D. Virzonis[1)], J. Puiso[4)], D. Adliene[4)]

[1)] *Faculty of Technologies, Kaunas University of Technology Panevezys Institute, Daukanto str. 12, LT-35212 Panevezys, Lithuania*
[2)] *Panevėžys Mechatronics Center, Daukanto str. 12, LT-35212 Panevezys, Lithuania*
[3)] *Department of Chemistry and Central Microscopy Research Facility, 85 Eckstein Medical Research Building, University of Iowa, Iowa City, Iowa 52242, USA*
[4)] *Department of Physics, Kaunas University of Technology, Studentų 50, LT- 51368, Kaunas, Lithuania*

Nanodot and nanopillar structures are of great interest to the common nanoelectronic devices, such as photonic crystals and surface plasmon resonance instruments. Generally this interest is determined by the possibility of photo-active surface modification, enabling fine-tuning and justification of physical properties. Vertically organized nanopillars are the most common structures in photoactive devices due their favorable orientation [1,2]. Reactive ion etching (RIE) was used to produce vertically oriented nanopillar structures. Self-organizing gold-chromium clusters were used as an etch mask. An anisotropic etching process based on CF_4 gases was used for silicon etching. Sidewall evolution during low radio frequency power etching has been analyzed. RIE recipes, with minimal mask sputtering, resulting with the aspect ratio 1:20 and better were developed. Our research resulted in high quality nanopillar arrays with lateral dimensions ranging from 10nm to 20nm.

References

[1]Fan Z., Ruebusch D.J., Rathore A.A., Kapadia R., Ergen O., Leu P.W., Javey A., Nano Res. 2009, 2/11: 829.
[2] Dong X., Tao J., Li Y., Zhu H., Applied Surface Science 2010, 256/8: 2532.

P-We-11

Microwave diagnostics technology of ion-irradiated silicon layers

I.A. Karpovich, V.B. Odzhaev, O.N. Yankovsky, E.I. Kozlova

Belorussian state university, Minsk, Republic of Belarus karpovich@bsu.by

The development of modern element base of microelectronics involves the improvement of the semiconductor materials' quality monitoring and diagnostics methods. The lifetime of nonequilibrium charge carriers is one of the most informative among the parameters in common studies. The value of these carriers is determined by the degree of the crystals' perfection, the presence of residual technological impurities, heat treatment conditions.

The lifetime value determination is the based on measurements of the photoconductivity rate decrease after pulse photoexcitation using the reflected microwave as a probe [1]. A characteristic feature of this work is the possibility to map the distribution of the effective lifetime of the nonequilibrium carriers on the surface of the semiconductor wafer.

Scanning of the Si wafers in the parameter distribution of the nonequilibrium carriers lifetime (NCL) in the plane of the construction of layered structures will present a visual quality picture of the technological operations execution (Fig. 1).

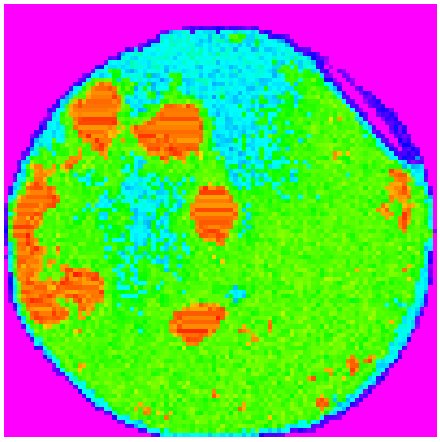

Fig.1: Map of the distribution of NCL on the surface of the silicon wafer

The method is designed for contactless measurements of the effective lifetime of nonequilibrium carriers in silicon ion-implanted wafers and epitaxial structures at various stages of their processing.

References

[1] Borodskij P.A., Buldygin A.F., Tokarev A.S. FTP, 2004, V. 38, №.9, P. 1043 – 1049.

P-We-12

RBS measurements of the low temperature formation of platinum silicide for Schottky high-power diodes

F. Komarov[1)], O. Milchanin[1)], J. Solovjov[2)], A. Turtsevich[2)], P. Zukowski[3)], Cz. Karwat[3)], K. Kiszczak[3)], Cz. Kozak[3)]

[1)] *Belarusian State University, 4 Nezavisimosti ave., 220030, Minsk, Belarus*
[2)] *Unitary enterprise "Transistor Plant", 220108, Minsk, Belarus*
[3)] *Lublin Technical University, 38A Nadbystrzycka Str., 20-618, Lublin, Poland*

Platinum silicide films are widely used in silicon devices. The crystallography, morphology and kinetics of formation of *PtSi* films has been the subject of much research due to the ability of these films to form near-ideal *n*- and *p*-type ohmic contacts and also Schottky contacts on substrates of silicon in the manufacture of various semiconductor devices. In particular, application of *PtSi* contact layer in Schottky high-power diodes allows to lower leakage current, to raise break-down voltage and also to increase temperature operating modes of devices.

In our work structural and electrical properties of contact platinum silicide layers for Schottky high-power diodes formed on silicon wafers by deposition of thin platinum layers (40 nm) and low temperature annealing (100-360°C, 30-480 min) were investigated. The depth distributions of *Pt* into the silicon matrix were analysed using RBS. In all cases the RBS measurements were performed in identical conditions with 1.4 MeV He^+. The structural-phase modifications of *Pt*/*Si* system after annealing have been studied by means of transmission electron microscopy in "plan-view" and "cross-section" geometries using a Hitachi H-800 instrument operating at 200 keV.

It is shown that process of silicide formation in *Pt/Si* system begins at temperatures of about 180 ºC. During heat treatment at 180-240°C only Pt_2Si phase is revealed. However, when the annealing of a 40 nm *Pt* layer occurs at 200-220°C, the Pt_2Si silicidation reaction is not fully completed even after 480 min. It is found that *PtSi* silicides are formed at the temperature above 240°C. There is no any influence of *Si* wafer doping on process of silicide formation. Thin layers of silicides, generated at lower temperatures (<260°C), are more perfect in depth, and also are characterized by more homogeneous grain sizes.

P-We-13

Structure and optical properties of silicon layers with GaSb nanocrystals created by ion-beam synthesis

F. Komarov[1)], L. Vlasukova[1)], O. Milchanin[1)], W. Wesch[2)], A. Mudryi[3)], B. Dunetz[1)]

[1)] *Belarusian State University, Nezavisimosti ave. 4, 220030 Minsk, Belarus*
[2)] *Friedrich Schiller University, Max-Wien-Platz 1, D-07743 Jena, Germany*
[3)] *Scientific and Practical Materials Research Center, National Academy of Sciences of Belarus, P. Brovki Str. 17, 220072 Minsk, Belarus*

A promising approach towards integration of III-V optoelectronic devices with Si electronics is the direct growth of III-V quantum dots in crystalline Si. GaSb is a narrow-gap A^3B^5 semiconductor with direct gap. Synthesis of GaSb quantum dots inside the crystalline Si is of interest for applications in light emitting diodes and photodetectors operating in IR range.

In this work, we present the results of structural and optical characterizations of GaSb nanocrystals (NCs GaSb) synthesized by high-fluence ion implantation in Si. (100) Si wafers were implanted subsequently with Sb and Ga ions. The ion energies were 350 keV for Sb and 250 keV for Ga and the fluence was 5×10^{16} cm^{-2} for both species. The implantation was carried out at 500°C. Afterwards, the samples were annealed at 700, 900 and 1100°C in an inert ambient using ordinary furnace annealing and RTA. The depth distributions of Ga and Sb in the implanted samples were evaluated by means of RBS/C. It has been found that "hot" implantation with the following annealing is accompanied by the significant diffusion redistribution of embedded atoms. The diffusion of both species towards the surface as the most effective sink for structure defects is predominated. The diffusion into the bulk of Si crystal is observed, too. The structure-phase transformations within the implanted layers and the influence of annealing regime on the size and depth distribution of GaSb nanocrystals have been investigated using TEM/TED technique. The optical properties of samples have been characterized using low-temperature photoluminescence (PL). It has been shown that modifying the regime of annealing may provide a way to control the optical and structural properties of Si layers with synthesized GaSb nanocrystals. A broad band at 0.9 eV has been registered in PL spectra of (Sb+Ga)Si samples annealed at 900°C. An annealing temperature growth up to 1100°C leads to disappear of the band at 0.9 eV and rearrangement of Si – NCs GaSb layer structure.

P-We-14

Nickel-platinum silicide formation on silicon by IBAD

F.F. Komarov[1)], O.V. Milchanin[1)], I. Konopljanik[1)], K. Kiszczak[2)], P. Zukowski[3)], Cz. Karwat[3)], Cz. Kozak[3)]

[1)] *Department of Physics, Belarussian State University, Minsk, Belarus*
[2)] *Maria Curie-Skłodowska University, Pl. M. Curie-Skłodowskiej 1, 20-031 Lublin, Poland*
[3)] *Lublin University of Technology*

Nickel silicide is now widely used in advanced devices thanks to its low formation temperature, low resistivity and low Si consumption. The stability of the sheet and contact resistance on nickel-silicide is an important issue. The main NiSi integration concern is its instability at high temperature. Ni (Pt) alloys introduction may considerably improve NiSi films thermal stability against agglomeration. Initial studies have shown that Pt addition could improve the thermal stability of NiSi films against transformation to $NiSi_2$, also. An amount of alloying element dissolved in NiSi determines structural and electrophysical properties of the formed layers. The one-beam ion mixing method using the truncated cones coated with layers of different materials makes it possible to modify near-surface metal or semiconductor layers by simultaneous deposition of one or several materials [1].

The truncated cones coated with Ni and Pt of different areas have been irradiated by 60 keV Ar^+ ions to the fluences of $2x10^{16}$ cm^{-2} and $5x10^{16}$ cm^{-2} at a beam current density of 10 $\mu A/cm^2$. The post-deposition furnace annealing as well as RTA in an inert ambient have been used to form or modify silicide layers. Auger electron spectroscopy and RBS with 1.5 MeV He^+ beam have been used for depth profiling over the whole modified structure. The as-deposited and annealed samples were characterized by TEM and XTEM. Silicide layer resistance was measured with four-point probe method. The structural and electrophysical properties of prepared samples are discussed as a function of Pt concentration and regimes of the layer deposition and thermal treatments.

References

[1] Zukowski P., Komarov F.F., Karwat Cz., Kiszczak K., Kozak Cz., Kamyshan A.S. Vacuum 2009; 83: 204-207.

P-We-15

Influence of hot implantation on residual radiation damage in silicon carbide

M. Kulik[1)], A. Drożdziel[1)], Li Lin[2)], S. Prucnal[1)], K. Pyszniak[1)], M. Rawski[1)], M. Turek[1)], J. Filiks[1)], Ł. Gluba[1)], J. Żuk[1)]

[1)] *Institute of Physics, Maria Curie-Skłodowska University, Pl. M. C. Skłodowskiej 1, 20-031 Lublin, Poland*

[2)] *Institute of Ion Beam Physics and Materials Research, Forschungszentrum Dresden-Rossendorf, P.O. Box 510119, 01314 Dresden, Germany*

Silicon carbide (SiC) is a wide band-gap semiconductor with promising applications as a high-power, high-temperature and high-frequency electronic material. Ion implantation plays an important role in SiC device production. However, the implantation process causes radiation damage which can lead to amorphization of subsurface SiC layers. Although annealing temperatures of SiC above 1500^{o}C are much higher than in Si, a complete recrystallization is often problematic in this material, especially for the samples implanted at room temperature (RT). Therefore ion implantation at elevated target temperatures (hot implantation) has become a way to decrease the amount of residual radiation damage in SiC.

In this study, the effects of Al^{+} sequential implantation into crystalline 6H-SiC at t=500^{o}C (hot implantation) were investigated by confocal micro-Raman spectroscopy and RBS/C, and compared with the implantation at RT. By performing hot implantation at 500^{o}C, the formation of a completely amorphous layer was suppressed, and further annealing at 1600^{o}C resulted in the Raman and RBS/C spectra almost indistinguishable from those of virgin SiC. These facts indicate clearly a crystalline order recovery in the implanted SiC layers.

The results of optical depth profiling of Al atoms by Particle Induced Photon Emission (PIPE) method are also shown in the present work. This technique employs detection of Al atomic line intensity during Bi^{+} ion beam sputtering of Al implanted SiC and subsequent measurement of a crater depth by a Talysurf profilometer. The obtained aluminium depth profile was compared with the calculated by SRIM simulations and a value of Bi^{+} sputtering yield for SiC was determined using the PIPE method.

Acknowledgement

The work was funded under Polish Ministry of Science and Higher Education silicon carbide programme as grant no. PBZ-MEiN-6/2/2006.

P-We-16

Application of the fractional-dimensional space approach to analysis of optical spectra in Al^+ hot-implanted GaAs

M. Kulik[1)], W. Rzodkiewicz[2)], A. Drożdziel[1)], K. Pyszniak[1], J. Żuk[1)]

[1)] *Institute of Physics, Maria Curie-Skłodowska University, Pl. M. C. Skłodowskiej 1, 20-031 Lublin, Poland*
[2)] *Institute of Electron Technology, Al. Lotników 32/46, 02-668 Warszawa, Poland*

Semi-insulating (100)GaAs single crystalline substrates have been Al^+ -implanted using subsequently ion beams of 250 keV energy (fluence, F=3.5x10^{16}cm^{-2}), and 100keV (F=9.6x10^{15}cm^{-2}). The ion implantation was carried out at six target temperatures ranging from 250 to 500^{o}C. The temperature at the hot stage was stabilized within ± 1^{o}C. The pressure in the collector chamber of the UNIMAS implanter was about 1x10^{-6} Torr during ion implantation processes. The optical spectra of hot-implanted GaAs were measured by Variable Angle Spectroscopic Ellipsometry (VASE) technique at incidence angles: 65^o, 70^o and 75^o in the wavelength λ range from 250 nm to 1000 mn with a step 2 nm. The implanted samples are described by a 4-phase theoretical model (an ambient, native oxide, implanted layer and crystalline substrate).

The model of fractional-dimensional space was applied to study optical transitions at van Hove critical points. Optical spectra of E_1 and $E_1+\Delta_1$ structures of Al^+-implanted GaAs at different implantation temperatures have been analyzed with the use of near first derivative spectra (fractional order of derivative $\xi \approx 1$). Symmetric line shapes were found both for crystalline and ion-implanted samples in the E_1 and $E_1+\Delta_1$ regions of the spectra near 2.9 and 3.1 eV, respectively. Using fractional differentiation, the dimension, as well as critical points parameters were directly determined.

P-We-17

Ion beam analysis of agricultural plants

Andrei Lagutin and Helena Gorodecka

Belarusian State Agrarian Technical University, 99 Nezavisimosti Av., 220023 Minsk, Belarus

Nuclear microprobes have been successfully applied to single-cell irradiation systems and elemental analysis techniques with RBS and PIXE. Numerous applications in biological samples take advantage of its versatility and easy operation, either at the tissue or individual cell scale. PIXE is the basic method employed for routine elemental mapping. In addition, micro-PIXE and other microbeam techniques complement each other to offer unique information [1].

In this review, different examples of investigation will be presented with emphasis placed on agricultural plants. The response of seed germination characteristics of some important agricultural plants to treatment in low pressure plasma of a capacitive coupled radio frequency (rf) discharge and in rf electromagnetic field has been studied. It has been shown that the pre-sowing plasma and radio-wave treatment of seeds contributes to their germination enhancement and sowing quality improvement [2].

References

[1] Lagutin A.E. *Device on the Basic of Insulating Capillaries for RBS and Other Applications*, 19th International Conference on Ion Beam Analysis, 7-11 Sept. 2009, University of Cambridge, UK. P. 187.

[2] Gorodecka H. A. et al. Influence of Plasma and Radio-Wave Treatment on Agronomical Properties of Seeds / XVIIIth Symposium on Physics of Switching Arc, 7-11 September 2009, Brno, Czech Republic. P. 170-173.

P-We-18

Structural changes in porous Si induced by high energy electron bombardment

Skirmantė Mockevičienė[1)], Diana Adlienė[1)], Igoris Prosyčevas[2)], Asta Guobienė[2)]

[1)] *Kaunas University of Technology, Studentų g. 50, LT-51368 Kaunas, Lithuania*
[2)] *Institute of Material Sciences, Kaunas University of Technology, Savanorių g. 271, LT-50131, Kaunas, Lithuania*

Porous silicon is widely used in differet areas of application due to its unique porous structure, which depends on the technological parmeters of the fabrication and can be modified bombarding initial structure with the accelerated particles. Possibility to controll the pore growth and to initiate a modification of porous structure, makes porous Si to the attractive material in the constructions of electronic devices, however reises the need for more detailed investigation. of porous Si sructures after their irradiation..

The aim of this work was to investigate porous Si structures after their bombardment with high energy (12 MeV) electrons and to compare these findings with the results obtained after the irradiation of the same initial structures with high energy (15 MeV) photons.

Porous Si layers were fabricated by vapor etching of Si (111) targets using a liquid mixture of the acids HF and HNO_3. Initial samples were irradiated by elctrons generated in medical linear accelerator Clinac 2100C (VARIAN). Bonding structure of porous Si layers was analysed using Raman scattering spectrometer (Yvon Jobin – System) and FT-IR spectrometer (Nicolet 5700 equipped with 10 Spec modality); while surface morphology of the samples was investigated using optical microscope MMU-3 supported with a digital camera Canon5, atomic force microscope (NANOTOP-206) and SEM FEI QUANTA 200FEG. Experimental results of electron irradiated samples were compared to those, obtained after the irradiation of the structures with high energy (15 MeV) X-Rays, generated in the same equipment. Irradiation dose to sample was the same in both cases - 2 Gy.

Radiation impact on the structure and morphology of porous silicon layers is analysed on the basis of sample preparation parameters as well as the mechanisms ongoing in irradiated porous structures is discussed.

P-We-19

Structure and electron-transport properties of photoresist implanted by Sb^+ ions

N. Vabishchevich[2)], D. Brinkevich[1)], V. Volobuev[1)], M. Lukashevich[1)], V. Prosolovich[1)], Yu. Sidorenko[1)], V. Odzhaev[1)], J. Partyka[3)]

[1)] Belarussian State University, 4 Nezavisimosti ave., Minsk-220050, Belarus
[2)] Polotski State University, 29 Blohina st., Novopolotsk, 211440, Belarus
[3)] Lublin University of Technology, 38d Nadbystrzycka st., 20-618 Lublin, Poland

Ion implantation is one of the effective technological method to change all physical properties of solids. In particular, conductivity of implanted polymers can increases up to 18 orders of magnitude with dose increasing and insulating or metallic regime of conductivity depending on kind of polymer matrix and ions, as well as implantation regimes can be obtained.

Photoresist with thickness d=1.8 μm have been deposited on to silicon substrate and implanted by 60 keV Sb^+ ions with fluence range $1 \cdot 10^{15}$-$5 \cdot 10^{16}$ cm^{-2} at ion current density 4 $\mu A/cm^2$. Atomic force microscopy, microhardness and microfrailness measrements were curried out at room temperature in air and temperature dependence of resistance measured in the temperature range 300-77K.

Ion implantation leads to decrease of surface roughness from about 0.7 nm (virgin sample) to 0.3 nm, while microhardness of near surface layer increases up to 2.5 GPa at maxima fluence $5 \cdot 10^{16}$ cm^{-2}. This value of microhardness is more than one order of magnitude higher than microhardness of virgin sample. Microhardness was higher near photoresist-silicon interface too.

As would be expected resistance decrease with fluence increasing because of production carbonaceous graphite like clusters, which at higher ion fluences may form system of conductive parth and may be responsible for enhanced electrical conductivity implanted samples. Independently of implantation fluence all samples show negative temperature coefficient of resistance. It means that all samples are on the insulating side of the insulator to metal transition. Mechanisms of surface roughness, microhardness and electrical conductivity change under the influence implantation Sb^+ ions are discussed.

P-We-20

Strength of the silicon implanted by high-energy ions of inert gases

D.I. Brinkevich[1)], V.S. Prosolovich[1)], Yu.N. Yankovski[1)], S.A. Vabishchevich[2)]

[1)] Belarussian State University, Nezavisimosti ave. 4, Minsk-220050, Belarus
[2)] Polotski State University, Blohina str. 29, Novopolotsk-211440, Belarus

Microhardness of n-Si monocrystall wafers implanted by Ne^+ (24.1 MeV, 1.10^{14}-5.10^{15} cm^{-2}), Ar^+ (46.9 MeV, 1.10^{14}-5.10^{15} cm^{-2}) and Kr^+ (150-210 MeV, 1.10^{12}-3.10^{14} cm^{-2}) ions was studied. The density of ionic current did not exceed 1 $\mu A/cm^2$. Measurements of microhardness were carried out by a standard technique along the direction <100>.

It was established, that the Ne^+ and Ar^+ implantation leads to hardening of surface layer of silicon monocrystals. The effect of surface irradiation hardening (increase of microhardness ΔH, depth of the strengthened layer) essentially depends on the mass and doze of implanted ions. This effect was observed only at fluencies (F) over 5.10^{14} sm^2 and did not leave on saturation even at the maximal fluence 5.10^{15} cm^2. High energy implantation by Ne^+ and Ar^+ ions increase the dispersion of casual distribution of microhardness. It testifies to formation of defects congestions on depths up to 1 micron at plate surface.

At Kr^+ implantation the effect of surface radiating hardening has been expressed much more poorly. So, depth of the strengthened layer at high-energy Kr^+ implantation did not exceed 1 micron. It was essentially less than at Ne^+ and Ar^+ implantation. Surface radiating hardening of silicon at Kr^+ implantation was observed only at small fluence ($F \leq 5.10^{12}$ cm^2) implantation. Reduction of microhardness took place at further increase F. Depths of the strengthened layer was reduced also. Furthermore, at fluence over 4.10^{13} cm^2 the surface dishardening was observed.

It is shown, that surface irradiation hardening of silicon is caused by electrically inactive interstitial defects. These defects are formed during diffusion to a surface of silicon own interstitial atoms from the layer broken by ionic implantation. Surface dishardening at Kr implantation is caused by vacancy defects.

Solar cell emitters fabricated by plasma immersion ion implantation and flash lamp millisecond annealing

S. Prucnal[1)], W. Skorupa[1)], B. Abendroth[2)], K. Krockert[2)], H.J. Möller[2)]

[1)] *Institute of Ion Beam Physics and Materials Research, Forschungszentrum Dresden-Rossendorf, P.O. Box 510119, 01314 Dresden, Germany*
[2)] *Institute for Experimental Physics, TU Bergakademie Freiberg, Leipziger Str. 23, 09599 Freiberg, Germany*

Cost reduction is the overall goal in the further development of solar cell technologies. Processing solar cells at lower temperatures helps reducing the energy cost and in thin film technologies may also facilitate the use of less temperature stable substrates such as normal glass or polymers foils. A high temperature step in conventional solar cell processing of silicon is the fabrication of the emitter by indiffusion of the doping element. In the present work a new technique will be presented and explored, which allows the implantation of the doping element by a plasma process and the subsequent annealing by a short time light pulse. Conventional ion implantation technique requires an accelerator and is not suitable for mass production of solar cells. Plasma Immersion Ion Implantation (PIII) technique is a new method that can be used for the emitter formation of solar cells. It is much easier to handle and has the potential for mass production. A dedicated PIII - machine has been built suitable for the implantation of doping impurities into silicon.

Both mono- and multicrystalline p-type silicon wafers were used for the implantation of phosphorous. Ion implantation is capable of producing a very shallow phosphorous doping profile near the surface of the wafer, typically 100 nm or less, without thermally affecting the bulk material. After ion implantation the silicon is strongly disordered or amorphous within the ion range. Therefore subsequent annealing is required to remove the implantation damage and to activate the doping element. Flash lamp annealing (FLA) offers here an alternative route for the emitter formation at an overall low thermal budget. During FLA, only the wafer surface is heated homogeneously to very high temperatures at ms time scales, resulting in the annealing of the implantation damage and an electrical activation of the phosphorous. However, variation of the pulse time also allows to modify the degree of annealing of the bulk region to some extent as well, which can have an influence on the gettering behaviour of metallic bulk impurities.

The μ-Raman spectroscopy showed that the silicon surface is amorphous after ion implantation. It could be demonstrated that FLA at 800^{o}C for 20 ms even without preheating is sufficient to recrystallize implanted silicon. The highest carrier concentration and efficiency and the lowest resistivity were obtained after annealing at 1200^{o}C for 20 ms both for mono- and multicrystalline silicon wafers. Photoluminescence results point towards P-cluster formation at high annealing temperatures which effects on metal impurity gettering within the emitter.

P-We-22

Different wavelength laser irradiation of amorphous carbon

A. Grigonis, Z. Rutkuniene, V. Vinciunaite

Kaunas University of Technology, Physics Department, Studentu st. 50, LT-51368, Kaunas, Lithuania

Coherent laser irradiation of amorphous carbon films formatted on Si substrate by ion beam deposition (IBD) and plasma enhanced chemical vapor deposition methods (PECVD) are analyzed in this work. a-C:H films have various sp^3/sp^2 phases ratio and different quantity of hydrogen, so they were conditional called as diamond like (DLC) (IBD formation method, quantity of H=(25-35)%, hardness by Vickers (HV)=15-25 GPa) and graphite like carbon films (PECVD method, H<20%, HV=6-12 GPa). Thin metallic (~20 nm, Au, Ni) layer or nanoisland (Ni, ~(20-40) nm of thickness and ~2nm of diameter) formatted on Si substrate stimulated nanotube formation during PECVD and increased hardness of films (~40GPa), refracting index (2.1-2.3), and slowly changed extinction coefficient.

Films were irradiated with nanosecond Nd:YAG laser (Ekspla NL301G) at the first (1064 nm; 6 ns), the second (532 nm, 4.2 ns) and the third (355 nm, 28 ns) harmonic by scanning or repeating (10 pulse to one point) regime. The same power was in both regimes, intensity was increased to the threshold of ablation. Irradiation by the first laser harmonic with the power density (30-70) MW/cm^2 stimulates a minor increasing of graphite phase. The peaks at ~800 cm^{-1}(intensive) and at ~970 cm-1 (weak) showed SiC formation. Formation of carbides was observed at the second harmonic irradiation when intensity of irradiation is low (<10 MW/cm^2). Graphitization becomes more intensive when intensity of radiation increased and films transform to the glass carbon and nano/micro crystallite compound at intensive ablations regime (~24 MW/cm^2). Ellipsometry measurements show not only the reduction but also high dispersion of film thickness. Micro relief analysis showed that film swelling proceeded during the graphitization process. Early ablation starts at irradiation by third laser harmonic with intensity of ~8 MW/cm^2 and roughness of Si substrate increased. Swelling of films was obtained when sample irradiated at the third harmonics with 1MW/cm^2.

P-We-23

Investigation of structural and optical properties of GDC thin films deposited by reactive magnetron sputtering

Jolita Sakaliūnienė, Jurgita Čyvienė, Brigita Abakevičienė

Kaunas University of Technology, Studentų str. 50, 51368 Kaunas, Lithuania

The purpose of this paper was to analyze structural and optical properties of gadolinia – doped ceria (GDC) thin films. At first the ceria – gadolinia multilayer systems (2-12 layers) were deposited using reactive magnetron sputtering in O_2/Ar gas mixtures [1]. Those systems (deposited on Si substrate) were annealed in air atmosphere at different temperature from 600^0C to 800^0C changing the annealing parameters (rise rate and annealing time). The thickness of all formed thin films was about 500 nm. The films were formed with ~90% ceria and ~10% gadolinia.

The GDC thin film structure was investigated by X-ray diffraction (XRD), scanning electron microscopy (SEM). The particle size of GDC films has been studied employing X-ray diffraction (XRD). The two major models such as known and employed in bulk materials. Both models are the integral breadth and the Warren-Averbach methods X-ray diffraction were used for the measurements [2]. The texture coefficient of GDC thin films was evaluated from XRD patterns. Optical properties of annealed GDC thin films were examined using a laser ellipsometer. Variation of porosity was estimated from refractive index *n* of GDC thin films.

Results show that the number of layers and annealing temperature have the influence on GDC thin film formation. Analysis of structural and optical properties of GDC presents that 12 layer system annealed at 600^0C for one hour has the highest refractive index n=2.17.

References

[1] Čyvienė J, Laurikaitis M, Dudonis J, Vacuum 2005;78:395.
[2] Bimbault L, Thin Solid Films 1996;275:40.

P-We-24

Thin superconducting NbN layers deposited on different substrates: Si, SiO_2, Si_3N_4, Al_2O_3 designed for superconducting single photon detectors

Wojciech Słysz[1)], Marek Guziewicz[1)], Michał Borysiewicz[1)], Jarosław Domagała[1)], Iwona Pasternak[1)], Krzysztof Hejduk[1)], Jan Bar[1)], Maciej Węgrzecki[1)], Piotr Grabiec[1)], Remigiusz Grodecki[1)], Iwona Węgrzecka[1)] and Roman Sobolewski[2)]

[1)] *Institute of Electron Technology, Lotników 32/46, 02-668 Warszawa, Poland*
[2)] *University of Rochester Rochester, NY 14627, USA*

We describe the collective fabrication and characterization of thin superconducting layers deposited on different substrates: sapphire Al_2O_3, monocrystalline Si, SiO_2, Si_3N_4. Usually single photon detectors (SSPD) are made of a superconducting NbN films deposited on sapphire or MgO wafers but very promising concepts of integrating them with advanced optical structures such as distributed Bragg reflectors (DBRs) and optical waveguides require different substrates.

We present technology of fabrication of thin NbN films using reactive RF magnetron sputtering. The films were deposited from a Nb target in a mixture of nitrogen and argon gas on substrates at temerature in range 700-850 C. The thickness of NbN layer we demonstrate were 5-50 nm.

Some superconducting and structural properties as well as morphology of the films attained from electrical measurement, ellipsometry, X ray difraction and atomic force microscopy AFM, respectivelly, will be shown. Our NbN layers are characterised by critical temperature T_c in range of 8-14 K, smoth surface and good structural properties. Moreover, we demonstrate here an improvement in the critical temperature of the superconducting layer by short time annealing at T=1000 C in Ar.

P-We-25

Influence of target materials on silver benzoate ion formation in LD ion source of time of flight mass spectrometer

Anna Smolira[*], *Robert Bicki, Agnieszka Gruszecka, Monika Szymańska-Chargot*

Institute of Physics, Division of Molecular Physics, Maria Curie Sklodowska University, 20-031 Lublin, Poland

Laser desorption (LD) time of flight mass spectrometry (TOF MS) is a wide spread method used for analysis of different compounds. In this technique, the analyte (sample) diluted in a proper solvent is put on the sample holder surface and dried. Next it is irradiated with a nanosecond laser pulse in order to form analyte's ions. Efficiency of this process depends of many factors. One of them is using different target materials in connection with sample holder (Figure 1).

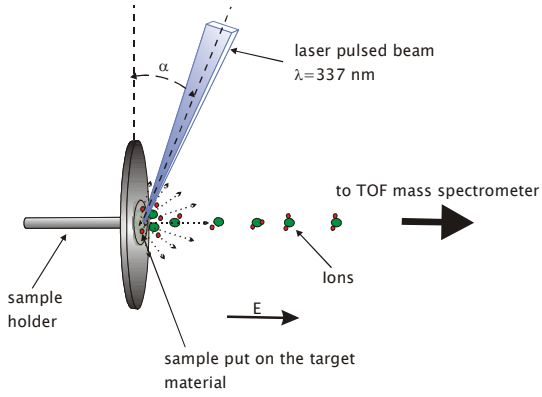

Fig. 1. The sample holder with a target material in the laser desorption (LD) ion source

In this paper results of measurements concerning influence of target materials on silver benzoate ion formation in laser desorption ion source are presented. Investigations concerned the effect of these materials on silver benzoate clustering and mass resolution of obtained mass spectra. The target materials used were glass, floppy disc, scotch tape or photocopy film.

[*] abajuk@telelab.umcs.lublin.pl

P-We-26

Detection of cathelicidins from porcine neutrophils by MALDI time of flight mass spectrometry

Joanna Wessely-Szponder[1)], Barbara Majer-Dziedzic[2)], Anna Smolira[3)], Ryszard Bobowiec[1)]

[1)] *Department of Pathophysiology, Chair of Preclinical Veterinary Sciences, Faculty of Veterinary Medicine, University of Life Sciences, Akademicka 12, 20-033 Lublin, Poland*
[2)] *Institute of Biological Bases of Animal Diseases, Sub-Department of Veterinary Microbiology, Faculty of Veterinary Medicine, University of Life Sciences, Akademicka 12, 20-033 Lublin, Poland*
[3)] *Institute of Physics, Division of Molecular Physics, Maria Curie Sklodowska University, 20-031 Lublin, Poland*

Cationic host defense peptides are important components of innate immunity in pigs and other mammalians. Most of these peptides have a direct antimicrobial activity and they also have a broad spectrum of effects on the host immune system, which may be taken into account in the introduction of novel therapeutics. The major antibacterial peptides, i.e. prophenin-1, prophenin-2, PR-39, and protegrins 1-3 were isolated from a porcine neutrophil crude extract and analyzed.

MALDI-TOF analysis was performed on the reflectron time of flight mass spectrometer (RTOF MS – built in the Institute of Physics, Division of Molecular Physics, UMCS Lublin, Poland, with an ion source MALDI). As a matrix, α-cyano-4-hydroxycinnamic acid (CCA, 189.2 Da, Sigma Aldrich) was used. The mass spectra of the investigated peptides were obtained in the linear mode of the spectrometer, collected at the nitrogen laser (337 nm) in the positive polarity of the ion source. The obtained molecular masses of prophenin-1 and prophenin-2 were 8683 Da and 8807 Da, respectively and were consistent with the predicted molecular masses. The molecular mass of 4716 Da, as revealed in MALDI TOF analysis corresponded to PR-39. Protegrins PG-1 to PG-3 were present and their obtained masses were as follows: 2154.5 Da for PG-1, 1955.6 Da for PG-2, and 2055.5 Da for PG-3.

P-We-27

Influence of substrate local heating on morphology of Al and Al_2O_3 nanofilms

Kazimierz Reszka[1)], Mieczysław Szczypiński[2)], Małgorzata Pomorska[3)]*

[1)] *Institute of Mechatronics, Nanotechnology and Vacuum Technique, Koszalin University of Technology, Śniadeckich str. 2, 75-435 Koszalin, Poland*
[2)] *TERMEX Ltd., Lniana str. 9, 75-213 Koszalin, Poland*
[3)] *Institute of Metallurgy and Materials Science, PAS, Reymonta str. 25, 30-059 Kraków, Poland*

Experimental investigations presented in this work were focused on the execution of a carousel system with its usability for step-by-step revolutions and the mechanism for clamping the heater, which made it possible to heat substrates individually within the range from 25°C to 300°C. This system was used for depositing the metallic Al films by the magnetron sputtering method on foil made of FeCrAl steel, which found application in production of metallic catalytic reactors. It was found that in case of not-heated foil the polycrystalline continuous Al film, which is separated from steel by amorphous oxide nanofilm obtained spontaneously under influence of weather conditions, was created. The deposition of aluminium on foil heated to the temperature of 300°C caused the film marked by fine grains integrated with small forces to be formed. These differences had an influence on morphology of oxide films.

Keywords:, alumina, oxide layers, heater, magnetron sputtering, whiskers

* Raclawicka str.15-17, 75-620 Koszalin, e-mail: kazimierz.reszka@tu.koszalin.pl, fax: +48 94 3478 489

P-We-28

Mass spectrometric study of the kinetic energy release of isopropanon isomer ions

E. Szot, L. Wójcik, K. Głuch

Institute of Physics, University of Maria Curie-Skłodowska, Pl. Marii Curie-Skłodowskiej 1, 20-031 Lublin, Poland

Investigations of small hydrocarbons has recently regained importance in the field of molecular physics as these molecules are considered to be prototypes of polyatomic molecules. They are important constituets in planetary and cometary atmospheres and in plasmas.

In the present work a ddouble focusing mass spectrometer of reversed Nier-Johnson type B-E geometry in research of ionization and fragmentation processes [1-3] of molecular ions produced from 1-propanol and its isomer 2-propanol was used. Experimental results of the high resolution kinetic energy release distribution (KERD) for these ions were compared. By using the same experiment parameters such as: accelerating voltage, electron ionization beam current and the pressure, we observed differences as well in mass spectrum as in ionization and appearance energies for both studied molecules. Moreover observed differences in fragmentation pattern and KERD, between molecular ions with the same mass but other structures allowed us to show differences in molecule structure and its energetic. These results allowed us to study how the structure of molecule influence on the fragmentation processes.

References

[1] K. Głuch, J. Fedor, S. Matt-Leubner, O. Echt, A. Stamatovic, M. Probst, P. Scheier and T.D. Märk, Kinetic-energy release in Coulomb explosion of metastable C3H52+, J. Chem. Phys., 118 (2003) 3090-3095.

[2] K.Gluch, J. Cytawa, L. Michalak, Int. J. Mass Spectrometry, 273 (2008) 20–2

[3] K.Gluch, J. Cytawa, L. Michalak, Int. J of Mass Spectrometry 278 (2008) 10–14.

P-We-29

Double focusing mass spectrometer in molecular structure investigatios

E. Szot, L. Wójcik, K. Głuch

Institute of Physics, University of Maria Curie-Skłodowska, Pl. Marii Curie-Skłodowskiej 1, 20-031 Lublin, Poland

The two sector field mass spectrometer of B-E (magnetic-electric) field configuration, enables to study in detail the kinetic energy release distribution (KERD) over a relatively wide range of molecular ions [1-4]. Using this device we have studied KERDs and deduced influence of molecule structure on this energy. By comparing high precision KERD measurements obtained from molecules built with the same atoms but in different arrangements, we obtained differences in our result concerning fragmentation and ionization processes.

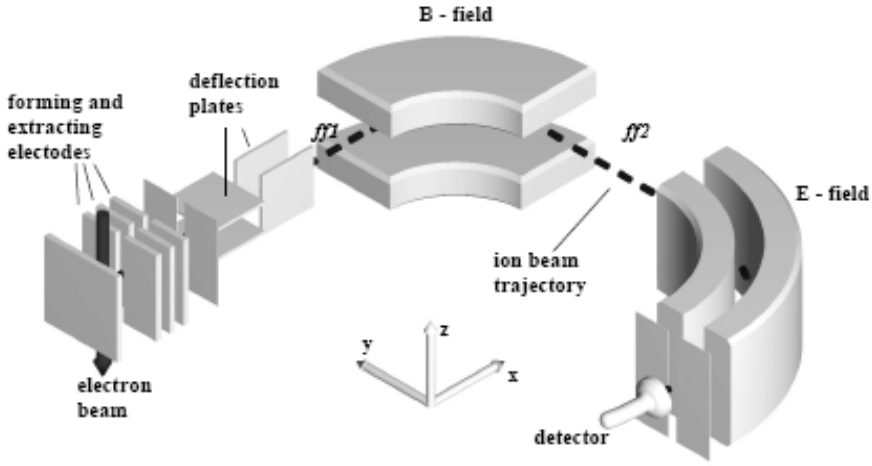

Fig. 1. Double focusing mass spectrometer

By detailed study of our result for simple hydrocarbon molecules we could deduced structures and energetic of the ions. In the present study the idea and the technique of usage of the double focusing mass spectrometer in investigations of the molecular structure is presented.

References

[1] K. Gluch, S. Matt-Leubner, O. Echt, P. Scheier, T. D. Märk, Vacuum 10/81 (2007), 1129-1132
[2] K. Gluch, J. Fedor, R. Parajuli, O. Echt, S. Matt-Leubner, P. Scheier, T. D. Märk, The European Physical Journal D - Atomic, Molecular, Optical and Plasma Physics 1-3/43 (2007), 77-80.
[3] K.Gluch, J. Cytawa, L. Michalak, Int. J. Mass Spectrometry, 273 (2008) 20-23.
[4] K.Gluch, J. Cytawa, L. Michalak, Int. J of Mass Spectrometry 278 (2008) 10-14.

P-We-30

Recombination properties of the ion-implanted silicon

M.I. Tarasik[1)], A.K. Fedotov[1)], A.M. Yanchenko[1)], A.N. Pyatlitski[2)], T.V. Piatlitskaya[2)], S.V. Shvedov[2)], P. Węgierek[3)], P. Zhukowski[3)]

[1)] *Belarusian State University, 4 Nezavisimosti ave., 220030, Minsk, Belarus*
[2)] *JS «INTEGRAL», 12 Korzhenevskogo st., 220108, Minsk, Belarus*
[3)] *Lublin University of Technology, 38d Nadbystrzycka st., 20-618 Lublin, Poland*

With help of microwave-photoconductivity method, lifetime of nonequilibrium charge carriers in Si-substrates N and P types after boron, phosphorus, helium [1] irradiation treatment with dose range $1x10^{13} \div 1x10^{15}$ at/cm^2 and heat treatment at (400÷850)^{o}C was investigated. Lifetime was measured by means of phase method with no more than 1% precision [2]. Photoconductivity excitation was performed by light-emitting diodes with different wavelength in 0.45÷0.85 μm range, which enables variation of light depth penetration in semiconductor.

Analysis of investigation results shows that after implantation and following heat treatment lifetime of nonequilibrium charge carriers, volume and near-surface, was increased. Essential increasing of nonuniformity in radial distribution was detected for some samples.

Lifetime increasing after ion implantation and heat treatment is explanated by gettering effect of metall impurities – recombination centers of nonequilibrium charge carriers by means of ion implantation damaged layer [3]. It was verified by spectral dependence of $\tau(\lambda)$.

Results of the present investigations may be useful for optimization of the process of solar cells production, for increasing of efficiency factor.

References

[1] M.I.Tarasik, A.K.Fedotov, A.M.Yanchenko and et al. IRS-2009. Proceedings of the 8-th International Conference. Minsk, Delarus, Stptember 23-25, 2009, P.207
[2] A.V.Burakov, S.N.Yakubenja, A.M.Yanchenko. IET, 1986, № 4, P.226
[3] A.R.Cheljadinskij, F.F.Komarov. Physics-Uspekhi, 2003, V.173, № 8, P.813-846

P-We-31

Effect of fluences of irradiation with 107 MeV krypton ions on recovery charge of silicon p^+n-diodes

N.A. Poklonski [1)], N.I. Gorbachuk [1)], M.I. Tarasik[1)], S.V. Shpakovski [2)], V.A. Philipenya[3)], V.A. Skuratov[4)], A. Wieck[5)], T. Kołtunovicz[6)]

[1)] *Belarusian State University, pr. Nezavisimosti 4, BY-220030, Minsk, Belarus*
[2)] *"Transistor Plant" Unitary Enterprise of the SPE "Integral", Korzhenevskogo 108, BY-220064 Minsk, Belarus*
[3)] *"Belmicrosystems" Research & Design Company of the SPE "Integral", Korzhenevskogo 12, BY-220108 Minsk, Belarus*
[4)] *Joint Institute for Nuclear Research, Joliot-Curie 6, RU-141980 Dubna, Moscow region, Russia*
[5)] *Ruhr-Universitaet Bochum, 150 Universitaetsstr., D-44780 Bochum, Germany*
[6)] *Lublin University of Technology, 38d Nadbystrzycka st., 20-618 Lublin, Poland*

The diodes under study were fabricated on the uniformly phosphorus doped single crystal silicon wafers with resistivity of 90 Ω·cm. The p^+-type region was created by implantation of boron ions. The depth of p^+n-junction occurrence was $x_j \approx 3.6$ μm, area was 4.41 mm^2. The contacts with thickness of 1.5 μm were formed by Al sputtering. The diodes were implanted with krypton ions from the side of p^+-region (energy 107 MeV, fluence Φ in the range $5 \cdot 10^7$-$4 \cdot 10^9$ cm^{-2}). The average projected range of krypton ions in Al-Si structure was $R_p \approx 15.0$ μm.

The reverse recovery charge Q_{rr} of the diodes was found to be inversely proportional to the square root of the irradiation fluence Φ value. The fraction of reverse recovery charge Q_{rrA} (which accounts for the phase of high reverse conduction) was found to decrease faster than Q_{rr} value with the fluence increasing. Thus, irradiation with high energy ions can be considered as one of the possible methods of creation of the Si-based fast diodes with soft recovery.

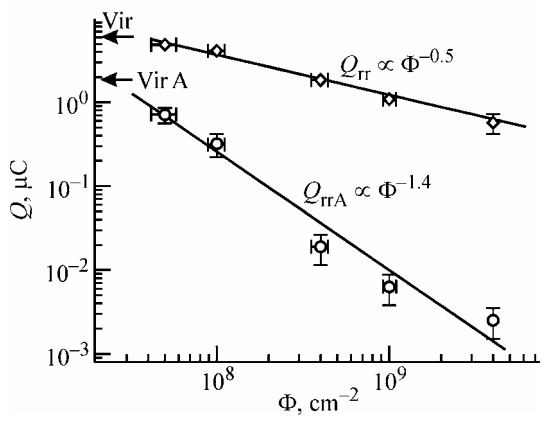

Fig. 1. Dependence of the total reverse recovery charge Q_{rr} and reverse recovery charge which accounts for the phase of high reverse conduction Q_{rrA} on the fluence Φ of irradiation of silicon diodes with krypton ions (arrows Vir and VirA marks values Q_{rr} and Q_{rrA} for non-implanted diodes)

P-We-32

Influence of Xe^+ irradiation on topography and wettability of graphite surface

Igor Tashlykov[1)], *Anton Turavets*[1)], *and Pawel Zukowski*[2)]

[1)] *Belarusian State Pedagogical University, Sovetskaja st.18, 220050 Minsk, Belarus*
[2)] *Lublin University of Technology, Lublin, Poland*

Graphite is candidate material for many technological applications, such as barrier or antifriction coating, foundry facings, etc. Thus the surface properties, like the morphology, mechanical properties and wettability, are important for the performance of the final system, therefore they have attracted considerable interests of many investigators for last years.

This work deals with influence of Xe^+ ions irradiation of graphite on its surface topography and wettability.

Graphite samples had typically size of 10x8 mm2 and a thickness of 3 mm. They were irradiated by 20 keV Xe+ ions. The beam current density was kept 1,2 μA/cm^2. The irradiation doses were $1\cdot10^{14}$, $3\cdot10^{14}$, $1\cdot10^{15}$, $3\cdot10^{15}$ ions/cm2. During irradiation, the vacuum pressure was $4\cdot10^{-4}$ Pa.

Atomic force microscopy (AFM) study of graphite samples were performed using NT-206 microscope in the contact mode with silicon cantilever tips. Contact angle measurements were based on the sessile-drop method described in [1].

The AFM three-dimensional pictures showed that after irradiation of graphite of Xe^+ ions with a dose of $3\cdot10^{15}$ cm^{-2} hemispherical grains (from 0.2 to 0.8 μm in diameter) appear on its surface, it could be attributed to the formation of xenon bubbles on the graphite surface. It was indicated that with an increase of the irradiation dose, the roughness average increases rapidly at first (when the sample was irradiated at the dose of $1\cdot10^{14}$ cm^{-2}) and then decreases. Contact angle measurement showed that irradiation of graphite of Xe^+ ions leads to a hydrophobic surface of graphite. We have observed that irradiation of graphite of Xe^+ ions can be used for receiving graphite surface with desirable topography and water wettability.

References

[1] Tashlykov I.S., Baraishuk S.M., Izvestia VUZov. Powder metallurgy and functional coatings 2008; 1: 30.

P-We-33

Effect of annealing on dope depth profiles in rapidly solidified Al-Ge alloys

Iya I. Tashlykova-Bushkevich[1)], Czeslaw Kozak[2)] and Vasiliy G. Shepelevich[3)]

[1)] *Belarusian State University of Informatics and Radioelectronics, P. Brovki Str.6, 220013 Minsk, Belarus*
[2)] *Lublin University of Technology, Nadbystrzycka Str. 38A, 20-618 Lublin, Poland*
[3)] *Belarusian State University, Av. Independence 4, Minsk 220050, Belarus*

Development of rapid solidification technologies and applications of rapidly solidified (RS) products in powder metallurgy as well as in microelectronics, mechanical engineering and the aircraft industry stimulates creation of mathematical models which include morphological stability analysis in Al alloys. One critical assumption is that current models of formation and growth of the competing solid phases and constituents requires a deeper understanding of the mechanisms by which kinetics determine RS solidification microstructure formation, including its scale, morphology and phase constitution. Therefore the investigation of microstructural changes taking place during Al alloy annealing is crucial improving the understanding of the surface segregation processes of solutes in the RS foils.

In this study, the solute depth redistribution as a function of the annealing temperature has been investigated for RS Al-Ge alloy foils by means of Rutherford backscattering spectroscopy (RBS) with application of computer simulation (RUMP). In adition, the annealed foils were characterized through scanning electron microscope and X-ray diffraction. The foil texture was studied using the inverse pole figures method. From the RBS spectra, nonuniform dope depth distribution profiles in the Al-Ge alloys were analyzed in respect to their microstructure and phase composition. It was found out that the dope surface segregation is remarkable at 500ºC in the samples. In fact, Ge content reaches 40 at % in a thin foil surface layer of annealed Al-5.0 at % Ge alloy. Carried out investigation of the layer-by-layer elemental composition emphasizes topics worthy of extensive research, aimed to advance present understanding of physical mechanisms which control the final RS microstructures of Al-based alloys.

P-We-34

Optical pattern fabrication in amorphous silicon carbide with high-energy focused ion beams

T. Tsvetkova[1)], S. Takahashi[2)], P. Sellin[3)], I. Gomez-Morilla[3)], O. Angelov[4)], D. Dimova-Malinovska[4)] and J. Żuk[5)]

[1)] *Institute of Solid State Physics, Bulgarian Academy of Sciences, 72 Tzarigradsko Chaussee Blbd., 1784 Sofia, Bulgaria*
[2)] *Centre for Nanostructured Media, School of Mathematics and Physics, The Queen's University of Belfast, Belfast BT7 1NN, UK*
[3)] *Surrey Ion Beam Centre, Advanced Technology Institute, School of Electronics and Physical Sciences, University of Surrey, Guildford, Surrey GU2 7XH, UK*
[4)] *Central Laboratory for Solar Energy and New Energy Sources, Bulgarian Academy of Sciences, 72 Tzarigradsko Chaussee Blvd., 1784 Sofia, Bulgaria*
[5)] *Institute of Physics, Maria Curie-Sklodowska University, Pl. M.Curie-Sklodowskiej 1, 20-031 Lublin, Poland*

Topographic and optical patterns have been fabricated in a-SiC films with a focused high-energy (1 MeV) H^+ and He^+ ion beam and examined with near-field techniques. The patterns have been characterized with atomic force microscopy and scanning near-field optical microscopy to reveal local topography and optical absorption changes as a result of the focused high-energy ion beam induced modification. Apart of a considerable thickness change (thinning tendency), which has been observed in the ion-irradiated areas, the near-field measurements confirm increases of optical absorption in these areas. Although the size of the fabricated optical patterns is in the micron-scale, the present development of the technique allows in principle writing optical patterns down to the nano-scale (several tens of nanometers). The observed values of the optical contrast modulation are sufficient to justify the efficiency of the method for optical data recording using high-energy focused ion beams.

P-We-35

Modification of "zirconium-on-silicon" system by dense compression plasma

V.V. Uglov[1)], N.T. Kvasov[2)], Yu.A. Petukhou[2)], R.S. Kudaktsin[1)], V.M. Astashynski[3)], A.M. Kuzmitski[3)], V.A. Ukhov[4)], A.V. Shashok[1)], P. Konarski[5)]

[1)] *Belarusian State University, 4 Nezalezhnasci ave., Minsk, Belarus*
[2)] *Belarusian State University of Informatics and Radioelectronics, 6 P. Brovka str., Minsk, Belarus*
[3)] *B. I. Stepanov Institute of Physics, National Academy of Sciences of Belarus, 68 Nezalezhnasci ave., Minsk, Belarus*
[4)] *"Semiconductor Device Factory" SOE, 12 Karzhaneuski str., Minsk, Belarus*
[5)] *Tele and Radio Research Institute, Ratuszowa 11, Warszawa, Poland*

The action of dense compression plasma flows (CPF) is a method for obtaining new compounds and unique structures in surface layer of materials. The feature of this method is that CPF acts on sample during 100 μs with energy density up to 40 J/cm^2. Such thermodynamic conditions provide essential phase and structural changes in surface layer of pure metals and semiconductors and their interface.

Metal-semiconductor system is widely used as contact for solar cells and microelectronic devices. Contact Zr-Si has special properties: low Shottky barrier, low resistivity and high thermal stability. In the present work we studied structure and phase changes of Zr layer deposited on silicon substrate after CPF action.

Silicon substrate with pre-deposited Zr coating was treated by a number of CPF with energy density 3-15 J/cm^2. Obtained samples were studied by X-ray diffraction, scanning electron microscopy and Auger-electron spectroscopy.

We found that the action of CPF with energy density 3-6 J/cm^2 results in the formation of modified layer (2-3 μm thickness) with atomic ratio of Zr 15 at.%. It consists of silicon dendrites with tip radius 0,2 μm and primary branch spacing 1 μm. Zirconium silicides ZrSi and $ZrSi_2$ are located between silicon dendrites. CPF action with energy density 10-15 J/cm^2 causes melting of Zr layer, mixing of Zr and Si in liquid and formation of ZrSi and $ZrSi_2$. Thickness of Zr-alloyed layer is 10-25 μm. This layer consists of silicon dendrites and $ZrSi_2$ in interdendritic space.

The formation of dendritic structure results in that contact area between silicon and zirconium silicides increases which provides potential improvement of electrical properties of contact.

This research was partially supported by BRFFR (project № F10M-127)

P-We-36

Hopping mechanism of electric conductivity in the n-type silicon implanted with Ne^+ neon ions

Paweł Węgierek and Piotr Billewicz

Lublin University of Technology, 38A Nadbystrzycka street, 20-618 Lublin, Poland

The article presents results of research on phosphorus-doped silicon of $\rho = 0{,}25\ \Omega\cdot cm$ resistivity, strongly defected by the implantation of Ne^+ neon ions of the $E = 100$ keV energy and a dose of $D=2{,}2\cdot10^{-14}\ cm^{-2}$. Values of measured electrical parameters (C_p, σ_p) have been recorded within the T_p temperature range from LNT to 373 K and at frequencies ranging from 50 Hz to 5 MHz. Research has been conducted on sample that has been isochronously annealed by the time of 15 minutes, within the T_a temperature range from 373 K to 873 K, with an average increase rate 50 K.

Results obtained in the process of sample testing have been analysed in the article in the context of activity of different mechanisms of electric conductivity in strongly defected silicon. For the annealing temperatures T_a=373 K and T_a=598 K it has been noticed that the frequency changes affects values of measured parameters. In addition, conductivity increase is connected with the increase of the capacity as long as the sample testing temperature (T_p) rises simultaneously. On the basis of dependences prepared for different T_p values it has been possible to estimate conductivity activation energy ΔE.

On the strength of conducted research it has been observed that there is strong correlation between certain electrical parameters and the annealing temperature. It has been determined that such correlation depends on changes of concentration of the radiation defects which is characteristic for each annealing temperature.

It has been concluded that in tested sample two different mechanisms of electric conductivity has appeared: the band one that dominates at low frequency values and the hopping one which is typical for high frequencies.

P-We-37

Formation of submicron n^+-layers in silicon implanted with H^+-ions

Yury Pokotilo[1)], Alla Petukh[1)], Aleksey Giro[1)], Paweł Węgierek[2)]

[1)] Belarussian State University, 4 Pr. Nezavisimosti, Minsk, Belarus
[2)] Lublin University of Technology, 38d Nadbystrzycka st., 20-618 Lublin, Poland

N^+-layers in commercial Mo-Si Schottky diodes with the active base region made of epitaxial phosphorusdoped silicon 5 μm in thickness, with a resistivity ρ=1.05 and 1.8Ω cm have been studied. The diodes were implanted with 300 keV H^+-ions at room temperature from the planar side through an Ag–Ni–Mo multilayer contact. The electron concentration profiles were obtained by standard C-V-measurements. The parameters of radiation-induced defects were determined by deep level transient spectroscopy (DLTS) at 1 MHz frequency. Postimplantation anneals were performed for 20 min at temperatures from 275 to 475°C.

At sufficiently high implant doses ($F \sim 10^{15}$ cm^{-2}) and temperatures from 350 to 475°C, there are at least two types of donors, present in roughly equal concentrations, one of which exhibits bistable behavior [1]. Our results lend further support to the bistability model based on the negative correlation energy of a singly ionized doubly charged donor. At ~475°C, the bistable H-donor is fully annealed, whereas the concentration of stable donors remains unchanged at annealing temperatures from 350 to 475°C. Under fixed post-implantation heat-treatment conditions (350°C, 20 min), it is the implant dose that determines which type of H- donor will form. In the range 10^{13} to 10^{14} cm^{-2}, H-donors of the former type are formed, and the maximum in their profile coincides with the projected ion range. In contrast, implant doses in the range 10^{14} to 10^{15} cm^{-2} produce H donors of the latter type, and the peak in their profile is located closer to the irradiated surface, in the region of the highest radiation damage.

Work partially support by BRFFI (grant №F09K-023).

References

[1] Pokotilo Yu.M., Petukh A.N., Litvinov V.V., Tsvyrko V.G., Neorganicheskie Materialy 2009;45;№11:1285

P-We-38

Time-dependent electron transport through the quantum dot based devices

Ewa Taranko, Małgorzata Wiertel, Ryszard Taranko

Institute of Physics, M. Curie-Skłodowska University, Pl. M. Curie-Skłodowskiej 1, 20-031 Lublin, Poland.

The electron transport in nanoscopic systems has mostly been studied in the case of constant values of the system parameters. However, in the context of the emerging field of quantum computing or experimental advances in the studies of the quantum dot (QD) subject to voltage pulses, it would be very desirable to perform the time-dependent calculations of the current in some QD based devices. The results of such calculations can be crucial for practical implementation of QD systems in a variety of electronic devices. We consider the different aspects of the time-dependent electron transport in systems of various combinations of the QDs and leads. Especially, the current transient effect and interference or beats phenomena are studied in the case of two double QDs (in parallel configuration) coupled with three or two leads. We observe the quantum beats of the resulting tunneling current, both at the source and drain electrodes or at the drain electrode only, depending on the configuration of QDs in the considered system. We consider also the asymptotic values of the current flowing in response to the sudden coupling of the electron reservoirs with the QDs system. The resulting current strongly depends on the bias voltage and the inter-QD coupling. The influence of the different forms of the QD energy level oscillations on the time-dependent current and its interference properties was also considered.

Acknowledgements: The work of R.T. has been supported by the Ministry of Science and Higher Education Grant No. N N202 109036.

P-We-39

Mass spectrometric study of ion-molecule reactions in H_2S and CH_4 mixtures

Leszek Wójcik and Artur Markowski

Institute of Physics, Maria Curie-Sklodowska University, Pl. M. Curie-Sklodowskiej 1, 20-031 Lublin, Poland

Investigation of ion molecule reactions were performed by authors for hydrogen sulfide – methane mixtures of different compositions. The concentration of methane in mixtures ranged from 10% to 90% (at 10% increments). The investigated gases of high spectral purity H_2S (99.8%) and CH_4 (99.99%) were supplied by Praxair and Merck, respectively. Pressure of the gas inside the ion source collision chamber was controlled by MKS Baratron manometer scaled in mTorr. Measurements were made by means of quadrupole mass spectrometer with special high pressure ion source constructed at the Institute of Physics in Lublin. Differential vacuum system to separate gas evacuation from ion source and analyzer was applied. Construction details were presented in earlier works [1-3]. Primary ions C^+, CH^+, CH_2^+, CH_3^+, CH_4^+, S^+, HS^+, H_2S^+ produced in gas by electrons with energy of 300 eV and secondary CH_5^+, $C_2H_5^+$, H_3S^+, $H_2{}^{34}S^+$, $H_3{}^{34}S^+$, CHS^+, CH_3S^+, S_2^+, HS_2^+, $H_2S_2^+$ and $H_3S_2^+$ from the ion-molecule reactions were observed. The gas pressure in the collision chamber of the ion source was varied from 0.7 to 33.3 Pa. Relative intensities for primary and secondary ions are presented as a function of potential of repeller electrode and concentration of methane in the mixture. Schemes of ion-molecule reactions were proposed. One of the criterion that helps to distinguish between primary and secondary ions arising in ion-molecule processes, is different dependence of ion intensity from the gas pressure. The other one is based on fact that probability of interaction between primary ions and neutral molecules that provide to ion-molecule reactions decreases with decreasing of residence time in ion chamber. Residence time can be changed by changes of the repeller potential. The influence of that potential on ion-molecule reactions efficiency for the examined mixtures of hydrogen sulfide and methane has been determined. The investigations of ion-molecule reactions in pure H_2S and mixtures of H_2S with CH_4 have been conducted using various mass spectrometric methods [4-8]. The obtained results were compared with those obtained in these works.

References

[1] Wójcik L. Ann Univ Mariae Curie-Sklodowska Sect AAA 1999;54:74.
[2] Wójcik L, Bederski K. Int J Mass Spectrom Ion Processes 1996;153:139.
[3] Wójcik L, Markowski A. Vacuum 2007;81:1393.
[4] Ruska WEW, Franklin JL. Int J Mass Spectrom Ion Phys 1969:3;221.
[5] Harrison AG, Thynne JCJ. Trans Faraday Soc 1966;62:3345.
[6] Bennett SL, Field FH. J Am Chem Soc 1972;94:6305.
[7] Huntress WT Jr, Pinizzotto RF Jr, Laudenslager JB. J Am Chem Soc 1973;95:4107.
[8] Wójcik L, Markowski A. Vacuum 2009;83:173.

P-We-40

Ion-molecule reactions in carbon tetrafluoride-helium mixtures

Leszek Wójcik and Artur Markowski

Institute of Physics, Maria Curie-Sklodowska University, Pl. M. Curie-Sklodowskiej 1, 20-031 Lublin, Poland

The studies of ion-molecule reactions are very important for understanding elementary processes in gas phase ion chemistry, but also for explaination the role of such processes in ionosphere. It's well known that presence of carbon tetrafluoride in atmosphere contributes to the decrease of stratospheric ozone level. The upper layers of earth's atmosphere contain mainly hydrogen and helium.

The main purpose of this work were measurements of ion-molecule reactions occuring in mixtures of carbon tetrafluoride with helium and their dependence on the pressure, for different composition of studied mixtures. Measurements were made by means of quadrupole mass spectrometer with a high-pressure ion source constructed by L. Wójcik and K. Bederski and presented in earlier works [1-3]. Mixture of investigated gases of required composition were made in separate leak system. The concentration of helium in mixtures with carbon tetrafluoride ranged from 10% to 90% (at 10% increments). The total mixture pressure pressure measured by MKS Baratron gauge, was changed from 0.7 to 33.3 Pa. These measurements in our opinion were carried out first time for such a wide range of the mixtures composition.

Primary ions were produced by electrons with energy of 300 eV. Electron current intensity was stabilized by keeping the constant value of total emission current from filament. Carbon tetrafluoride and helium used in experiment were supllied by Merck. The purity of both gases reached 99.99%. Gas pressure inside the collision chamber of the ion source was controled by MKS Baratron manometer. All measurements were made at constant repeller potential fixed at 10 V. Differential pumping of the mass spectrometer is used for increase the maximum gas pressure inside the high-pressure ion source keeping low pressure in quadrupole mass analyzer regions.

Primary and secondary ions He^+ (m/q=4), C^+ (m/q=12), F^+ (m/q=19), CF^+ (m/q=31), CF_2^+ (m/q=50) and CF_3^+ (m/q=60) were observed. Relative values of ion currents for these ions were determined as a function of total gas pressure inside the collision chamber of the ion source for different mixtures compositions.

The ionic processes occurring in the mixture of CF_4-He were studied extensively by many investigators using various methods [4-7]. Obtained results were compared with that presented in literature.

References

[1] Wójcik L, Bederski K. Int J Mass Spectrom Ion Processes 1993;127:11.
[2] Bederski K, Wójcik L. Int J Mass Spectrom Ion Processes 1996;154:145.
[3] Markowski A, Wójcik L, Gruszecka A. Vacuum 2009;83:178.
[4] Chau M, Bowers ML. Int J Mass Spectrom Ion Phys 1977;27:191.
[5] Ellen R, Weber ME, Armentrout PB. J Chem Phys 1990;92:2296.
[6] Huang FY, Kushner MJ. J Appl Phys 1995;78:5909.
[7] Bederski K. Vacuum 2007;81:1374.

P-We-41

Improved light extraction efficiency by two-dimensional triangular photonic crystal arrays using focused ion beams

B.H. Tsai[1)], C.F. Wu[2)], S.F. Kung[1)] and G.M. Wu[1)]*

[1)] *Institute of Electro-Optical Engineering, Chang Gung University, Taoyuan 333, Taiwan R.O.C.*
[2)] *Department of Applied Mathematics, National Dong Hwa University, Hualien 974, Taiwan R.O.C.*

Nitride-based thin-film materials have become increasingly important for the high brightness light-emitting diode (LED) applications. The improvements in light extraction and lower power consumption are highly desired. Although the internal quantum efficiency of GaN-based LED has been relatively high, only a small fraction of light can be extracted because of the interface refraction between GaN and the contact materials. In this study, two-dimensional photonic crystal arrays have been prepared on the top p-GaN layers to improve the light extraction efficiency by focused ion beam technology using a dual-beam nanotechnology workstation system SMI 3050. The acceleration voltage of the Ga ion beam was fixed at 30 kV and the ion beam current was 100 pA. The LED area was designed to be 350×350 μm^2 with both top and bottom pads. The cylindrical air holes exhibited the diameter of 150 nm, and two different periods of 300 nm and 700 nm were examined. The micro photo-luminescence analysis results showed that the light output was 1.2 times and 1.5 times higher than that of the non-patterned LED control sample, while the photonic crystal period was set at 300 nm and 700 nm, respectively. In addition, we developed Bandsolve simulation tools for the photonic crystal band structures. The correlations in structure-property would be further discussed.

* Corresponding author E-mail: wu@mail.cgu.edu.tw

P-We-42

Mechanisms of electric conductivity in gallium arsenide exposed on poly-energy implantation of H^+ ions

Paweł Żukowski, Paweł Węgierek, Piotr Billewicz, Tomasz Kołtunowicz

Lublin University of Technology, 38A Nadbystrzycka street, 20-618 Lublin, Poland

In the article have been presented results of research on electrical parameters of gallium arsenide of $\rho = 0{,}1\ \Omega\cdot cm$ resistivity, modified in the process of poly-energy implantation of H^+ ions of the energy ranging from 40 keV to 250 keV. Ranges of energy and dose of the implantation have been strictly selected in order to obtain a distribution of radiation defects as homogeneous as it had been possible. Sample has been isochronously annealed by the time of 15 minutes. Values of conductivity have been recorded within the temperature range from LNT to 433 K and at frequencies ranging from 50 Hz to 5 MHz.

On the basis of correlation between conductivity and frequency prepared for annealing temperatures T_a from 523 K to 663 K and sample testing temperature T_p from 77 K to 153 K it has been possible to calculate values of the frequency coefficient α, according to the formula $\sigma \sim f^{\alpha}$. Then the correlation between the defects relaxation time τ and temperature has been determined and activation energy has been estimated.

After analysing obtained results it has been noticed that conductivity changes are the function of sample testing temperature, frequency and annealing temperature. In particular, as long as values of T_p and T_a increases it is possible to observe the increase of those frequencies which are connected with hopping mechanism of electric conductivity. On the strength of the analysis of dependences $\alpha = f(f)$ it has been observed that the increase of T_p and T_a also causes that the highest rates of α coefficient are moving towards higher values of the frequency. Described phenomena are probably connected with changes of the type and the concentration of radiation defects, caused by the rise of annealing temperature.

Results of research proved that in tested sample two types of electric conductivity occurred: the band mechanism which is typical for low frequencies and the hopping one that dominates at high frequencies.

P-We-43

Calculation of concentration and mobility of free charge carriers and own defects in monocrystal epitaxial films PbTe at α-irradiation

V. Wojcik, Ya. Saliy, P. Zukovskiy, D. Freik

Physical-Chemical Institute of Vasyl Stefanyk Precarpathian National University, 57, Shevchenka str., Ivano-Frankivsk, 76026, Ukraine

Was shown, that size effects in monocrystal films n-PbTe under α-irradiation, grown on mica wafers by method of hot wall, connected with distributions of donors and dispersion centers of free charge carriers. Made approximation of experimental effective dependence from thickness of conductivity σ(d) and product of Hall coefficient and conductivity $R(d)\sigma(d)^2$ by theoretical dependences with using local concentrations n(x) and mobilities μ(x) of free charge carriers. It is gained spatial parameters of dependence of defects of growth on boundary wafer-film and dislocations on next layer.

For the purpose of studying of distribution of electrical active defects and dispersion centres of free charge carriers in films n-PbTe, and also their division, was improved the method used by us earlier for receiption of distribution of radiating defects in films PbTe and own defects in metal films. Spatial parameters of distribution and peak values of concentration of donors defects in a thick film, and also similar values of the characteristic for the dispersion centers are received.

Local concentrations of donor defective conditions are presented by the sum of two normal distributions on a background of even one and local concentrations of dispersion centers – by one normal distribution on a homogeneous background.

Mobility of free charge carriers is inversely proportional to concentration of dispersion centers.

Spatial characteristics of distributions d and b weakly depend on temperature. Peaks of distribution centers are situated on depth $d_3 = 0.033$ μm, that is in 1,5 times closer to wafer than peaks of distribution of sources $d_1 = 0.050$ μm. Boundaries of both distributions d + b in which there is a basic part of defects, situated on 0.1 μm from a wafer, difference between them makes 0.01 μm. Distribution of defects of the second type extends from 0.6 to 2.1 μm, their peak concentration in 15 times is less, than defects of the first type.

P-We-44

Features annealing of silicon implanted with argon ions

V.B. Odzhaev[1)], V.S. Prosolovich[1)], Yu.N. Yankovski[1)], V.A. Belous[1)], P. Zhukowski[2)]

[1)] Belarussian State University, 4 Nezavisimosti ave., 22005, Minsk, Belarus
[2)] Lublin University of Technology, 38d Nadbystrzycka st., 20-618 Lublin, Poland

The processes of generation, transformation, annealing defects and activation diffusion of impurities in silicon implanted with ions of argon have been studied by means of Rutherford backscattering, SIMS, IR-absorption, neutron activation analysis and measurement of Hall effect. Silicon wafers of n-type were implanted with 50 keV, 100 keV and 46.9 MeV Ar^+ ions in the fluencies ranging from $1 \cdot 10^{12}$-$1 \cdot 10^{16}$ cm^{-2}.

For silicon implanted with 50 and 100 keV argon ions maximum in the distribution of radiation defects at a depth 0.8-0.9 R_P was observed. It was found that annealing reduces the concentration of radiation defects and their joint diffusion with argon atoms to a surface of wafers. Probably, in this case diffusion occurs on clusters of radiation damage created by argon.

The formation of two regions of radiation defects in silicon implanted with 46.9 MeV argon ions is observed. The first (approximately 0.3 R_P) is caused divacancies. The second (on depth 0.8-0.9 R_P) is associated with regions of disorder. The redistribution of profiles of technological impurities (Au, Cu, Fe, Na) is not observed for all implantation energies. That means that the radiation-induced diffusion of this impurities is absent during ion implantation. The displacement of a maximum argon depth profiles after rapid thermal and furnace annealing was not observed.

The profile shape of implanted argon after RTA at 1000^0C during 30 s is unchanged also. This profile is broadened after furnace annealing at 1000^0C during 30 minute due to the diffusion of argon in depth and to the wafer surface. The redistribution of technological impurities due to their gettering argon have been observed too. The profiles of their distribution practically corresponded to the distribution profile of argon.

Authors Index

Abadias G. 23
Abakevičienė Brigita 141
Abd El Aal S. 103
Abd El Aal Shaaban 45, 65
Abd El Hady M.M. 66
Abdi S. 94
Abendroth B. 139
Adliene D. 128
Adlienė Diana 136
Ajayeva L.V. 69, 118
Ali Mona 22
Alontseva D.L. 21, 67
Andrearczyk T. 43
Angelov O. 152
Armstrong B.M. 56
Assmann W. 90
Astashynski V.M. 115, 153
Aubert P. 32
Azarko I.I. 69, 118
Azarko Igor 68

Baidak V.A. 96
Baine P. 56
Bak-Misiuk J. 119
Bak-Misiuk Jadwiga 28
Bakulin A. 69, 118
Balcerski Józef 111
Baltrusaitis J. 128
Bar Jan 142
Baranowska J. 75
Barcz A. 119
Barcz Adam 28
Barlak Marek 19, 29, 55, 60, 70, 71, 106
Barocio S.R. 93
Bederski K. 121
Belous V.A. 162
Belov Alexey 50
Berdaliev D.T. 101
Beresnev V.M. 96, 98, 107
Beresnev Vyacheslav M. 95
Bersnev V.M. 97
Bicki Robert 143
Bieliński Dariusz M. 42
Billewicz Piotr 154, 160
Bobowiec Ryszard 144
Bocheńska Katarzyna 19, 29, 55, 70, 71, 106
Bonchyk O. 88
Boniecki M. 32
Borysenko Oleksey 95
Borysiewicz Michał 142
Brinkevich D. 137
Brinkevich D.I. 138
Brzozowski R. 63, 91
Buca D. 54
Budziak A. 88
Burinskas Aleksandras 76

Caliebe W. 119
Chaplanov A.M. 122
Chen Y.F. 34
Cherenda N.N. 115
Cherkouk C. 57
Chien H.W. 123
Chow Lee 28
Chugrov Ivan A. 49
Cichomski Michał 111, 124
Craciun L. 109
Curuia M. 109

Čyvienė Jurgita 141

Dąbrowski Ludwik 19
Debelle A. 32
Debelle Aurélien 31
Dem'yanenko A.A. 96
Demyanov Serguey 30
Dimova-Malinovska D. 152
Dobrzanski L. 26
Dolecki K. 91
Domagala J.Z. 119
Domagała J.Z. 43
Domagała Jarosław 142
Domaradzki Jarosław 72
Droździel A. 43, 48, 61, 133, 134
Duda P. 58
Dudonis Aleksandras 76
Dudonis Julius 85
Dunetz B. 131
Dynowska E. 119

Erdybaeva N.K. 97
Ershov Alexey 50
Ershov Alexey V. 49
Ershov Andrew A. 49

Fassbender J. 89

Fedchenko Helena..... 99
Fedotov A. 125
Fedotov A.K..... 80, 126, 148
Fedotov Alexander..... 30
Fedotov Alexander K. 79, 116
Fedotova Julia 30
Fedotova Julia A. 116
Fedotova V.V. 80
Fedotova Vera..... 30
Fedotova Vera V. 79
Fendler R. 54
Filiks J..... 39, 133
Fillon A. 23
Filossofov D.V. 110
Fouad M. 103, 104
Frantskevich A.V. 126
Frantskevich N.V. 126
Freik D. 127, 161
Fryska S. 75

Gamble H.S..... 56
Garrido Frédérico..... 31
Gawlik Grzegorz..... 37
Gebel Thoralf..... 54
Ghasemi S. 74
Ghomi H. 74
Ghomi Hamid 73
Giro Aleksey..... 155
Gluba Ł. 133
Głuch K..... 146, 147
Gomez-Morilla I. 152
Gorbachuk N . I 149
Gorodecka Helena..... 135
Gorshkov Oleg..... 50
Grabiec Piotr..... 142
Grigonis A..... 140
Grodecki Remigiusz..... 142
Gröetzchel Rainer 70
Gruszecka A..... 121
Gruszecka Agnieszka..... 143
Guobienė Asta..... 136
Guziewicz Marek..... 142

Haeberlein S..... 54
Hallen A. 119
Heera V. 54
Heidarnia A. 74
Hejduk Krzysztof..... 142
Helm M. 46, 57
Herrmannsdörfer T..... 54
Hładki P. 58
Hurley R..... 56

Ignatenko Oleg 68
Il'yashenko M.V..... 96, 97, 98, 107
Il'yashenko Maxim..... 95
Iljinas Aleksandras 76
Ion M. 109
Ismail B. 103, 104
Ivanou Dmitry 30
Ivanov S.A. 21
Ivanova Yulia 30

Jagielski J. 26, 32
Jagielski Jacek 31, 37
Jakucionis L..... 128
Jaouen C. 23
Jozwik I. 26, 32
Jóźwik Iwona..... 37

Kaczmarek Danuta 72
Kaczorek K..... 25
Kaliasas R. 128
Kamyshan A.S. 81
Kamyshan Alexander 52
Kanjilal A. 46, 48
Karpovich I.A. 129
Karpovich Igor 68
Karvat Cz..... 96
Karwat C. 122
Karwat Cz..... 130, 132
Katkauske Oresta..... 85
Kavaliauskas Zydrunas..... 77
Kaverin M.V..... 96, 97, 98, 107
Kaverin Mikhail 95
Khalfaoui N. 90
Khoramabadi Mansour 73
Kiszczak K. 78, 130, 132
Kolisnichenko O.V. 107
Kolitsch Andreas 70
Kolos V.V..... 122
Koltunowicz T.N. 80
Koltunowicz Tomasz N. 30, 79, 116
Kołtunovicz T. 149
Kołtunowicz T.N. 125, 126
Kołtunowicz Tomasz..... 160
Komarov F..... 53, 130, 131
Komarov F.F. 81, 97, 132
Konarski P. 25, 115, 153
Konarski Piotr 60
Konopljanik I..... 132
Korman A. 22, 66
Korolik O..... 125
Kostyuk Alexey..... 50
Kośla Katarzyna 111, 124

Kotb H.S. 66
Kowalczyk Paweł 47
Kowalski Zbigniew W. 82
Kozak Cz. 130, 132
Kozak Czeslaw 151
Kozak M. 98
Kozlov Zh.A 109
Kozlova E.I. 69, 118, 129
Kozłowski Witold 124
Krockert K. 139
Krysztof Michał 84, 108
Krzyżanowska H. 43
Kucharski S. 86, 87
Kudaktsin R.S. 153
Kulik Igor 95
Kulik M. 43, 53, 74, 133, 134
Kung S.F 159
Kunitskyi Yu.A. 107
Kurchenko V.P. 69, 118
Kuzmitski A.M. 153
Kvasov N.T. 153
Kwiatkowska J. 100
Kwietniewski Norbert 47
Kylyshkanov M.K. 97

Labdi S. 32
Lagutin Andrei 135
Larkin Andrey V. 116
Laukaitis Giedrius 85
Lehmann J. 46
Levintant-Zayonts N. 86, 87, 88
Liedke B. 89
Liedke M.O. 89
Lin Li 133
Low Y.W. 56
López-Callejas R. 93
Lu H.C. 34
Lukashevich M. 137

Maciejak O. 32
Mahgoub G. 22
Majer-Dziedzic Barbara 144
Makhmudov N.A. 96, 98, 107
Makhmudov Nemat A. 95
Maksimkin O.P. 101
Mantl S. 54
Marcinauskas Liutauras 77
Markevich M.I. 122
Markowski Artur 157, 158
Marszalek Marta 99
Mateescu G. 109
Mazalski P. 89
Mazanik A. 125
Mazanik A.V. 126
Mazanik Alexander 30
Maziewski A. 89
Mączka D. 61, 78
Mączka Dariusz 36
McNeill D.W. 56
Meftah A. 90
Mercado-Cabrera A. 93
Mezhylovska L. 127
Michalec M. 88
Michel A. 23
Mihul A. 110
Mikhaylov Alexey 50
Mikhaylov Alexey N. 49
Mikolajunas M. 128
Milchanin O. 53, 130, 131
Milchanin O.V. 132
Milcius Darius 18, 85
Milčius Darius 76
Misevra S.Ya. 21
Misiuk Andrzej 28
Mitchell S.J.N. 56
Mockevičienė Skirmantė 136
Möller H.J. 139
Moneta M. 91, 92
Mudryi A. 53, 131
Muecklich A. 41
Munnik F. 66
Muñoz-Castro A.E. 93

Nickel F. 38
Niknam A.R. 94
Nowicki L. 35, 41, 51
Nycz Barbara 19, 55, 60, 70, 71

Odzhaev V. 137
Odzhaev V.B. 129, 162
Odzhaev Vladimir 68
Opielek Marek 20
Oprea C. 63, 109, 110
Oprea I.A. 63, 109, 110

Padureanu I. 109
Partyka J. 137
Partyka Janusz 95
Pasternak Iwona 142
Pawłowska Marta 37
Pawłowski B. 91
Pągowska K. 35, 41
Peña-Eguiluz R. 93
Petukh Alla 155
Petukhou Zu.A. 153
Philipenya V.A. 149

Piatkowska A. 32
Piatlitskaya T.V. 148
Piedad-Beneitez A.de la 93
Piekoszewski Jerzy . 19, 29, 55, 70, 71, 106
Pochrybniak Cezary 19, 29, 55, 70, 71, 106
Pogrebnjak A.D. 20, 21, 96, 97, 98, 107
Pogrebnjak Alexander D. 95
Poklonski N . A 149
Pokotilo Yury 52, 155
Pomorska Małgorzata 145
Posselt M. 54
Postolnyi Bogdan 95
Potzger K. 27
Pranevicius Liudas 18
Pranevicius Liudvikas 18
Pranevicius Liudvikas 77
Proba M. 63
Prociow Eugeniusz L. 72
Prokhorenkova N.V. 21
Prosolovich V. 137
Prosolovich V.S. 138, 162
Prosyčevas Igoris 136
Protsenko Serhiy 99
Prucnal S. 48, 61, 133, 139
Przybytniak Grażyna 42
Pshyk A.P. 96
Pshyk A.V. 98
Puiso J. 128
Puszkarz A. 92
Puzyrev Mihail 68
Pyatlitski A.N. 148
Pyszniak K. 43, 48, 53, 61, 133, 134
Pyszniak Krzysztof 36

Radzimski Zbigniew 72
Rainey P. 56
Rajchel B. 100
Rastkar A.R. 94
Ratajczak R. 35, 41, 51
Rawski M. 133
Rebohle L. 46, 57
Reszka Kazimierz 145
Rodríguez-Méndez B.G. 93
Rogowski Jacek 124
Rogoz V. 98
Romanowski P. 119
Runka T. 26
Russakova A.V. 101
Rutkuniene Z. 140
Rzodkiewicz W. 134

Saad A.M. 80
Saad Anis 30
Saad Anis M. 79
Sadowski J. 43
Saied S.O. 33
Sakaliūnienė Jolita 141
Saliy Ya. 127, 161
Sallam A. 103, 104
Sarnecki Jerzy 37
Sartowska Bożena ... 19, 55, 60, 70, 71, 106
Sattonnay Gaël 31
Savitskij G. 88
Sellin P. 152
Semenov V.A. 109
Senkara J. 25
Shaaban A. 22
Shalimov A. 48
Shashok A.V. 115, 153
Shepelevich Vasiliy G. 151
Shpakovski S . V 149
Shvedov S.V. 148
Shymanski V.I. 115
Shypilenko A.P. 97
Shypylenko A.P. 98, 107
Sidorenko Yu. 137
Sihame A. 22
Skorupa W. 46, 48, 54, 57, 139
Skuratov V.A. 149
Słowiński B. 58, 78
Słówko Witold 84, 108
Słysz Wojciech 142
Smolira A. 121
Smolira Anna 143, 144
Sobol O.V. 96, 98
Sobolewski Roman 142
Sochacki Mariusz 47
Solovjov J. 130
Starosta Wojciech 19, 60, 70, 106
Stas'kov N. 125
Stefanescu I. 109
Stefaniv N. 127
Stelmakh V.F. 122
Stępkowska Aneta 42
Stoch Paweł 19
Stonert A. 22, 35, 41, 51, 66
Studer F. 90
Sullivan J.L. 33
Surma Barbara 28
Svito Ivan 30
Swiatek Z. 88
Szalanski P.J. 63, 109, 110
Szczypiński Mieczysław 145
Szmaja Witold 111, 124
Szmidt Jan 47
Szot E. 146, 147

Szymanska-Chargot M. 121
Szymańska-Chargot Monika 143
Szymczak R. 43

Takahashi S. 152
Taranko Ewa 156
Taranko Ryszard.....156
Tarasik M.I. 148
Tashlykov Igor 150
Tashlykova-Bushkevich Iya I. 151
Tashmetov M.Yu. 98
Tashmetov Mannab 95
Templier Claude 18
Tetelbaum David 50
Tetelbaum David I. 49
Thomé L. 32
Thomé Lionel 31
Timofeev A.A. 21
Toulemonde M. 90
Trautmann C. 90
Tsai B.H. 159
Tsay K.V. 101
Tsvetkova T. 152
Tsvyrko Viktor 52
Tuleta Marek 112
Tuleushev Yu.Zh. 97
Turavets Anton 150
Turek M. 48, 61, 133
Turek Marcin 36, 113
Turos A. 22, 35, 41, 51, 66
Turtsevich A. 130
Tyurin Yu.N. 20
Tyutyunnikov Serguey 30

Uglov V.V. 115, 153
Ukhov V.A. 153

Vabishchevich N. 137
Vabishchevich S.A. 138
Valatkevicius Pranas 77
Valencia Alvarado R. 93
Velichkov A.I. 110
Vinciunaite V. 140
Virbukas Darius.....85
Virzonis D. 128
Vlasukova L. 53, 131
Voelskow M. 46
Volobuev V. 137
Voss K.-O. 90

Wajler A. 32
Waliś Lech 19, 70, 106
Wang W.L. 123
Wegierek Pawel 116
Werner Zbigniew 19, 29, 70
Wesch W. 131
Wessely-Szponder Joanna 144
Węgierek P. 148
Węgierek Paweł 154, 155, 160
Węgrzecka Iwona 142
Węgrzecki Maciej 142
Wieck A. 149
Wiertel Małgorzata 156
Wierzchowski Wojciech 36
Wieteska Krzysztof.....36
Wilczyńska Teresa 60
Wiśniewski Roland 60
Wojcik V. 161
Wosiński T. 43
Wójcik L. 146, 147
Wójcik Leszek 157, 158
Wójtowicz A. 48
Wroński Z. 39
Wu C.F. 159
Wu G.M. 34, 123, 159
Wündisch C. 54

Yakuschenko Ivan.....95
Yanchenko A.M. 148
Yankovski Oleg 68
Yankovski Yu.N. 138, 162
Yankovsky O.N. 129
Yastrubchak O. 43

Zagojski A. 26
Zhukowski P. 80, 148, 162
Zhukowski Pawel.....79, 116
Zubrzycki J. 78
Zukovski P.V. 97, 107
Zukovskiy P. 161
Zukowski P. 130, 132
Zukowski Pawel.....99, 150

Żuk J. 43, 48, 53, 133, 134, 152
Żukowski P. 125, 126, 127
Żukowski Paweł.....160